

INFORMATION TO USERS

This manuscript has been reproduced from the microfilm master. UMI films the text directly from the original or copy submitted. Thus, some thesis and dissertation copies are in typewriter face, while others may be from any type of computer printer.

The quality of this reproduction is dependent upon the quality of the copy submitted. Broken or indistinct print, colored or poor quality illustrations and photographs, print bleedthrough, substandard margins, and improper alignment can adversely affect reproduction.

In the unlikely event that the author did not send UMI a complete manuscript and there are missing pages, these will be noted. Also, if unauthorized copyright material had to be removed, a note will indicate the deletion.

Oversize materials (e.g., maps, drawings, charts) are reproduced by sectioning the original, beginning at the upper left-hand corner and continuing from left to right in equal sections with small overlaps.

Photographs included in the original manuscript have been reproduced xerographically in this copy. Higher quality 6" x 9" black and white photographic prints are available for any photographs or illustrations appearing in this copy for an additional charge. Contact UMI directly to order.

ProQuest Information and Learning
300 North Zeeb Road, Ann Arbor, MI 48106-1346 USA
800-521-0600

UMI[®]

Static and dynamic properties of epileptogenic lesions

By

Li Li Min

Department of Neurology and Neurosurgery
McGill University, Montreal

March, 2000

A thesis submitted to the Faculty of Graduate Studies and Research
in partial fulfillment of the requirements of the degree of

Ph.D.

© Li Li Min, 2000



**National Library
of Canada**

**Acquisitions and
Bibliographic Services**

**395 Wellington Street
Ottawa ON K1A 0N4
Canada**

**Bibliothèque nationale
du Canada**

**Acquisitions et
services bibliographiques**

**395, rue Wellington
Ottawa ON K1A 0N4
Canada**

Your file Votre référence

Our file Notre référence

The author has granted a non-exclusive licence allowing the National Library of Canada to reproduce, loan, distribute or sell copies of this thesis in microform, paper or electronic formats.

The author retains ownership of the copyright in this thesis. Neither the thesis nor substantial extracts from it may be printed or otherwise reproduced without the author's permission.

L'auteur a accordé une licence non exclusive permettant à la Bibliothèque nationale du Canada de reproduire, prêter, distribuer ou vendre des copies de cette thèse sous la forme de microfiche/film, de reproduction sur papier ou sur format électronique.

L'auteur conserve la propriété du droit d'auteur qui protège cette thèse. Ni la thèse ni des extraits substantiels de celle-ci ne doivent être imprimés ou autrement reproduits sans son autorisation.

0-612-64604-1

Canada

ABSTRACT

A series of studies were undertaken with the aim of assessing the static and dynamic profiles of the most common types of epileptogenic lesions: hippocampal sclerosis and cortical developmental malformations. Neuronal metabolic dysfunction measured by proton magnetic resonance spectroscopic imaging (^1H -MRSI) overlaps the structural lesion displayed by magnetic resonance imaging (MRI). The extent of neuronal metabolic dysfunction, however, tends to be wider than the MRI-visible lesion and may reflect the intrinsic nature and extent of the original epileptogenic damage. In addition, neuronal metabolic dysfunction and synchronized neuronal firing often coincide spatially and vary together in intensity possibly reflecting the severity of the epileptogenic process.

Non-foreign tissue lesional, temporal lobe epilepsy (TLE) syndrome is a heterogeneous condition, which displays a spectrum of neuronal damage. The different patterns of neuronal damage measured by MRI volumetry (MRIVol) and ^1H -MRSI enable accurate probabilistic prediction of TLE lateralization and discrimination of TLE from extra-TLE. Furthermore, both MRIVol and ^1H -MRSI have a prognostic value in surgical TLE patients, which can be used to streamline surgical candidates.

The neuronal damage is present in the early stages of the epileptogenic process in patients with localization related epilepsy. This process is dynamic and shows a slow progressive neuronal loss and dysfunction in TLE patients, which is not related to seizure burden. Neuronal metabolic dysfunction, lesions, spikes, cognitive decline, and psychiatric disorders are part of the epileptogenic process. These different domains parallel each other in

a given time, although their pathophysiological processes are distinct. Thus seizures and neuronal damage co-exist but are not causally related.

Normalization of neuronal metabolic function is seen in post-operative seizure-free patients, with a recovery half time of six months. However, the process of neuronal recovery does not occur in patients who are seizure-free due to antiepileptic medication. The epileptogenic process causes disruption of normal neuronal network and in order to reverse this disruption the epileptogenic area must be isolated or resected surgically. The epileptic state is a translation in time of the activity of the epileptogenic process. Seizures, stereotyped behavioral manifestations, are the hallmark of the epileptogenic process. Absence of seizures, however, does not reflect inactivity of the epileptogenic process. Neuronal damage as measured by NAA/Cr can serve as a surrogate marker of the epileptogenic state.

RÉSUMÉ

Nous avons entrepris une série d'études, dans le but de déterminer les états basal et longitudinal des types les plus fréquents de lésions épileptogènes: la sclérose hippocampique et les malformations du développement cortical. Les modifications du métabolisme neuronal détectés par imagerie spectroscopique de résonance magnétique (ISRM) se superposent aux lésions anatomiques visualisées par imagerie de résonance magnétique (IRM). Cependant, l'étendue des modifications métaboliques sont souvent plus larges que celle des lésions détectées par IRM, et peuvent mettre en évidence la nature même et l'étendue de la région épileptogène initiale. De plus l'étendue ainsi que l'intensité des modifications métaboliques neuronales coïncident souvent avec les décharges neuronales synchronisées, ce qui reflète la sévérité du processus épileptique.

Le syndrome de l'épilepsie temporale (ETL) non-lésionnelle consiste en un large spectre d'atteinte neuronale. L'IRM volumétrique et l'ISRM permettent de latéraliser avec précision l'épilepsie temporale et de la discriminer de l'épilepsie extra-temporale à l'aide d'une analyse multi-paramétrique. Enfin ces deux méthodes d'investigation permettent d'établir un pronostique chez des patients candidats à une chirurgie.

L'atteinte neuronale est observée des les premières phases du processus épileptique chez les patients présentant une épilepsie localisée. Les variations de ce processus sont accompagnées d'une perte ou d'un dysfonctionnement neuronal, chez les patients présentant une ETL, qui n'est pas corrélée avec la fréquence des crises. Le processus épileptique peut présenter plusieurs aspects tels que des modifications métaboliques, des lésions anatomiques,

des décharges neuronales, un déclin cognitif, et des maladies psychiatriques. Parmi ces derniers, certains peuvent coexister malgré une pathophysiologie distincte. Ainsi, il n'y a pas de corrélation entre l'observation des crises comitiales et d'une atteinte neuronale.

Chez les patients ne présentant plus de crises après chirurgie, on observe une normalisation du métabolisme neuronal après une demie-période de récupération de six mois. Cependant, ce phénomène n'est pas démontré chez les patients ne présentant plus de crise sous traitement médicamenteux. Le processus épileptique entraîne des altérations du réseau neuronal, qui peuvent être corrigées ou limitées par une résection de la région épileptogène. Alors que les crises comitiales ou un comportement stéréotypé constituent les signes du processus épileptique, l'absence de crises ne reflète pas une inactivité du processus épileptique. Par contre, l'atteinte neuronale, mesurée par le rapport métabolique de NAA/Cr, constitue un marqueur substitutif du processus épileptique.

ABSTRACT	II
RÉSUMÉ	IV
ACKNOWLEDGEMENT	VIII
ABBREVIATION	IX
PREFACE	X
INTRODUCTION (RATIONALE AND OBJECTIVES).....	XIII
CHAPTER I	17
Review of the literature	17
Epidemiology.....	17
Etiology.....	18
Role of Antiepileptic Drugs in Epilepsy.....	21
Surgical Treatment of Epilepsy.....	23
Impact of MR-based Techniques in Epilepsy.....	25
Neuronal Damage and Recovery in Epilepsy.....	36
CHAPTER II.....	43
Anatomo-functional relationships in epileptic lesions	43
Paper 1: Neuronal metabolic dysfunction in patients with cortical developmental malformations: a proton MR spectroscopic imaging study.....	44
Paper 2: Spatial extent of neuronal metabolic dysfunction measured by proton MR spectroscopic imaging in patients with localization related epilepsy.....	58
Paper 3: Relation of interictal spike frequency to ¹ H-MRSI-measured NAA/Cr.....	83
CHAPTER III	98
Clinical relevance of new types of MR-based techniques	98
Paper 4: Magnetization transfer contrast in the lateralization of temporal lobe epilepsy.....	99
Paper 5: Lateralization of temporal lobe epilepsy (TLE) and discrimination of TLE from extra-TLE using pattern recognition on MR spectroscopic and volumetric data.....	105
Paper 6: Prognostic value of proton MR spectroscopic imaging in surgical outcome of patients with intractable temporal lobe epilepsy and bilateral hippocampal atrophy.....	130

CHAPTER IV	143
Dynamic changes in lesions underlying epilepsy	143
Paper 7: Neuroimaging evidence of progressive neuronal loss and dysfunction in temporal lobe epilepsy.	144
Paper 8: Time course of postoperative recovery of N-acetyl-aspartate in temporal lobe epilepsy.	167
Paper 9: Proton MR spectroscopic imaging studies in patients with newly diagnosed partial epilepsy.	188
 CHAPTER V	 202
Conclusion and summary	202
Neuronal metabolic dysfunction in relation to lesions and spikes	202
Clinical relevance of new types of MR-based techniques	204
Neuronal damage and recovery in the epileptogenic process.....	205
Epileptic State.....	207
 REFERENCE.....	 209

ACKNOWLEDGEMENT

This thesis was made possible with the help of many people. I would like to acknowledge:

Dr. Douglas L. Arnold, my supervisor, for providing his support and the means necessary to carry out this project.

Dr. Frederick Andermann, my advisor, for giving me the opportunity to come to the Montreal Neurological Institute, and for guidance and training in the field of epilepsy.

Dr. Jean Gotman, my advisor, for guidance and direction of this project.

Dr. François Dubeau for providing insightful comments on many of the papers.

My friends and colleagues at the MRS lab, Fernando Cendes, Edwin Tasch, Wolfgang Serles, Samson Antel, Sridar Narayanan, Zografos Caramanos, Carmela Tartaglia, and Ellie Tobman, for their extensive help in this project. Neda Bernasconi and Dominique Sappey-Marinier for the French translation of the abstract.

The granting agencies: Savoy Foundation for Research in Epilepsy of Canada, Medical Research Council of Canada and Jeanne-Timmins-Costello Fellowship for financing this project.

My family for providing me with unconditional and endless support.

ABBREVIATION

MR = magnetic resonance

¹H-MRSI = proton magnetic resonance spectroscopic imaging

MRVol = magnetic resonance volumetric study

MT = magnetization transfer

CDM = cortical developmental malformation

TLE = temporal lobe epilepsy

Extra-TLE = extra-temporal lobe epilepsy

NAA = N-acetylaspartate

Cr = creatine + phosphocreatine containing compounds

Cho = choline containing compounds

CA= Cornu Ammonis

CPS = complex partial seizure

SGTC = secondarily generalized tonic clonic seizure

AED = anti-epileptic drug

PREFACE

This Ph.D. aims to evaluate the structural and metabolic characteristics of the epileptogenic lesion and its dynamic changes, with special emphasis on diagnosis, prognosis, and clinical evolution of partial epilepsies. I have chosen the option offered in “Guidelines Concerning Thesis Preparation” that allows inclusion of original articles as part of the thesis.

This thesis is based on nine original articles. In six of them I have done all the research work, performed the statistical analysis and written the manuscript. In the remaining three I have done part of the work; in paper 7, I participated in the conceptualization of the idea, analysis and interpretation of the data. In papers 3 and 8, I participated in the conceptualization of the idea, collection, analysis and interpretation of the data, and writing part of the manuscript. All the authors of these nine articles have contributed significantly and thus have co-authorship as specified in uniform requirements for manuscripts submitted to biomedical journals Vancouver group, fifth edition (1997, <http://www.thelancet.com/newlancet/sub/author//uniform1.html>). Two papers (papers 1 and 7) have been published in peer-reviewed journal of international reputation. Two papers (paper 3 and 6) have been accepted for publication. Five papers (paper 2, 4, 5, 8 and 9) have been submitted.

This thesis is divided into five chapters. The first chapter reviews the current findings and state of knowledge in the field of epilepsy with special emphasis on the two most common types of epileptogenic lesions: hippocampal sclerosis and cortical developmental malformations, their clinical manifestation, diagnosis and prognosis.

The core experimental findings of this thesis are presented in three parts in the second,

third and fourth chapters.

The second Chapter deals with the anatomo-functional relationships of epileptogenic lesions. This chapter comprises three papers, in which we assess the relationship amongst neuronal metabolic dysfunction as measured by proton magnetic resonance spectroscopic imaging (^1H -MRSI), structural brain lesion as detected by MRI, and epileptic neuronal firing as measured by EEG. We demonstrated in the largest series of patients with cortical developmental malformations, confirming the findings of Kuzniecky et al.,¹ that different types of cortical developmental malformations present distinct degrees of neuronal metabolic dysfunction, and in some cases, the neuronal metabolic dysfunction extends beyond the MRI defined lesion (paper 1). We also demonstrated that neuronal metabolic dysfunction can extend beyond the primary epileptogenic area in about 40-50% of cases (paper 2). We were the first to demonstrate that frequency of interictal neuronal firing is negatively related to the degree of neuronal dysfunction (paper 3).

The third Chapter focuses on the clinical relevance of new MR-based techniques. This chapter comprises three papers which assess the clinical utility of magnetization transfer ratio in temporal lobe epilepsy (paper 4), a sophisticated mathematical approach towards MR data sets for TLE lateralization and discrimination between TLE and extra-TLE (paper 5), and the prognostic value of ^1H -MRSI in surgical outcome (paper 6). We demonstrated that magnetization transfer ratio is not useful for lateralization of TLE, contrary to a preliminary report from the Queen Square group². We were the first to report that TLE patients present MR characteristics that allow a probabilistic prediction, which further refines the lateralization of TLE and discrimination between TLE and non-TLE patients (paper 5). We were the first to report the surgical prognostic value of ^1H -MRSI in refractory TLE (paper 6).

The fourth Chapter focuses on the dynamic changes in lesions underlying epilepsy. This chapter comprises three papers which assess the issue of neuronal damage and recovery in TLE. Using MRIVol and 1H-MRSI, we were the first to demonstrate that there is evidence of progressive neuronal loss and dysfunction in patients with intractable TLE (paper 7). Normalization of NAA is seen in post-operative seizure-free patients and we were the first to show that NAA recovery can be modeled as an exponential function with a recovery half time of 6 months (paper 8). We were also the first to show that the normalization of NAA in this case appears to be due to removal and/or disconnection of the epileptogenic area (paper 9).

The fifth Chapter provides a conclusion and summary.

INTRODUCTION (RATIONALE AND OBJECTIVES)

There is a dynamic interplay between epileptic lesions, seizures, and neuronal structural-functional state in the brains of patients with partial epilepsy. However, it is unclear what are the strengths of these relationships and their biological and clinical relevance for the diagnosis and prognosis of partial epilepsy. Magnetic resonance (MR) based techniques allow for the non invasive *in vivo* study of the structural and functional state of the human brain. Thus, these different MR-markers of neuronal integrity can be used to improve (i) understanding of pathophysiological mechanisms of underlying epileptogenic lesions and (ii) diagnosis of epilepsy, and ultimately these knowledge can be applied to (iii) improve our management of patients with epilepsy.

There are a wide variety of epileptogenic lesions; hippocampal sclerosis and cortical developmental malformations are the most common types. These types of lesions are often seen in patients with refractory epilepsy. Fortunately, surgical therapy is an effective alternative treatment in many of these patients in whom an epileptogenic area can be defined and excised without major neuropsychological sequelae. The surgical outcome has been less satisfactory in cortical developmental malformations compared to hippocampal sclerosis. The poor results have been blamed on a more widespread microscopic abnormality. If this were the case, one would expect to find a more widespread neuronal metabolic abnormality in cortical developmental malformations. In temporal lobe epilepsy, the neuronal metabolic dysfunction often involves contralateral homologous region, however, it is unclear whether neuronal metabolic abnormality can also extend to non-homologous regions of brain, and if present

what are the mechanisms underlying the widespread neuronal dysfunction. The anatomical distribution of interictal spikes and the neuronal damage often co-localize with the epileptogenic area. An increase in spike frequency has been observed after seizures, and it was suggested to represent neuronal damage, if this is the case, one could expect to find a relationship between spikes and neuronal metabolic dysfunction.

There is a small proportion of patients with refractory partial epilepsy with no MRI-identifiable lesion called "MR-negatives". This group of patients represents a major challenge for defining the epileptogenic area. The solution to this problem lies in the development of more sensitive pre- and/or post-processing techniques or implementation of already available MR sequences used in other pathologies. Magnetization transfer (MT) is a magnetic resonance sequence used in other pathologies such as multiple sclerosis. MT is highly sensitive to demyelinating lesions, and a preliminary report in three patients with epilepsy showed promising results, thus MT might be clinically useful for epileptic patients. MRI volumetry (MRIVol) of amygdala and hippocampus and proton magnetic resonance spectroscopic imaging (^1H -MRSI) of the temporal lobes are sensitive to mesial temporal lobe neuronal damage. The side of maximal abnormality often coincides with EEG lateralization. The specificity of temporal lobe ^1H -MRSI, however, is less clear. It is possible that application of a more sophisticated mathematical approach to both MRIVol and ^1H -MRSI data sets can provide additional information on lateralization and also localization of the seizure focus. The pattern of volume loss detected by MRIVol has shown surgical prognostic value, with best outcome seen in patients with unilateral hippocampal atrophy, and with worst outcome seen in patients with bilateral hippocampal atrophy or no atrophy. Although, temporal lobe ^1H -MRSI can lateralize the side of seizure origin in TLE patients, it remains unknown whether this type of examination has surgical prognostic value that can add information to MRIVol.

There is a debate whether neuronal damage is progressive and caused by seizures, and if neuronal damage is present at early stages of epileptogenic process. Since MR-based techniques can provide measurement of neuronal integrity, these issues can be assessed using two methodological designs: longitudinal and cross-section. The longitudinal design would be more appropriate, but its major drawback would be time necessary to detect any changes in the measurements, as this could be years. An alternative would be a cross-sectional design study. Neuronal metabolic dysfunction can be reversible in patients with TLE who become seizure-free after surgical ablation/disconnection of epileptogenic area. The time course of recovery from neuronal metabolic dysfunction is unknown, and this information may help understand mechanism underlying normalization of neuronal metabolic function in epilepsy.

We undertook a series of studies trying to answer these questions. The studies in this thesis were divided into three interrelated chapters; the first part studies the anatomic-functional relationships in epileptogenic lesions, the second part evaluates the clinical relevance of new types of MR-based techniques, and the third part investigates the dynamic changes in lesions underlying epilepsy. Specifically, the objectives of this thesis are to assess:

I. Anatomo-functional relationships in epileptic lesions

- The extent and degree of neuronal metabolic dysfunction in patients with cortical developmental malformation and epilepsy.
- The anatomical distribution of neuronal metabolic dysfunction in partial epilepsy and the clinical differences between patients with more widespread vs. localized neuronal metabolic dysfunction.
- The relationship between interictal scalp spike frequency and the underlying brain

neuronal metabolic dysfunction.

II. Clinical relevance of new types of MR-based techniques

- The clinical usefulness of magnetization transfer in the lateralization of patients with TLE.
- The use of pattern recognition of temporal lobe proton MR spectroscopic imaging (¹H-MRSI) and MR volumetric (MRVol) data for the lateralization and discrimination between temporal lobe epilepsy (TLE) and extra-TLE.
- The clinical relevance of ¹H-MRSI in the prognosis of surgical patients with refractory TLE and bilateral hippocampal atrophy.

III. Dynamic changes in lesions underlying epilepsy

- Progression of neuronal damage in TLE patients.
- The time course of postoperative NAA recovery in patients with refractory TLE.
- The degree of neuronal metabolic dysfunction in the temporal lobes of patients with newly diagnosed partial epilepsy, and the reversibility of this dysfunction with anti-epileptic medication.

CHAPTER I

Review of the literature

Epidemiology

Epilepsy is defined as non-provoked, recurrent, stereotyped seizures. In the general population of developed countries, the prevalence of epilepsy has been estimated to be about five to 10 people in 1,000 inhabitants with an annual incidence affecting 50 to 75 people in 100,000³⁻⁵. Current anti-epileptic drugs (AEDs) can achieve seizure control in about 80% of patients with epilepsy^{6,7}. The remaining 20% comprise a group of patients with refractory epilepsy. Extrapolating these figures to Canada, in a population of 26 million, there are approximately 30,000 to 40,000 cases of chronic epilepsy. Of the 15,000 new cases every year, 20% will die in 5 years^{8,9}, leaving 12,000 cases. Of these, 80% are well controlled on AEDs, and the remaining 20% (~ 2,000) of new cases will be added to the backlog of patients with chronic epilepsy every year.

The natural history of epilepsy is unclear. The first effective medication, bromide, has been in use long before the advent of a proper epidemiological study design. Therefore, much of the knowledge about the dynamics of epilepsy is based on the clinical evolution of treated epilepsy.

Patients with epilepsy have a higher morbidity and mortality risk than the general population. Sudden death has been estimated to be 6 times higher than the general

population¹⁰. Some of the risk factors include difficulty controlling epilepsy¹⁰⁻¹², and associated cardiovascular disorder¹³. Furthermore, the social stigma associated with epilepsy and the prejudice towards patients with epilepsy undermine the patient's confidence and cause psychological stress.

Etiology

There are a number of factors known to cause epilepsy, ranging from genetic to acquired. Progress has been made in the molecular genetics of epilepsies¹⁴⁻¹⁶. Genetic factors are considered to be of etiological significance in 40% to 60% of cases¹⁷. Mutations in genes responsible for epilepsy can be categorized into (i) alteration in ion channels, (ii) disruption of normal brain development, (iii) progressive neuronal degenerative processes, and (iv) impairment of neuronal cell energy metabolism. For example, autosomal familial nocturnal frontal lobe epilepsy presents a clinical phenotype characterized by seizures beginning in childhood with clusters of short lasting tonic posturing seizures arising from sleep, and normal EEG¹⁸, often misdiagnosed as a sleep disorder^{19,20}. A locus was mapped to chromosome 20q13.2-q13.3 (Phillips et al.,²¹), with a mutation in the gene that encodes the $\alpha 4$ subunit of the nicotinic acetylcholine receptor^{22,23}. The consequence of this mutation is unclear, but it is thought to cause alterations in Ca^{2+} channel permeability²⁴. In cortical developmental malformation (CDM), for instance band heterotopia, an X-linked disorder²⁵, commonly referred to as 'double cortex' because of the extra ectopic layer of gray matter²⁶, two research groups cloned the mutated gene that encodes a novel protein, named doublecortin^{27,28}. The function of doublecortin is yet unclear, possibly it plays a role in the signal transduction pathway²⁹. Another X-linked disorder, familial periventricular nodular heterotopia has a

phenotype characterized by female, normal intelligence, with seizures often of the partial type beginning in the second decade and presenting with contiguous smooth ectopic neurons along the lateral aspects of the third ventricle^{25,30-32}. Eksioglu et al.³³ mapped the locus to chromosome Xq28. The candidate region includes regions that encode for protein filamin 1³⁴, which is an important regulator in cell migration.

Interestingly, MRI has brought new insights in the phenotype expression of some familial partial epilepsies. For example, Fernandez et al.³⁵ reported on two families with several members who had a history of febrile convulsions. They found that patients who had experienced febrile convulsion as well as unaffected members had significant hippocampal asymmetry as compared to normal controls. In a parallel study, VanLandingham³⁶ reported MRI findings in 27 infants who had febrile convulsions. The results suggested that some patients had a pre-existing abnormality. Two of the 27 who had prolonged lateralized febrile seizures had follow-up scans that showed the development of hippocampal sclerosis. In a similar line of research in familial temporal lobe epilepsy, which presents a heterogeneous clinical manifestation³⁷, Kobayashi et al.³⁸ showed in their preliminary results in 15 unrelated families that many of the affected and unaffected members presented an MRI phenotype with atrophy and/or morphological alterations of the mesial temporal structures.

Examination of *post-mortem* and surgically removed specimens from patients with chronic refractory TLE reveals that hippocampal sclerosis (HS) is the most common type of pathology followed by CDM.³⁹ Hippocampal sclerosis is often present as part of the temporal lobe epilepsy syndrome. This syndrome is characterized by a constellation of clinical signs and symptoms of temporal lobe type seizures, neuro-cognitive impairment, and temporal lobe spikes. Association with a history of childhood febrile convulsions is found in up to 30-40%

of the cases⁴¹⁻⁴², followed by a latent “silent” period until early adolescence when seizures begin. The type of precipitating factor in HS appears to be important in the pattern of atrophy. Free et al.⁴³ demonstrated that unilateral HS was associated with a history of early febrile convulsions while bilateral HS was more closely linked to a history of meningitis and encephalitis.

Raymond et al.⁴⁴ studied 100 patients with CDM and refractory epilepsy and found that pre- and perinatal problems occurred in one third of patients, however, less than 5% of these problems were considered severe. The clinical manifestation of CDM was quite variable and classified as generalized in 16 and localization-related in 84 patients. Even in patients with localization-related epilepsy, the syndromes were variable and classified as frontal (32%), temporal (31%), parietal (14%) and occipital (7%) lobe epilepsy.

Moreover, patients with refractory epilepsy can present with both HS and CDM on MR imaging series⁴⁵⁻⁴⁸. The association between HS and an extra-hippocampal lesion is known as a dual pathology and is observed in approximately 5% to 20% of patients with refractory epilepsy in MRI series⁴⁵⁻⁴⁸. In a pathological series this figure rises to 30% of patients⁴⁹. In a series of 167 patients with lesional epilepsy studied by Cendes et al.,⁴⁶ using MRI the most common types of concomitant extra-hippocampal lesions seen in dual pathology were early gliotic scars and CDM independent of the lesion location. The authors suggested that a common pathogenic mechanism during pre- or perinatal development may explain the occurrence of concomitant HS and associated developmental abnormalities or predisposition to prolonged febrile convulsions.

These particular types of pathologies highlight the complexity and heterogeneity of factors causing epilepsy. In most cases the pathophysiology mechanisms is likely to be

multifactorial, genetic and acquired, rather than an isolated factor participating in the epileptogenic process.

Role of Antiepileptic Drugs in Epilepsy

Anti-epileptic drugs can be divided into major categories depending on the mechanism of action^{6:7:50}: (i) sodium currents, (ii) T-calcium currents, (iii) GABA_A currents, and (iv) NMDA currents. Many of the AEDs have multiple mechanisms of action. The first line AEDs target primarily the sodium channels while the most recently developed drugs act on GABA and NMDA systems^{51:52}.

The short term effect of AEDs in epilepsy is quite well established, that is to prevent the recurrence of seizures, however their long term effects are not so well defined⁵³. Much of this is due to the limited knowledge on the natural history of epilepsy. It is not known in what situation the AEDs could actually cure the epileptogenic process and/or prevent the progression of this process. In some patients, the epileptogenic process is self limited. An example is Rolandic epilepsy with onset of infrequent seizures in childhood and remission by mid adolescence⁵⁴. The assumption that epilepsy progresses is controversial. Although this is not a general phenomenon, it has been observed to different degrees in some patients, manifesting itself by progressive memory decline, appearance of behavioral problem, and exacerbation of seizure frequency and severity.

There is experimental evidence, however, that the newly developed AEDs, because of their action on NMDA or GABA systems, are also neuroprotective⁵⁵⁻⁵⁹ and can prevent epileptogenesis and progression of neuronal damage and its consequences.

Pitkanen et al.,⁶⁰ compared the efficacy of carbamazepine, a sodium channel blocker, and vigabatrin, an irreversible GABA_A transaminase inhibitor, in preventing hippocampal and amygdaloid damage in the perforant pathway stimulation model of status epilepticus in the rat. They found that both drug treatments were equally effective in decreasing the number and severity of seizures during electrical stimulation. However, in the vigabatrin group, the damage to the hippocampus was significantly less severe than in the carbamazepine group. The severity of neuronal damage in the hippocampus did not differ between carbamazepine and vehicle-treated animals.

Loscher et al.,⁶¹ reported an interesting finding on the novel anticonvulsant, levetiracetam, in amygdala-kindling in rats, a model of temporal lobe epilepsy. The mechanism of action of levetiracetam is unclear, but it has been suggested that it acts on the GABA system⁶². They found that after termination of daily treatments with levetiracetam, amygdala stimulations elicited shorter lasting behavioral seizures and afterdischarges in the amygdala compared to vehicle treated controls. These data indicate that levetiracetam did not simply mask the expression of kindled seizures through an anticonvulsant action, but exerted a true antiepileptogenic effect.

There are several “newly marketed” AEDs such as vigabatrin, lamotrigine, topiramate, gabapentin, which have been shown to be very effective in controlling seizures⁶³, however, the long term effects of these drugs remain to be seen.

All AEDs, however, are not devoid of side effects, which can range from mild somnolence to life-threatening hepatic failure. Some side effects only became apparent after a number of years. For instance, felbamate was withdrawn from the market after it was linked to fatal bone marrow aplasia⁶⁴. More recently, vigabatrin has been implicated in causing visual

field constriction⁶⁵.

Surgical treatment is an alternative for those 20% of patients with epilepsy in which the current AEDs show no benefit.

Surgical Treatment of Epilepsy

The success of a surgical treatment for seizure control depends on the definition and extent of the resection of the epileptogenic area ⁶⁶⁻⁶⁹. However, approximately only 30% of patients undergoing extensive pre-surgical investigation will eventually undergo surgery⁷⁰ due to (i) inadequate technology for defining the epileptogenic area, and (ii) epileptogenic area is too large or is located in an eloquent region which prevents surgical intervention. Therefore, to have a cost/effective surgical program for epilepsy, two major lines of research should be carried out: 1) develop new strategies for seizure localization, and 2) improve pre-selection mechanisms for candidates undergoing extensive pre-surgical investigation. It would be important to have a mechanism that can rapidly select suitable surgical candidates for investigation. Localization of the epileptogenic area has evolved over time and relies largely upon current knowledge and the available technology at a given time and site.

The first epilepsy surgery performed by Sir Victor Horsley was guided solely by semiology. Currently, there are several different techniques available for seizure localization including: radio-ligand imaging techniques (SPECT, PET), magnetic resonance techniques (MR imaging, and MR spectroscopy), neuropsychological testing, magnetoencephalography, and video-EEG monitoring. It is difficult to make a non-biased comparison of these different types of tests, as they each provide insight into the different facets of epilepsy. Thus, the definition of the epileptogenic area is a multimodal task and relies on the convergence of

various results to the same location in the brain.

Gloor⁶⁹ proposed a seizure localization approach based on the conceptualization of the epileptogenic area and the epileptogenic lesion. He made three assumptions: 1) in partial seizures, a lesion must exist. 2) if a structural or functional lesion can be demonstrated, the chances of that lesion being the cause of seizures is high, and 3) the area from which seizures originate is likely to overlap or to be in the vicinity of the lesion. In Gloor's words the definition of the epileptogenic area in anatomical and pathophysiological terms is impossible. Although defining a lesion has been simplified in the past decade with the advent of modern neuroimaging techniques, especially MRI, some difficulties remain (*i*) epileptogenic area varies in extent, (*ii*) within the epileptogenic area there are different degrees of seizure induced potential, and (*iii*) the epileptogenic area's properties present dynamic changes in the time domain.

Lüders and Awad⁷¹ proposed a more Cartesian approach and subdivided the epileptogenic area into (*i*) pacemaker (*ii*) lesion, (*iii*) irritative zone, (*iv*) symptomatogenic zone, and (*v*) functional zone. This subdivision is supported by the findings from different complementary examinations and clinical manifestations. The pacemaker corresponds to the area of the brain from which seizures originate. The epileptogenic lesion corresponds to a structural lesion, which can be revealed by MRI in many cases. The irritative zone corresponds to an area of abnormal neuronal firing as defined by EEG. The symptomatogenic zone refers to the areas in the brain responsible for the behavioral manifestation of the seizures. The functional zone corresponds to the impairment of cerebral function related to the epileptogenic process.

Although all of the different examinations play a role in seizure localization, video-

EEG remains the gold standard. Video-EEG monitoring is conducted in hospitals for a period of days or weeks, because this is usually done after drug reduction with the aim of recording seizures. The duration of the monitoring is usually dictated by the number of recorded seizures required. In some patients with no clear localization, an invasive neurophysiological approach (surgical placement of intracranial electrodes) is performed, which increases the overall risk as well as the complexity of the exam. In light of the costs and risks associated with video-EEG, other techniques have been investigated in order to help in seizure localization with the aim of decreasing the duration of monitoring and to avoid invasive recording in some cases.

Impact of MR-based Techniques in Epilepsy

MR imaging

MRI is based on the detection of a signal derived mainly from water. The concentration and mobility of water in various structures presents different relaxation times in a magnetic field. The spatial differences of the relaxation times confer the contrast and anatomic resolution in MRI.

MRI has played an important role in the pre-surgical evaluation of patients with refractory epilepsy because it can display underlying epileptogenic lesions, including HS and CDM^(36,72-79). In the pre-MRI era, many of the epileptogenic lesions, especially HS and CDM, were “invisible” on the available neuroimaging techniques and were only seen in *post-mortem* studies.

Mesial temporal sclerosis is characterized by selective neuronal loss affecting

predominantly areas CA4, CA3, and CA1 of the hippocampus, variable degrees of gliosis, and mossy fiber sprouting. The degree of damage is variable, ranging from severe, which is readily identified on visual inspection of MRI as volume loss, and changes in MR signal ($T_2\uparrow$ and $T_1\downarrow$), to subtle, which is not apparent on qualitative assessment. In fact, because (i) structural volume and (ii) MR signal changes are the MR hallmark of this type of lesion, other sequences such as FLAIR⁸⁰⁻⁸², and post-processing quantitative measurements such as volumetric studies⁸³⁻⁸⁸ and T_2 relaxometry⁸⁹⁻⁹¹, have been applied with very good results. Volumetric studies of mesial temporal structures have been the most common formal evaluation of patients with seizure disorder⁹²⁻⁹³, particularly in those with temporal lobe epilepsy.

The pathological findings of CDM are quite variable and so are their MRI correlates⁹⁴⁻⁹⁶. The type of abnormality can range from extensive which is easily identified, as in lissencephaly, to non evident as in microdysgenesis. The diagnosis is improved when other sequences and qualitative and quantitative techniques are applied. Bastos et al.,⁹⁷⁻⁹⁸ demonstrated that application of curvilinear reconstruction can display subtle forms of CDM, which would otherwise go undetected on high resolution MRI.

Although there is an increased yield of detecting brain lesions when different quantitative MRI analyses are used in conjunction with qualitative MRI inspection (see figure), there is still a small group of patients in whom no abnormality is detected. This group of 'MR-negative' patients remains a challenge for those searching for new imaging alternatives.

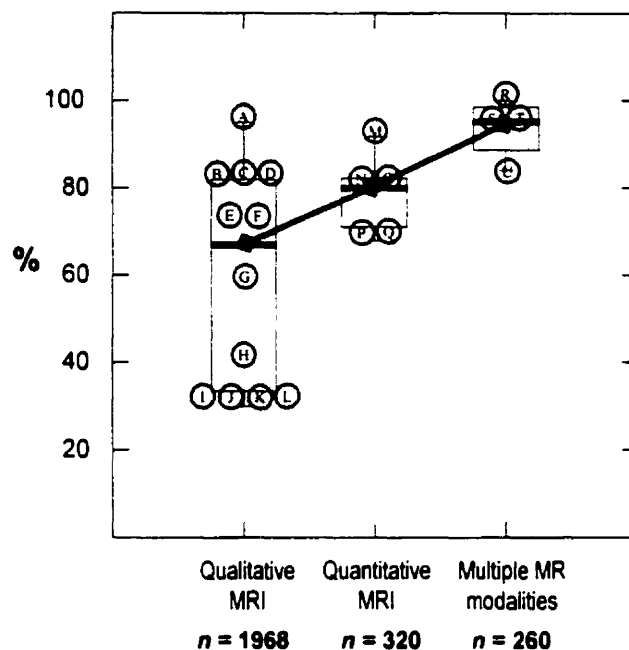


Figure: Box-and-whisker plots of percentage of abnormalities detected by qualitative MRI, quantitative MRI and multiple MR modalities. The detection of abnormalities increases as quantitative analyses are added to qualitative inspection of MRI. The qualitative MRI series comprise mostly patients with refractory partial epilepsy, and the wide range reflects different sequences used, and populations being studied (A= Bronen et al.,⁹⁹ B= Peretti et al.,¹⁰⁰ C= Zentner et al.,¹⁰¹ D= Ryvlin et al.,¹⁰² E= Menzel et al.,¹⁰³ F= Li et al.,⁴⁵ 1995, G= Ferone et al.,¹⁰⁴ H= Wang et al.,¹⁰⁵ I= Kramer et al.,¹⁰⁶ J= Kilpatrick et al.,¹⁰⁷ K= Convers et al.,¹⁰⁸ L= Paterson et al.,¹⁰⁹). Quantitative MRI series comprises in patients with refractory TLE investigated with T₂ relaxometry (M= Namer et al.,¹¹⁰) and MRVol (N= Lawson et al.,¹¹¹ O= Christensen et al.,¹¹² P= Cascino et al.,¹¹³ 1991, Q= Adam et al.,¹¹⁴). Multiple MR modalities series comprises patients with refractory TLE investigated with MRVol plus ¹H-MRSI (R= Cendes et al.,¹¹⁵ 1997, S= Kuzniecky et al.,¹¹⁶ 1998) or MRVol plus T₂ relaxometry (T= Woermann et al.,⁹¹ 1998, U= Van Paesschen et al.,¹¹⁷ 1997).

MR spectroscopy

Brain proton MR spectroscopy (¹H-MRS) permits the quantification of cerebral metabolites^{118;119}. In contrast to MRI, ¹H-MRS measures metabolite concentrations 10,000

times less than the concentration of water. The metabolites present distinct resonance frequencies in a magnetic field that allows differentiation among them.

In brain ¹H-MRS, the most intense signal is visible at 2.02 ppm and corresponds to N-acetyl groups, mainly N-acetyl aspartate (NAA) ^{118;119}. NAA is synthesized in the brain mitochondria from acetyl-CoA and aspartate by the enzyme L-aspartate N-acetyltransferase¹²⁰⁻¹²³. Monoclonal immunocytochemistry has shown that NAA is found exclusively in neurons and neuronal processes of the mature brain^{124;125}. Urenjak et al.¹²⁶ using high field spectrometer on extracts of cultured cerebellar granule neurons, cortical astrocytes, oligodendrocyte-type 2 astrocyte (O-2A) progenitor cells, oligodendrocytes, and meningeal cells, found a large amount of NAA in neurons, but also in O-2A progenitors. This may pose a problem in assessing NAA in infants but is not an issue in adults.

The precise role of NAA is unknown, and it has been implicated in many processes of the nervous system: *(i)* regulation of neuronal protein synthesis¹²⁷, *(ii)* fatty acid synthesis¹²⁸⁻¹³¹, *(iii)* the metabolism of several neurotransmitters such as N-acetyl-aspartyl-glutamate^{123;132} and *(iv)* brain osmoregulation¹³³.

NAA undergoes changes during brain development and maturation. Kato et al.,¹³⁴ assessed the developmental changes in NAA in human fetal and child brains using ¹H-MRS. They found that NAA was detected in the cerebral cortex and white matter of fetuses at 16 weeks gestation. NAA increased gradually from 24 weeks gestation and remarkably from 40 weeks gestation to 1 year of age. Kreis et al.,¹³⁵ studied 77 subjects between 34.5 and 926 weeks gestational age and demonstrated that NAA gradually reaches adult values over the first two years of life. Saunders et al.,¹³⁶ examined the effect of aging on brain metabolite concentrations using short echo single voxel proton spectroscopy in 30 healthy volunteers

ranging in age from 24-89 years. They found no significant trend in changes of concentrations of NAA, total creatine, total choline or myo-inositol with age.

Since the NAA signal in the mature brain derives only from the neuronal pool, areas of decreased NAA signal intensity are interpreted as either (i) neuronal loss and/or (ii) dysfunction. The assumption of neuronal loss is supported by both experimental¹³⁷⁻¹⁴⁴ and clinical observations¹⁴⁵⁻¹⁵⁰. For instance Strauss et al.¹³⁸ showed that the NAA measured by ¹H-MRS was decreased in areas of neuronal loss induced by quinolinic acid, an excitotoxic agent. Similarly, Ebisu et al.¹⁴¹, Najm et al.^{139;140} and Tokumitsu et al.¹⁴² showed that neuronal loss caused by kainate induced status epilepticus in rat brains correlates well with the reduction of NAA signal detected on ¹H-MRS.

The assumption of neuronal dysfunction is supported by *in vivo*¹⁵¹⁻¹⁵⁴ and *in vitro*^{144;155;156} studies showing the ability of the NAA signal to recover. De Stefano et al.¹⁵¹ reported on a series of patients with acute brain injury, multiple sclerosis or mitochondrial encephalopathy, who had significant NAA decrease and lactate increase during the acute phase of disease with NAA normalization paralleling the clinical recovery. Balm et al.¹⁵³ performed ¹H-MRSI in 16 patients with symptomatic carotid artery stenosis before and after endarterectomy. They found that metabolic changes seen pre-operatively (↓NAA, ↑lactate) normalized four days after endarterectomy. Matthews et al.¹⁵⁵ showed that neurons under stress conditions *in vitro* express less NAA and this reverses with optimization of the culture media, reflecting the survival of a population of viable neurons. Bates et al.¹⁵⁶ showed that inhibition of mitochondrial oxygen consumption and ATP synthesis also inhibited NAA production, suggesting that impaired neuronal mitochondria function, if not reversed, may result in irreversible neuronal death.

Creatine plus phosphocreatine containing compounds (Cr) are seen at 3.02 ppm. Cr participates in the energy metabolism cycle to generate ATP. In vitro, glial cells present higher Cr concentration than neurons. In normal and some pathological conditions, Cr is homogeneously distributed throughout the brain and used as a reference peak. In epilepsy, Cr has been shown to undergo minor changes¹⁵⁷⁻¹⁶¹. Petroff et al.¹⁶⁰ used high field spectrometry to analyze temporal lobe tissue excised from patients with epilepsy. They found that the Cr concentration in epileptic brains was not different from normal control values.

Choline containing compounds (Cho) are seen at 3.24 ppm. Cho is involved in membrane synthesis and degradation. A decrease and increase in the Cho signal have been observed in different disease. Acute demyelination lead to increase of Cho signal, possibly reflecting myelin breakdown with increase in free mobile Cho pool¹⁶².

Lactate is not usually detected in normal brains. An increased lactate signal seen at 1.33 ppm reflects abnormal energy metabolism and has been seen in several conditions, which include stroke¹⁴⁸, mitochondrial disease¹⁶³⁻¹⁶⁶, and brain tumors¹⁶⁷.

Using short echo times, editing sequences, and high field strengths, other signals can be detected, such as GABA¹⁶⁸ and glutamate/glutamine¹⁶⁹.

In epilepsy, ¹H-MRS has often been used for presurgical investigation, mainly for lateralization of TLE. Both single and multivoxel studies have proven to be equally useful for TLE lateralization. Table 1 and 2 summarize these findings.

Table 1: Single voxel ¹H-MRS studies of TLE

Authors	Patients n	Concordant Lateralization	Discordant Lateralization
Connelly et al., 1994 ¹⁵⁸	25	15 (60%)	3 (12%)
Breiter et al., 1994 ¹⁷⁰	7	7 (100%)	0
Cross et al., 1996 ¹⁵⁷	20	11 (55%)	0
Achten et al., 1997 ¹⁷¹	21	17 (81%)	0
Duc et al., 1998 ¹⁷²	11	11 (100%)	0
Total	84	61 (72%)	3 (3%)

Table 2: Multivoxel ¹H-MRS studies of TLE

Authors	Patients n	Concordant Lateralization	Discordant Lateralization
Hugg et al., 1993 ¹⁷³	8	8 (100%)	0
Vainio et al., 1994 ¹⁷⁴	7	7 (100%)	0
Cendes et al., 1994 ¹⁷⁵	10	8 (80%)	0
Ng et al., 1994 ¹⁷⁶	25	21 (84%)	2 (8%)
Hetherington et al., 1995 ¹⁷⁷	10	10 (100%)	0
Ende et al., 1997 ¹⁷⁸	16	16 (100%)	0
Cendes et al., 1997 ¹¹⁵	100	84 (84%)	2 (2%)
Kuzniecky et al., 1998 ¹¹⁶	30	29 (97%)	1 (3%)
Total	229	183 (80%)	5 (2%)

MRVol and ¹H-MRSI of temporal lobes are complementary examinations and have shown good agreement with results from prolonged video-EEG^{115,116}. The results of both

MRVol and ¹H-MRSI of temporal lobes are usually expressed in terms of lateralization, *i.e.* left, right, or bilateral. This kind of approach is simple and useful, however, it is possible that a more sophisticated way of analyzing these data sets can bring an additional information.

The neuronal metabolic dysfunction within the volume of interest detected by ¹H-MRSI in patients with partial seizure tend to be more diffuse than EEG localization and MRI. Concomitant contralateral temporal lobe NAA reduction can be seen in 18% to 50% of patients with unilateral TLE^{115;157;176;178}. Interestingly, in a pathological series reported by Margerison and Corsellis¹⁷⁹, approximately 50% of patients with TLE also had evidence of bilateral hippocampal sclerosis. The bilateral NAA reduction may represent bilateral disease in some patients. On the other hand, the NAA reduction may reflect secondary neuronal dysfunction due to the primary epileptogenic area. It has been observed that a lesion in one area of the brain can cause dysfunction in distant, interconnected areas. Fulham et al.¹⁸⁰ demonstrated that NAA is reduced in cases of trans-synaptic cerebellar diaschisis. Furthermore, Rango et al.,¹⁸¹ performed an elegant experiment wherein axonal lesions were induced by stretch injury in the guinea pig right optic nerve (95-99% crossed fibers). The trans-synaptic concentration of NAA, Cr, and the NAA/Cr ratio in the lateral geniculate bodies (LGB) and superior colliculi (SC) sample extracts were measured 72 hours later using high resolution ¹H-MRS. In the left LGB/SC, which is where the right optic nerve fibers project, reductions of NAA and NAA/Cr were found whereas Cr levels were normal. NAA, NAA/Cr, and Cr values were all normal in the right LGB/SC. Histology and electron microscopy findings revealed no abnormalities. At day seven, the left LGB/SC NAA and NAA/Cr values were in the normal range. In epilepsy, there are a number of factors assumed to cause secondary neuronal dysfunction, these include (i) clinical seizures, (ii) subclinical epileptic activity, and (iii) epileptic lesion.

It remains unclear whether the NAA decreases observed at the epileptogenic focus also extend to other non-homologous areas of the brain. Bertolino et al.,¹⁸² performed an experiment, in which they assessed the repercussions of a focal brain lesion occurring early in development throughout the developing brain. They induced mesial temporo-limbic lesions in 12 monkeys, six had a lesion within three weeks of birth and the remaining six at approximately five years of age. ¹H-MRSI of the prefrontal cortex of these monkeys were acquired and they found significant bilateral reductions of NAA relative signals exclusively in the prefrontal cortex of the neonatal lesion group in comparison with control and adult lesion groups.

In epilepsy, the spatial relationship between the NAA decrease and the underlying mechanisms causing neuronal damage is unclear. The above mentioned studies suggest that the neuronal damage as measured by NAA can extend to areas at a distance from the lesion, and that the timing of the insult may contribute to the widespread neuronal damage. It remains to be seen if this is relevant for epileptic patients.

The NAA signal is used as a parameter of neuronal integrity. The side of maximum NAA reduction often coincides with the side of EEG abnormality. Interictal spikes are intermittent, transitory, electrical phenomenon which reflect underlying, synchronized, neuronal depolarization caused by an imbalance in the excitatory/inhibitory neuronal circuitry. The relationship between spiking frequency and underlying neuronal function and epileptogenic state is unclear. Gotman^{183;184} has demonstrated that spikes do not appear to modulate ictal seizure onsets. On the other hand, the spiking frequency increases after seizures^{185;186}, which suggests the possibility of neuronal damage. Peeling and Sutherland¹⁸⁷ used high-resolution ¹H-MRS to determine the concentrations of several metabolites (lactate,

alanine, NAA, gamma-aminobutyrate, glutamate, aspartate, creatine, choline, taurine, inositol, and succinate) in tissue from patients undergoing surgical treatment for intractable epilepsy. They correlated the metabolite profiles with the results of histopathological analysis of the excised tissue and the spike activity. Surprisingly, they found no differences in metabolite levels for tissue from actively spiking or nonspiking neocortical sites.

Magnetization transfer

Traditional MRI of brain produces images whose intensity reflects the distribution of water. Hydrogen nuclei associated with various semi-solid (macro-molecular) components have an extremely short T₂ (<~100 μs) and are not directly detectable on MRI scanners since minimum echo times are typically 2-orders of magnitude longer. However, interaction between semi-solid and bulk water protons results in a continuous exchange of magnetization referred to as cross-relaxation or magnetization transfer^{188,189}. Magnetization transfer ratio (MTR) imaging detects this exchange by selectively saturating the semi-solid magnetization pool and measuring the resulting decrease in the water signal due to transfer of this saturation in regions undergoing exchange¹⁹⁰⁻¹⁹⁴. The biological meaning of magnetization transfer is still unclear, though abnormal MTR has been shown to correlate with low NAA in other pathologies¹⁹⁵. Abnormal MTR has been demonstrated in the TLs of patients with TLE², possibly reflecting a disruption of structural integrity. Magnetization transfer imaging could potentially be applied in the investigation of patients with seizure disorders, particularly where the conventional MRI shows no abnormality.

MR findings and surgical outcome

Once the epileptogenic area is identified and epilepsy surgery is indicated, it is

important to determine and to inform patients of the potential risk/benefit of the procedure along with the anticipated post-operative results. It is apparent that different types of underlying pathology carry distinct surgical outcomes.

Hippocampal sclerosis, CDM, tumors, vascular malformations, and traumatic injuries are the most common types of lesions encountered in patients with refractory epilepsy^{39;45;196}. Surgical results in patients with CDM appear to depend on the type and extent of the underlying CDM^{31;96;197-199}. A poorer surgical outcome is often attributed to more widespread malformations that usually extend beyond the lesion defined on MRI. Palmieri et al.^{198;199} have proposed that both MRI-visible lesion and actively spiking tissue should be removed in order to achieve satisfactory surgical results. They reasoned that actively spiking tissue might reflect microdysgenesis, which is invisible on MR imaging. Eriksson et al.¹⁹⁶ reviewed histopathological and clinical findings in 139 children and adults with epilepsy who had surgical treatment. In their series, microdysgenesis had the worst surgical results, only 40% of patients became seizure free.

Hippocampal sclerosis is the most common type of pathology seen in excised surgical material of patients with refractory TLE. The surgical approach is usually anterior temporal lobectomy or selective amygdalo-hippocampectomy. Most centers attain total seizure control in 2/3 of cases²⁰⁰.

Results derived from volumetric studies have predictive value for surgical outcome²⁰¹⁻²⁰⁵. For example, Arruda et al.²⁰¹ studied 74 TLE patients treated surgically. They divided the patients into three groups according to the volumetric findings: unilateral, bilateral, or no atrophy of the amygdala-hippocampal formation on quantitative MRI. Outcome was assessed according to Engel's classification at least one year after surgery. Ninety-three percent of the

patients with unilateral atrophy, 61.7% of those with bilateral atrophy, and 50% of the group with no significant atrophy of the mesial temporal structures had excellent results (Engel's class I-II).

¹H-MRSI has become useful in providing prognostic information for other conditions affecting the central nervous system²⁰⁶⁻²⁰⁸. Friedman et al.²⁰⁸ showed that NAA measured with ¹H-MRS soon after a traumatic brain injury predicted overall neuropsychological performance 6 months later. ¹H-MRS has a higher sensitivity to neuronal damage than MRI and can provide additional diagnostic and prognostic information on those patients with pathologies associated with poorer prognosis, *i.e.*, patients with CDM, bilateral hippocampal atrophy or no atrophy.

Neuronal Damage and Recovery in Epilepsy

Neuronal damage: cause or consequence of seizures

Hippocampal sclerosis is found in about 50% to 75% of the surgical specimens obtained from patients with refractory TLE. It is debatable whether the neuronal loss seen in HS is the cause or the consequence of long-standing seizures. Studies using an experimental model of partial epilepsy or based on clinical observations of *post-mortem* and surgical materials have been carried out to assess this question.

Cavazos et al.²⁰⁹ used quantitative stereological methods to determine the distribution and time course of neuronal loss induced by electrical kindling in rats. Three groups were analyzed: 3, 30, and 150 kindled generalized tonic-clonic seizures in hippocampal, limbic, and neocortical pathways. Neuronal loss was observed in the hilus of the dentate gyrus and CA1

after three generalized tonic-clonic seizures, and the neuronal loss increased in these areas after 150 seizures. Neuronal loss was also observed in the CA3, the entorhinal cortex, and the rostral endopyriform nucleus after 30 seizures and was detected in the granule cell layer and CA2 after 150 seizures.

On the other hand, Bertram and Lothman²¹⁰ studied the effect of intermittent kindled seizures on the dentate gyrus. They compared 3 groups of rats: (1) those that had experienced 1500 intermittent kindled seizures, (2) those that had experienced a single episode of limbic status epilepticus and (3) control rats. The results showed that absolute neuronal counts were decreased in the hilus after status epilepticus but no change followed kindling. Both groups, however, had decreased neuronal densities in the hilus when compared to controls, but, the decreased density after status epilepticus was secondary to neuronal loss, while that which followed kindling was the result of the expansion of the hilar neuropil without a change in the number of neurons.

Liu et al.²¹¹ demonstrated that stereological estimates of neurons in regions CA1, CA3 and the dentate granule cell layer in the dorsal hippocampus showed a dose-dependent neuronal loss in the CA3 and CA1 subregions of the pilocarpine rat model of epilepsy. No progressive neuronal loss was observed in these regions studied after 3, 6 and 12 weeks of spontaneous recurrent seizures.

Using human autopsy material, Mouritzen-Dam²¹² demonstrated that frequent generalized tonic-clonic seizures (>2 seizures per month) were positively correlated with significant reductions in the number of neurons in fields H₁ and H_{1,2} when compared with patients who had suffered only a few such seizures (<6 per year). This neuronal loss increased throughout life with the duration of the disorder.

Meencke and Veith²¹³ studied 650 autopsied brains of epilepsy patients and found HS in 30% of cases. They found that (i) patients with early manifestation of epilepsy (<1 year) more frequently showed HS than those with late onset epilepsy (>21 year), (ii) the incidence of HS was not correlated with the duration of epilepsy, and (iii) there was no correlation between incidence of HS and frequency of generalized tonic-clonic seizures.

Mathern et al.,²¹⁴⁻²¹⁹ have taken a more moderate stance, suggesting that hippocampal sclerosis results from an “initiating precipitating event” followed by progressive damage.

Secondary neuronal damage due to seizures has been investigated using new MR-based techniques that allow the *in vivo* assessment of the structural and functional integrity of epileptogenic lesions. Cendes et al.²²⁰ performed volumetric studies in 70 patients with epilepsy: 50 had refractory TLE, 10 had extra-TLE, and 10 had generalized epilepsy. They found no significant correlation amongst duration, frequency and life time estimated seizures with degree of hippocampal and amygdala atrophy.

In contrast, Kalviainen et al.²²¹ performed volumetric studies and T₂ relaxometry in 3 groups of patients with TLE (18 newly diagnosed, 14 well controlled and 32 drug resistant chronic epilepsy) and found a significant difference in seizure severity and degree of hippocampal atrophy among the groups. In addition, they observed that estimated life-time seizure burden had a significant negative correlation with hippocampal atrophy and a positive correlation with T₂ signal.

Theodore et al.²²² performed volumetric MRI studies on the hippocampal formation of 35 TLE patients. Using a multivariate analysis, the effect of duration, but not age at onset or scan, was found to be significantly associated with hippocampal atrophy. Patients with a

history of febrile seizures did not have earlier epilepsy onset or longer duration.

Van Paesschen et al.²²³ used MRI including hippocampal quantitation to study 63 adult patients with newly diagnosed partial seizures. They found that 76% of patients had normal MRI findings, 10% had hippocampal sclerosis, and 14% had MRI abnormalities other than hippocampal sclerosis. Patients with hippocampal sclerosis had a worse prognosis than patients with other MRI findings with respect to seizures.

These studies are inconclusive as to the presence or absence of neuronal loss as a consequence of seizures. Future studies are required to settle this issue.

Neuronal recovery: relevance of seizure control

Seizures have been shown to induce changes in gene expression, cellular morphology and function²²⁴. It could be assumed that blocking the seizures would allow dysfunctional neurons to recover. Evidence from PET²²⁵⁻²³⁰, ¹H-MRS^{161,231-233}, and neuropsychological testing²³⁴⁻²³⁹ support this assumption. For instance, Hajek et al.²²⁸ studied 25 patients with interictal 18F-fluorodeoxyglucose (18F-FDG) PET, a marker of glucose metabolism, before and after selective surgery for TLE. They divided the patients into three groups: (i) patients with neocortical TLE (n = 5), (ii) patients with mesiobasal limbic TLE associated with mesial gliosis (n = 14), and (iii) patients with mesiobasal limbic TLE and small mesial tumors (n = 6). Postoperatively, patients in group (ii) and five of six patients in group (iii) were seizure-free; the remaining sixth patient had one generalized seizure. Patients with neocortical TLE had more than a 90% reduction of seizure frequency. The main postoperative metabolic findings were as follows: (1) marked increase of regional cerebral metabolic rate of glucose (rCMRglu), both in the ipsilateral and, significantly, in the contralateral hemisphere in group (ii), patients with

mesial gliosis; (2) decrease of rCMRglu values in the contralateral mesiobasal temporal lobe cortex in all patient groups, and (3) a trend toward the normalization of rCMRglu values in the ipsilateral temporal neocortex 12 months after surgery in patients with mesial temporal sclerosis.

Savic et al.,²²⁹ using PET measurements with [11C]flumazenil, demonstrated the normalization of the benzodiazepine receptor density in four patients with TLE one year after complete seizure control following surgical removal of the epileptogenic area. Similarly, NAA has been shown to normalize after successful surgical treatment in the temporal lobe ipsi-^{161,231-233} and contralateral¹⁶¹ to the side of resection. The NAA recovery has been observed to occur as early as two months postoperatively²³³.

Neuropsychological series showed a similar trend. Jokeit and Ebner²³⁴ measured full scale intelligence quotient (FSIQ) in 127 TLE patients preoperatively and 6 months postoperatively. Retesting 6 months after surgery showed that seizure free patients (n=85) had a significant improvement in their FSIQ.

The improvement observed in different domains of brain function as shown in PET, ¹H-MRS, and neuropsychological series, resulted from surgical treatment and the improvement of these parameters with drug therapy is less evident.

Selwa et al.²³⁵ performed serial cognitive testing in TLE patients treated either with pharmacological or surgical therapies. Cognitive testing was repeated at intervals ranging from 1 to 8 years in 47 adult TLE patients. The results showed that the nonsurgical group showed no significant change in intellect or memory compared to controls, and variance over time was similar to test-retest norms in healthy controls. In the surgical group, however, only the

patients who had undergone surgery on the right side improved significantly in FSIQ and tended to improve in logical memory on postoperative testing.

Preliminary results from the National Institute of Health-USA²⁴⁰ in children with newly diagnosed epilepsy showed follow-up FDG-PET normalization one year later in two seizure-free patients, while in those with poor seizure control, deterioration or no change was observed on the follow-up FDG-PET exam. Whether the glucose metabolism disturbance is a marker of poor seizure control is unclear, since it is known that FDG-PET results are influenced by peri-scanning seizures²⁴¹.

Mendes-Ribeiro et al.²⁴² reported temporal lobe ¹H-MRS findings in 10 seizure free TLE patients treated with AEDs. Two patients had significant NAA/Cr reduction despite a long period of seizure freedom (3 years) using AEDs. Interestingly, these two patients had a past history of poor seizure control.

Holopainen et al.²⁴³ performed ¹H-MRS of mesial temporal regions, in two groups of children with epilepsy; in children with a history of complex febrile convulsions (CFCs) (n = 7; mean age 7.1 years) and in children without any history of CFCs, (n = 6; mean age 7.6 years). In both groups, NAA/(Cho + Cr), NAA/Cho, and NAA/Cr were significantly decreased ipsilaterally to the seizure focus when compared with the control group, but no significant differences were detected between the epilepsy groups. In this study metabolite abnormalities in the mesial temporal region were detected in both children with intractable and with AED controlled epilepsy. Unlike FDG-PET, NAA/Cr appears not to be influenced by peri-scanning seizures²⁴⁴. In addition, NAA is a more specific marker of neuronal integrity.

The temporal profile of neuronal damage and recovery is unclear. Studying these

processes would shed light on the dynamic changes caused by the epileptogenic lesion and consequently provide guidance in the clinical management of patients with epilepsy.

CHAPTER II

Anatomo-functional relationships in epileptic lesions

We do not know the precise the relationship between the lesions seen on MRI (cortical developmental malformations) and functional measures (NAA reduction and EEG spikes). MRI can demonstrate cortical developmental malformations, but the neuronal metabolic profile of these types of lesions is unclear. The side of NAA reduction often coincides with the side of epileptic focus, but the anatomical localization of these two variables is less clear. The relationship between spikes and neuronal metabolic dysfunction is also unknown. Thus we undertook the following studies to clarify of these issues.

Paper 1: Neuronal metabolic dysfunction in patients with cortical developmental malformations: a proton MR spectroscopic imaging study.

Li LM, Cendes F, Bastos AC, Andermann F, Dubeau F, Arnold DL.
Neurology 1998;50:755-759.

Lippincott Williams & Wilkins

SUMMARY

Background: Cortical developmental malformations are best diagnosed by MR imaging and are often the cause of refractory epilepsy. The extent of neuronal metabolic dysfunction in cortical developmental malformations is unclear.

Objective: To assess the neuronal metabolic profile of patients with cortical developmental malformations and refractory epilepsy.

Patients/Methods: We studied 23 patients with cortical developmental malformations and refractory epilepsy using proton MR spectroscopic imaging. Mean age was 28 years (range, 9 - 47 years). The lesions examined were: focal cortical dysplasia (5), heterotopia (4 band, 6 periventricular, 2 subcortical), polymicrogyria (3), tuberous sclerosis (2), and polymicrogyria and periventricular nodular heterotopia (1). We measured the relative signal intensity of N-acetylaspartate/creatine (NAA/Cr) in the lesion, in the peri-lesional region, and remote region from the visible lesion. The values were compared to those from similar brain regions of 25 normal control subjects.

Results: The mean NAA/Cr z-score values for the 23 patients were: lesion = -2.20 (Standard error [SE] = 0.32, N [number of patients] = 21), peri-lesional region = -1.01 (SE = 0.38, N = 15), and distant region = -0.03 (SE = 0.34, N = 18), with $p < 0.0002$. Despite the presence of a large number of neurons, heterotopia showed a relative decrease of NAA in some patients, suggesting that the neurons present were dysfunctional.

Conclusion: The maximal NAA/Cr decrease, metabolic dysfunction, co-localized to the structural malformation as defined by MRI and extended to normal-appearing regions adjacent to the visible lesion.

INTRODUCTION

Brain development is a complex process regulated by many factors. After neural induction, neuroblasts proliferate and differentiate into neural or glial cells. From the germinal plate neuroblasts migrate to their final destination. Once the individual cells established their identities, they extend their axons and establish synaptic connections. Disruption at any of these critical periods of formation of the nervous system leads to different types of cortical developmental malformations (CDM). These may be gross abnormality such as lissencephaly or microscopic and invisible on conventional MRI. The appearance of the abnormal cells also varies depending on the timing of the insult.

The clinical presentation of CDM is variable. CDMs have been recognized as a common cause of seizures in patients with medically refractory epilepsy being evaluated in tertiary centers^{30,44,45,72}. Magnetic resonance imaging (MRI) has played an important role in presurgical evaluation of these patients in helping to define the structural epileptogenic abnormalities. Surgical results in these patients depend on the type and extent of the underlying CDM^{31,197}. Poorer surgical outcome is often explained by the fact that the malformations are usually widespread, and often extend beyond the lesion defined on MRI^{44,245,246}.

Magnetic resonance spectroscopy of brain enables non-invasive quantification of metabolites *in vivo*. The most intense signal in the proton MR spectrum of brain originates from the N-acetyl groups, mainly N-acetylaspartate (NAA). Less intense signals arise from creatine plus phosphocreatine (Cr) and choline-containing compounds (Cho). NAA is localized exclusively in neurons and neuronal processes in the mature brain^{124,125,160}, and can be used as neuronal marker^{175,247}. Decreased NAA is observed in areas of neuronal loss or

dysfunction^{160;175;247}. Cr, which may be more concentrated in glia than neurons¹⁶⁰, is relatively homogeneously distributed in normal brain and can be used as internal standard in this circumstance.

This study was designed to assess whether proton magnetic resonance spectroscopic imaging (MRSI) measurements of NAA could detect abnormalities associated with neuronal lesion in CDMs, whether the abnormalities extend outside the lesion visible on MRI, and whether different types of CDM exhibit different abnormalities in the proton spectrum.

PATIENTS AND METHODS

We studied 23 patients (10 women) with different types of CDM. All 23 patients had medically refractory epilepsy. The mean age at study was 28 years (range, 9 - 47 years).

All patients underwent detailed evaluation including prolonged video-EEG monitoring to record seizures. The diagnosis of CDM was based on MR imaging findings. Three patients had histopathological confirmation. The patients studied represent most of the patients admitted to the epilepsy service with CDM over a two year period. A few patients were not included for logistic reasons. These occurred at random and patients who were included represent a reasonable sample of patients with CDMs and refractory epilepsy seen in this institution, and others⁴⁴.

Diagnostic MRI scans were acquired using a 1.5 T scanner, combined imaging and spectroscopic system (ACS III Philips Medical Systems, Best, The Netherlands). We acquired sagittal and coronal T1-weighted (TR 550, TE 19 ms) images, followed by transverse proton density (TR 2000, TE 20 ms) and T2-weighted (TR 2100, TE 20, 78 ms) images. T1-weighted gradient-echo volume acquisition of the whole brain (TR 18 ms, TE 10ms, 30° angle, 1 mm

thick contiguous slice) was acquired for multiplanar reconstruction.

Proton MRSI studies were performed in a separate examination. After scout images in axial and sagittal planes, a multislice transverse spin-echo MRI (TR 2000, TE 30) was obtained. A large volume of interest (VOI), including the lesion, was defined for selective excitation. A water suppressed proton MRSI was acquired from the VOI (TR 2000 ms, TE 272 ms, 250x250 mm FOV, 32x32 phase-encoding steps), followed by a proton MRSI without water suppression (TR 850 ms, TE 272 ms, 250x250 mm FOV, 16x16 phase-encoding steps). Post-processing included zero-filling the water unsuppressed MRSI to obtain 32x32 profiles, followed by application of mild Gaussian k -space filter and an inverse 2D Fourier transformation to both water suppressed and unsuppressed MRSI^{248;249}. Residual water signal was removed by applying the linear HSVD fitting method²⁴⁹. Resonance intensities in individual spectra were determined by integration of peak areas using locally developed software.

The definition of the region (figure 1A - B) corresponding to lesion, peri-lesional tissue and tissue remote from the lesion were based on MR imaging and done by one of us (ACB) who was unaware of the MRSI results. The peri-lesional region was defined as normal-appearing tissue surrounding MRI visible lesion. Remote regions within the volume of interest (VOI) were defined as being more than 2 voxel (approximately 2 cm), at least, away from the MRI visible lesion, and appearing normal on MRI. Values for NAA, Cho, Cr, were determined by averaging values from spectra in these three regions.

The size of the VOI for spectroscopy was 75mm to 100mm in the left-right axis, 75mm to 105mm in the antero-posterior axis, and 18mm to 20mm in thickness. The size of the individual voxel after post-processing was approximately 1.2 cm x 1.2 cm x 1.8-2 cm

(thickness of the box). The number of voxels averaged for each of the three regions (lesion, peri-lesion, and distant from the lesion) ranged from 2 to 15.

Z-scores (standardized scores that express the original raw values in terms of standard deviations [SD] from the mean of the normal control group) were used because they allowed uniform comparison of the degree of reduction of NAA/Cr values in the lesion, the perilesional region, and regions remote from the lesion. Z-scores were obtained for each individual patient by subtracting NAA/Cr values from the mean NAA/Cr value obtained from a similar region of a group of 25 age-matched normal controls, and dividing the result by the normal controls' SD for that region. Analysis of variance (ANOVA) was performed to assess statistical differences among the z-scores of NAA/Cr ratio from these three regions (lesion, peri-lesion, and remote from the lesion).

In six patients with unilateral lesion, we also assessed the percentage differences of NAA, Cr and Cho between the lesion and contralateral homologous regions.

The objectives of this study were explained to all patients and informed consent obtained.

RESULTS

The CDM studied were: focal cortical dysplasia in 5 patients, heterotopia in 12 (4 band, 6 bilateral periventricular, 2 unilateral subcortical), bilateral perisylvian polymicrogyria in 3, tuberous sclerosis in 2, and unilateral perisylvian polymicrogyria plus bilateral periventricular nodular heterotopia in 1. Seventeen of the 23 patients had bilateral structural abnormalities.

We obtained spectroscopic information from the three regions (lesion, peri-lesion, and remote regions) in 12 patients, from at least two of these regions in 7 patients, and from only

one region in 4 patients (table 1).

Table 1: NAA/Cr values converted into z-scores for 23 patients with cortical developmental malformations

Pt/sex/age (yrs)	Type of CDM	Lesion	Peri-lesion	Remote from the lesion
1/f/38	FCD	-	-0.95	-0.19
2/m/22	FCD	-4.31	-1.91	-1.23
3/m/30	FCD	-1.73	-0.72	-1.39
4/f/19	FCD	-2.15	0.02	-0.03
5/m/29	FCD	-4.57	-	-
6/f/31	Ht-band	-4.13	-	-
7/m/9	Ht-band	-1.20	-	-
8/f/11	Ht-band	-0.42	-0.63	-
9/m/11	Ht-band	-2.48	-	1.65
10/f/45	Ht-PNH	-4.39	-4.35	-2.10
11/f/23	Ht-PNH	-4.68	-2.58	-
12/m/25	Ht-PNH	-3.46	-1.96	-1.39
13/f/39	Ht-PNH	-1.62	0.04	-1.01
14/f/36	Ht-PNH	0.75	-	0.54
15/m/24	Ht-PNH	-0.98	0.67	1.54
16/m/16	Ht-sub	-3.33	-3.41	0.58
17/m/23	Ht-sub	-1.57	-	0.84
18/m/34	PMG	-1.25	0.56	1.73
19/m/33	PMG	-0.72	-0.48	-0.07
20/f/20	PMG	-0.39	1.22	-0.52
21/m/30	PMG+PNH	-1.03	-0.67	1.10
22/f/47	TS	-	-	-1.433
23/m/43	TS	-2.56	-	0.92
Mean●	-	-2.20	-1.01	-0.03

● = Analysis of variance with $p < 0.0002$

FCD = focal cortical dysplasia. Ht = heterotopia. PNH = periventricular nodular heterotopia. sub = subcortical. PMG = polymicrogyria. TS = tuberous sclerosis.

The mean NAA/Cr Z-scores values for the 23 patients were:

- lesion = -2.20 (Standard error [SE] = 0.32, N [number of patients] = 21),
- peri-lesion = -1.01 (SE = 0.38, N = 15),
- remote from the lesion = -0.03 (SE = 0.34, N = 18).

There was significant difference among these regions with $p < 0.0002$ (ANOVA) (see table 1).

The mean NAA/Cr Z-scores values for patients with focal cortical dysplasia were:

- lesion = -3.19 (SE = 0.52, N = 4),
- peri-lesion = -0.89 (SE = 0.52, N = 4),
- remote from the lesion = -0.71 (SE = 0.52, N = 4)

There was significant difference among these three regions with $p < 0.02$ (ANOVA).

The mean Z-scores values for patients with polymicrogyria were:

- lesion = -0.85 (SE = 0.41, N = 4),
- peri-lesion = 0.15 (SE = 0.41, N = 4),
- remote from the lesion = 0.56 (SE = 0.41, N = 4)

There was no significant difference among these three regions with $p > 0.09$ (ANOVA).

The mean Z-scores values for patients with heterotopia were:

- lesion = -2.07 (SE = 0.49, N = 12),
- peri-lesion = -1.49 (SE = 0.61, N = 7),
- remote from the lesion = 0.08 (SE = 0.57, N = 8)

There was significant difference among these three regions with $p < 0.02$ (ANOVA).

In unilateral CDM, comparison between ratios of NAA in the lesion/NAA in contralateral homologous region and the mean controls' NAA ipsilateral to patient's lesion side/mean controls' NAA in the contralateral hemisphere showed relative reduction of NAA resonance intensity of 5% to 51% (mean = -21%, median = -11%, SD = 16) in the lesion. We used the same method of comparison for Cr and Cho. Cr showed a mean reduction of 1% (median = -3%, SD = 25, range -37% to 27%). Cho showed a mean increase of 12% (median = 6%, SD = 51, range from -49% to 100%). Increase in Cho were mainly observed in FCD.

The interictal EEG abnormalities were localized in 6/23 patients, regional in 7/23, multifocal or generalized in 8/23, and silent in 2/23. We observed very active interictal EEG activity, characterized by frequent runs of poly-spikes, in ten patients (table 1, patients 1, 2, 3, 4, 6, 8, 9, 16, 17, and 20). There was no relationship between the extent and degree of active interictal spiking and NAA/Cr ratio values.

DISCUSSION

We found relatively decreased NAA/Cr signal intensity in some types of CDM suggesting abnormal neuronal metabolism in these malformations. The relative decreased NAA signal intensity, when present, was maximal in the lesion, decayed in areas surrounding

it, and was less marked or absent in areas far from the lesion (figure 1C).

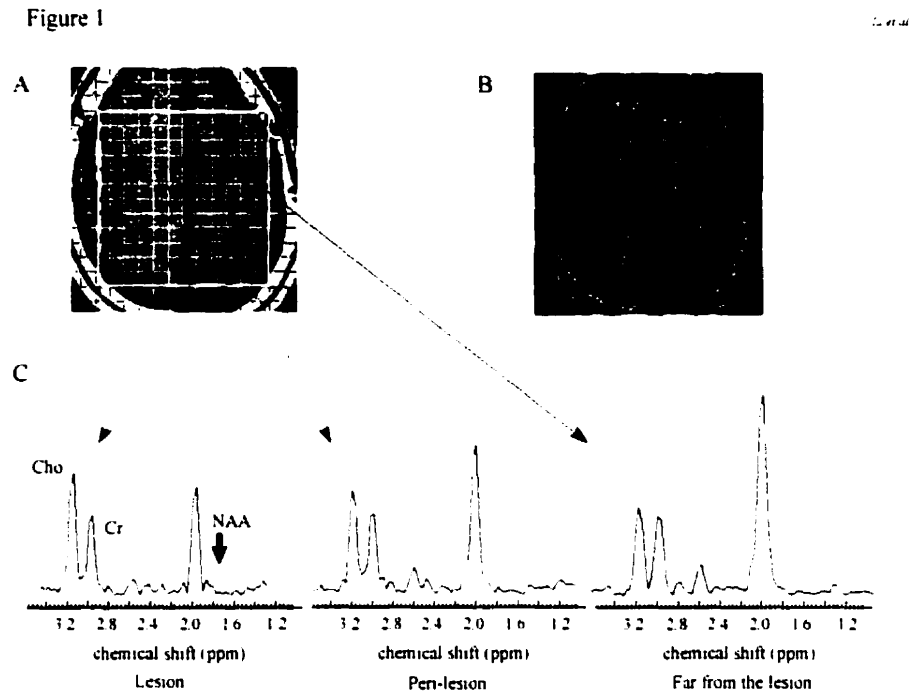


Figure 1: Twenty-two year old man, with seizures since age 5 years. A) Scout MR image showing the VOI with superimposed phase-encoding grid, and the three regions of interest; lesion, peri-lesion, and far from the lesion. B) Axial T1 weighted image showing left parietal focal cortical dysplasia (arrow). C) Average spectra from the three regions of interest. The reduction in NAA signal intensity is greatest in the lesion and decreases with distance from the lesion.

Possible explanations for the low NAA outside the visible lesion include: 1) microscopic abnormalities that extend outside the lesion visible on MRI, 2) depression of NAA by epileptic activity, or 3) altered relaxation time of NAA or Cr. The presence of microscopic abnormalities more extensive than the lesion visible on MRI would be consistent with pathological^{250,251} and clinical^{44,245,246,252} observations, and could explain, at least in part, the poor surgical results sometimes observed in patients with CDM. Palmini et al.,¹⁹⁸ have found that active residual repetitive cortical spiking had negative influence on surgical outcome

and suggested that additional resection of the spiking cortex surrounding CDMs, should be performed, speculating that this type of epileptiform activity reflects underlying microscopic cortical malformation. Ongoing interictal epileptic abnormality or recurrent seizures could lead to secondary neuronal dysfunction through secondary involvement of areas connected to the primary epileptogenic region²⁵³⁻²⁵⁵. This is consistent with our recent observation that NAA in the remaining temporal lobes increases after successful anterior temporal lobectomy¹⁶¹. We do not believe that altered relaxation times are responsible for the altered NAA/Cr, as the nature of the pathology would not be expected to produce changes in relaxation times, especially changes that would affect NAA and Cr sufficiently differently to alter their ratio significantly.

We did not perform absolute quantification of metabolite signal intensities, but rather used Cr as an internal standard to normalize intensities between subjects. In patients who had unilateral lesion visible on MRI we compared the metabolites to the homologous normal appearing region of the contralateral hemisphere. In these patients, Cr in the lesion was similar to Cr in the contralateral homologous normal-appearing region (mean difference = -1^o%, maximum increase of 27^o%). Thus, increases in Cr cannot explain the magnitude of the observed decreases in NAA/Cr which must, therefore, represent NAA decrease.

Distinct developmental malformations result from insults occurring at different stages of cell generation, proliferation, differentiation and migration into the cerebral cortex²⁵⁶. We demonstrate that different types of CDM may also show different degrees of relative NAA decrease (figure 2).

For instance, in focal cortical dysplasia we found very low NAA/Cr ratios. This disorder results from abnormal neuronal and glial cell differentiation and proliferation, and the

lesion contains structurally abnormal neurons and, at times, balloon cells. Both are probably dysfunctional cells with abnormal synaptic activity and connectivity, and presumably this explains the reduced NAA/Cr values. In polymicrogyria the malformation is due to abnormal cortical organization. The timing of the insult is post-migrational, and neurons are thought to be mature. More normal cellular structure and the presence of synaptic integrity may explain why patients with polymicrogyria have normal NAA/Cr ratios (figure 2).

Figure 2

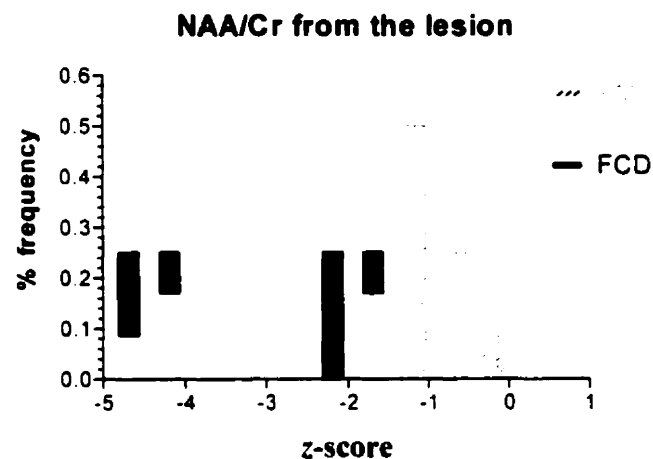


Figure 2: Frequency distribution of NAA/Cr z-scores for different types of CDM. Seventy-five percent of patients with focal cortical dysplasia had NAA/Cr more than 2 SD below the normal mean. All cases of polymicrogyria had NAA/Cr within the normal range. Heterotopia were variable with half of the patients having NAA/Cr more than 2 SD below the normal mean.

Heterotopia consist of a large number of neurons that failed to initiate or complete the migration process. In heterotopia because of the clustering of an abnormally high number of neurons one would expect a relative increase of NAA signal. This assumption is based on histopathological studies showing normal-appearing neurons and evidence of active

synapses²⁵⁷, and on FDG-PET findings showing patterns of glucose uptake similar to normal cortex²⁵⁸. However, we found NAA to be variably normal or abnormal in this group. This suggests that at least some of these apparently normal neurons are, in fact, dysfunctional (figure 3).

Figure 3:

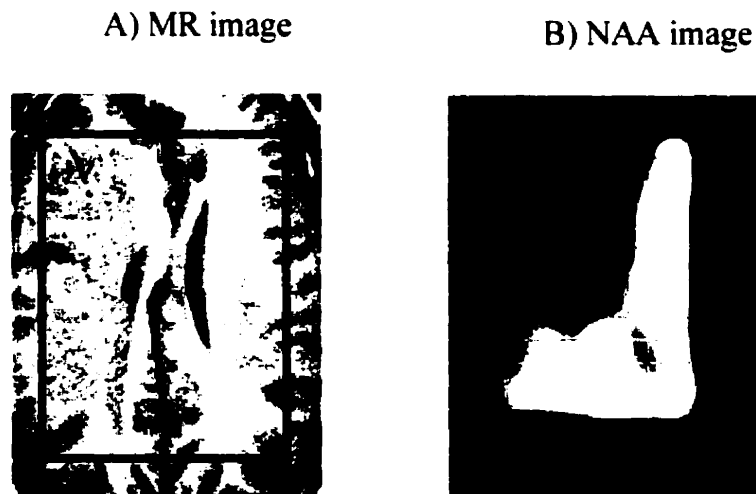


Figure 3: 16 year old boy with seizures. A) MR image showing a large unilateral heterotopia. The black rectangle shows the VOI for MRSI. B) The corresponding NAA image shows a relatively low signal intensity from NAA over the heterotopia compared to the contralateral normal side.

Two case reports have also shown variability of NAA signal intensity in heterotopia^{259,260}. One possible explanation is that the neuronal populations in heterotopia may consist of neurons at different stages of maturation, some of them being immature and improperly connected, and therefore expressing less NAA¹³⁵.

The degree of interictal EEG activity, and the extent of the EEG abnormalities (localized or generalized), did not correlate with the NAA/Cr values in our series. Kuzniecky et al.,²⁶¹ also failed to find correlation between relative NAA/Cr values and EEG abnormalities in their series. The differences in NAA/Cr between types of CDMs appear to reflect more the type of malformation than the amount of interictal EEG abnormality. This suggests that the decrease in NAA is not entirely secondary to interictal epileptic activity. However, in this series all patients had clinically refractory epilepsy, and further studies in patients with CDMs and well controlled epilepsy might provide some answer about the relationship between the seizure severity and NAA signal intensity.

There is as yet no consensus on the classification of malformations of the cerebral cortex, this is due to our incomplete understanding of the mechanisms underlying the pathophysiology of CDM³⁰. Proton MR spectroscopy may be useful in studying the biology of CDMs and, as with brain tumors¹⁶⁷, help refine the classification and differential diagnosis in different types of brain lesions. Three out of 24 patients in this study underwent surgical resections. This number is too small to make any meaningful clinico-pathological correlation. Multimodal image co-registration techniques^{262,263} that allow visualization of the relationship between structural lesions and cellular metabolism (PET, MRSI), or function (fMRI, EEG) may offer new dimensions for surgical planning and resection of malformations in patients with refractory lesional epilepsy.

Paper 2: Spatial extent of neuronal metabolic dysfunction measured by proton MR spectroscopic imaging in patients with localization related epilepsy.

Li LM, Cendes F, Andermann F, Dubeau F, Arnold DL.
Epilepsia 2000 (in press).

Lippincott Williams & Wilkins

SUMMARY

Background: In patients with unilateral temporal lobe epilepsy, low NAA can be seen in both temporal lobes in 18 to 60% of patients. It is possible that analogous widespread reduction of NAA might also extend to areas of the brain not primarily involved in the seizure generation.

Objectives: i) Assess the spatial extent of the decrease in the neuronal marker N-acetyl-aspartate (NAA) relative to creatine (Cr) in patients with localization-related epilepsy, and ii) assess the clinical differences between patients with and without widespread NAA/Cr reduction.

Patients/Methods: We studied 51 patients with localization-related epilepsy. Patients were divided into three groups according to their clinical and EEG investigation: 1) temporal lobe epilepsy (TLE, n=21), 2) extra-temporal lobe epilepsy (extra-TLE, n=20), and 3) multilobar epilepsy (patients with a wider epileptogenic zone, n=10). We acquired proton MR spectroscopic imaging (¹H-MRSI) of temporal and fronto-centro-parietal regions in separate examinations both for patients and controls. NAA/Cr values 2 standard deviations below the mean of normal controls were considered abnormal.

Results: Twenty-three patients (45%) including 12 with TLE had normal MR imaging including volumetric studies of the hippocampus. Forty-nine patients (96%) had low NAA/Cr indicating neuronal dysfunction in either temporal and/or extra-temporal ¹H-MRSIs; 38% of patients with TLE and 50% of patients with extra-TLE also had NAA/Cr reduction outside the clinical and EEG defined primary epileptogenic area. The NAA/Cr reduction was more often widespread in the multilobar group (6/10 [60%]) than in the temporal or extra-temporal

groups (5/16 [31%]). Non-parametric tests of: a) seizure duration, b) seizure frequency, and c) life-time estimated seizures, showed no statistically significant difference ($p > 0.05$) for TLE and extra-TLE patients with or without NAA/Cr reduction outside the seizure focus.

Conclusion: 40-50% of patients with localization-related epilepsy have neuronal metabolic dysfunction that extends beyond the epileptogenic zone defined by clinical-EEG and/or the structural abnormality defined by MRI.

INTRODUCTION

Proton MR spectroscopy ($^1\text{H-MRS}$) of brain is a non-invasive technique that enables detection of different metabolites *in vivo* based on distinct resonance characteristics of the substance in a magnetic field. The most intense signal in a normal brain, seen at 2.02 parts per million (ppm), is derived from the N-acetyl groups, mainly composed of N-acetyl aspartate (NAA)^{119;247}. NAA is found exclusively in mature neurons and neuronal processes^{124;125}. Several studies have demonstrated that an area of brain with relative reduction of NAA correlates with either neuronal loss^{137-144 145-150} or dysfunction^{144;151-156;161;231-233}. The two other signals easily identified in normal brain spectra are Choline-containing compounds (Cho) and Creatine and phospho-creatine containing compounds (Cr), seen at 3.2 and 3.0 ppm respectively^{119;247}. Cr, a metabolite important for energy metabolism, is found in neurons and glia cells, and is relatively homogeneously distributed throughout the normal brain.^{187;264;265}.

Both single voxel^{115;157;158;170;172;266} and multivoxel $^1\text{H-MRS}$ ($^1\text{H-MRSD}$)^{115;116;159;173-176;178} have high sensitivity for detecting low NAA indicative of temporal lobe neuronal loss or dysfunction in temporal lobe epilepsy, and the maximum NAA reduction is often associated with the side of seizure origin defined by prolonged video-EEG monitoring. In patients with unilateral temporal lobe epilepsy, low NAA can be seen in both temporal lobes in 18 to 60% of patients^{115;157;158;176;178}. It is possible that analogous widespread reduction of NAA might also extend to areas of brain not primarily involved in the seizure generation.

The objectives of the present study were: i) to assess the spatial extent of NAA/Cr reduction in patients with localization-related epilepsy, and ii) to assess the clinical differences between patients with more widespread as opposed to focal decreases in NAA/Cr.

PATIENTS AND METHODS

Patients were recruited from the Epilepsy Service at the Montreal Neurological Hospital. The majority had medically intractable epilepsy and underwent detailed pre-surgical evaluation including prolonged video-EEG monitoring to record seizures. The anatomic classification of epilepsy was based on the clinical data and prolonged video-EEG monitoring findings. The objectives of the study were explained to all patients and informed consent was obtained.

Seizure duration was expressed in years and defined as the period between onset of habitual seizures and the ^1H -MRSI scan. Seizure frequency in the five years prior to the scan was obtained from direct interview with the patients and review of the medical chart. The seizure frequency was variable and Engel's seizure frequency score²⁶⁷ was applied: 1-3 per year = 1; 4-11 per year = 2; 1-3 per month = 3; 1-6 per week = 4; 1-3 per day = 5; 4-10 per day = 6; and more than 10 per day = 7. Frequency of secondarily generalized tonic-clonic seizures was categorized into three groups: rare = < 3 per year, monthly = < 4 per month, and weekly = occurring at least once a week. A seizure cluster was defined as a tendency for attacks to occur one after another during a short period of time. Estimated life-time seizure scores were obtained by multiplying the seizure frequency score by seizure duration.

For those who underwent surgical treatment for epilepsy, Engel's outcome score²⁶⁷ was used (class I = seizure-free or residual auras; class II = less than 3 CPS a year; class III = reduction of >90% of seizures; class IV = reduction of < 90% of seizures).

Temporal and extratemporal lobe ^1H -MRSI protocols.

We performed prospective ^1H -MRSI in 38 consecutive patients during their

investigation. We also included 13 other patients with refractory partial epilepsy who in the past had ¹H-MRSIs of both temporal and extra-temporal regions. The main reason why these 13 patients had both examinations was because the seizure localization was not clear at the time of their initial investigation. The mean age of the 51 patients was 31.5 years (range 12 to 60 years).

¹H-MRSI studies were performed in separate examinations using a Philips 1.5 T combined imaging and spectroscopy system (Philips Medical Systems, Best, The Netherlands). After scout images in axial and sagittal planes, a multislice transverse spin-echo MRI (TR 2000, TE 30) was obtained. The volume of interest (VOI) of the extra-temporal lobe protocol included a large portion of the frontal and part of the parietal lobes (see Figure 1a). The size of the VOI for extra-temporal protocol spectroscopy was 75mm to 100mm in the left-right axis, 75mm to 105mm in the antero-posterior axis, and 18mm to 20mm in thickness. The VOI of the temporal lobe protocol included part of the body and tail of the hippocampus and portions of gray and white matter from the mid and posterior temporal lobe (see Figure 1b). The size of the VOI for temporal lobe protocol spectroscopy was 85-100mm in the left-right axis, 75-95mm in the antero-posterior axis, and 20mm in thickness. The size of the individual voxel after post-processing was approximately 1.2 cm x 1.2 cm x 1.8-2 cm. Detailed descriptions and results of these two protocols have been described elsewhere^{115,268}. Water suppressed proton MRSI was acquired from the VOI (TR 2000 ms, TE 272 ms, 250x250 mm FOV, 32x32 phase-encoding steps), followed by a proton MRSI without water suppression (TR 850 ms, TE 272 ms, 250x250 mm FOV, 16x16 phase-encoding steps). Post-processing included zero-filling the water unsuppressed MRSI to obtain 32x32 profiles, followed by application of a mild Gaussian *k*-space filter and an inverse 2D Fourier transformation to both water suppressed and unsuppressed MRSI. For the extra-temporal protocol residual water signal was removed

by applying the linear HSVD fitting method²⁴⁸. For the temporal lobe protocol the resulting time domain signal was left shifted and subtracted from itself to improve water suppression²⁶⁹. This procedure reduces the amplitude of water and nearby resonances and results in relatively high ratios of NAA/Cr.

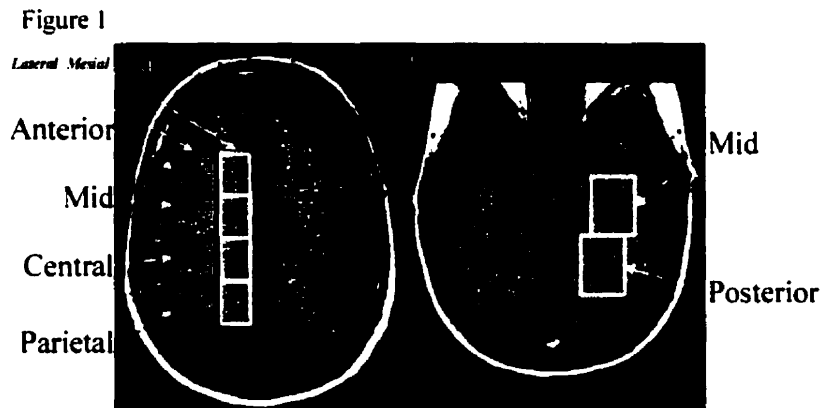


Figure 1: ¹H-MRSI volume of interest in extra-temporal (a) and temporal (b) protocols. The VOI of the extra-temporal protocol was subdivided into 16 subregions. The VOI of the temporal protocol was subdivided into four subregions. The averaged NAA/Cr from each subregion was compared to homotopic NAA/Cr values from a group of normal control subjects (30 controls in the temporal and 25 controls in the extra-temporal protocols). The patient's NAA/Cr values two standard deviations below the mean of the normal controls were considered abnormal.

The spectroscopist was unaware of the results of EEG and MRI. Resonance intensities in individual spectra were determined by integration of peak areas using locally developed software. The number of spectra averaged for each subregion within the VOI (Figure 1) was 10 ± 2 for the temporal lobe protocol and 8 ± 2 for the extra-temporal lobe protocol for both patients and normal control subjects. Voxels on the edge of the VOI, that were affected by chemical shift artifact and voxels that were artifactually broadened were excluded from the analyses. The resonance intensity of NAA was normalized to intravoxel Cr. In epilepsy, Cr is relatively stable^{157;158;160;161;177} so that changes in the NAA/Cr ratio reflect

changes in NAA and neuronal loss or dysfunction.

The same procedure was performed for specific group control data (25 for extra-TL and 30 for TL protocols). Patients' NAA/Cr ratios 2 standard deviations (SD) below the normal mean were considered abnormal.

MR imaging and MR volumetric measurements

All the patients had diagnostic MR imaging acquired separately using the same scanner. The protocol consisted of sagittal and coronal T1 weighted (TR 550, TE 19 ms) images, followed by axial proton density (TR 2000, TE 20 ms), and T2 weighted (TR 2100, TE 20, 78 ms) images. T1 weighted 1mm thick contiguous slice gradient-echo volume acquisition of whole brain (TR 18, TE 10 ms, 30° angle, isotropic voxel) was also acquired for multiplanar reconstruction and volumetric study of mesial temporal structures. The volumetric protocol and its previous results have been published elsewhere^{85,270}. Corrected amygdala or hippocampal volumes 2 SDs below the normal mean were considered abnormal

RESULTS

We used the ILAE 1989 syndromic classification²⁷¹ to classify the 51 patients into two groups based on the clinical features and EEG findings: 1) temporal lobe epilepsy, and 2) extra-temporal lobe epilepsy. We performed a separate analysis based exclusively on patients with well-localized EEG. We added a third multilobar group. Patients were classified into the multilobar group if the epileptogenic zone was widespread, involving two or more lobes, or electro-clinical features were not clearly localizing or if there was discordance between the EEG findings and clinical manifestations to a point where it was not possible to resolve whether the clinical manifestations were related to a given location or a reflection of seizure

spread from a distance.

The clinical data, EEG findings, MRI and ¹H-MRSI results are displayed in Tables 1, 2 and 3 respectively.

Patients with temporal lobe epilepsy

Twenty-one patients (10 women) with a mean age of 35 years (range 17 – 60 years) were classified as having TLE.

MR IMAGING AND VOLUMETRIC MEASUREMENT OF MESIAL TEMPORAL STRUCTURES:

Diagnostic MR imaging and MRVol showed hippocampal atrophy in 10 (6 bilateral), cortical dysgenesis in 4 (2 had associated hippocampal atrophy), and no abnormality in 8 (38%). With the exception of periventricular nodular heterotopia, all the lesions were located in the temporal lobe.

¹H-MRSI:

TL-MRSI showed significant NAA/Cr reduction in all patients (100%), concordant to the side of EEG lateralization in 19/21, and discordant in two (Table; patients 32 and 49). The NAA/Cr reduction in the temporal lobes was unilateral in only 7/21. Extra-TL-MRSI showed an additional NAA/Cr reduction in 8 (38%) patients (4 unilateral, 3 bilateral localized, and 1 diffuse) with TLE. Seven of these eight patients with reduction of NAA/Cr in the extra-TL regions also had bilateral NAA/Cr reduction in the temporal lobes. The lateralization given by extra-TL MRSI was concordant with TL-MRSI in 2, discordant in 2, and non-lateralized in 4.

¹H-MRSI AND CLINICAL CORRELATES:

Mann-Whitney U test rank comparison between those with and those without

NAA/Cr reduction in extra-TL regions showed no significant difference for the sum of the ranks for age of seizure onset (95 vs. 136, $p = 0.61$), for seizure duration (82 vs. 149, $p = 0.66$), for seizure frequency scores (68.5 vs. 141.5, $p = 0.68$), and for estimated life-time seizure scores (63.5 vs. 146.5, $p = 0.43$). Chi-square showed no significant association between additional extra-TL NAA/Cr reduction and frequency of secondary generalized tonic-clonic seizures (rare [42%] vs. monthly [33%] vs. weekly [0%]), Chi-square (2) = 0.808, $p = 0.67$. Fisher's exact test showed no significant association between additional extra-TL NAA/Cr reduction and clustering of seizures, $p = 1$, 2 tailed.

Seven patients underwent surgical resection in the temporal lobe. Two of five patients without, and neither of the two patients with extra-TL NAA/Cr reduction were seizure-free (Fisher's exact test with $p > 0.05$, 1 tailed)

Patients with extra-temporal lobe epilepsy

Twenty patients (13 women) with a mean age of 28 years (range 12 – 56 years) were classified as having extra-TLE.

MR IMAGING AND VOLUMETRIC MEASUREMENT OF MESIAL TEMPORAL STRUCTURES:

Diagnostic MR imaging and MRVol showed cortical dysgenesis in 5, hippocampal atrophy in 3 (2 bilateral), hippocampal asymmetry in 2, hemispheric atrophy in 2, and were normal in 9 (45%).

¹H-MRSI:

Extra-TL-MRSI showed NAA/Cr reduction in 14 patients (70%) and the side of the abnormality was concordant with EEG lateralization in all. The extra-TL-MRSI NAA/Cr reduction was unilateral and localized in 9, bilateral and localized in 5. TL-MRSI showed

NAA/Cr reduction (5 bilateral and 5 unilateral) in 10 patients (50%). In these 10 patients with TL-MRSI abnormality, the extra-TL-MRSI was normal in four, abnormal in six, and in two of them the NAA/Cr reduction was on the side opposite the TL-MRSI lateralization.

¹H-MRSI AND CLINICAL CORRELATES:

Mann-Whitney U test rank comparisons between those with and those without NAA/Cr reduction in the extra-TL regions showed no significant difference for the sum of the ranks for age of seizure onset (103.5 vs. 106.5, $p = 0.909$), for seizure duration (128.5 vs. 81.5, $p = 0.075$), for seizure frequency scores (111 vs. 99, $p = 0.638$), and for estimated lifetime seizure scores (127.5 vs. 82.5, $p = 0.088$). Chi-square showed no significant association between additional TL NAA/Cr reduction and frequency of secondarily generalized tonic-clonic seizures (rare [50%] vs. monthly [50%] vs. weekly [50%]), Chi-square (2) = 0.0, $p = 1$. Fisher's exact test showed no significant association between additional TL NAA/Cr reduction and clustering of seizures, $p = 0.170$, 2 tailed.

Four patients underwent surgical removal of a lesion. One patient had TL NAA/Cr reduction and was not seizure-free. One of three patients without TL NAA/Cr reduction was seizure-free.

In a separate analysis, we excluded the 13 patients that were retrospectively studied to ensure that our findings were not bias because of them. We found that 7 of 15 patients with extra-TLE (46%), and 7 out of 18 patients with TLE (39%) had associated low NAA/Cr in the temporal and extra-temporal ¹H-MRSI, respectively. These figures are similar to those in the analysis that included the 13 patients; 50% for the extra-TLE and 38% for the TLE patients.

Patients with multilobar epilepsy

Ten patients (3 women) with a mean age of 32 years (range 13 - 52 years) were classified as having multilobar epilepsy. Six had electro-clinical features more suggestive of TLE and four of extra-TLE.

MR IMAGING AND VOLUMETRIC MEASUREMENT OF MESIAL TEMPORAL STRUCTURES:

Diagnostic MR imaging and MRVol showed cortical dysgenesis in 2, bilateral hippocampal atrophy in 2, fronto-central atrophy in 1, and no abnormality in 6 (60%).

¹H-MRSI:

TL-MRSI showed significant reduction of NAA/Cr in 9/10 (5 bilateral, 4 unilateral). The side of maximum NAA/Cr reduction was concordant to the side of EEG lateralization in all patients. Extra-TL-MRSI showed reduction of NAA/Cr in 8/9 (4 unilateral, 3 diffuse, and 1 bilateral localized). One patient with non-lateralizing seizures had TL-MRSI with maximal NAA/Cr reduction in one temporal lobe and the extra-TL-MRSI showed NAA/Cr decrease in the opposite side.

¹H-MRSI AND CLINICAL CORRELATES:

Five patients had surgery (4 anterior temporal resection, and 1 parietal resection). Only one patient who had temporal lobe resection was seizure-free, the others were in class III-IV.

Patients with well-localized ictal EEG

Considering only patients with well-localized ictal EEG changes (Table: patients 6, 10-14, 18, 28, 30, 35, 37, 40, 41, 43, 46, 47, and 49), we found that the NAA/Cr reduction was present at the site of ictal EEG abnormality in 16 / 17 (94%) of patients. The NAA/Cr reduction also extended to region distant from the localized ictal EEG abnormality in 6/17 patients (35%).

DISCUSSION

¹H-MRSI is very sensitive for detection of neuronal metabolic dysfunction in patients with localization-related epilepsy. In this series 23 patients (45%) had normal MRI including volumetric studies, while 49 patients (96%) had either temporal and/or extra-temporal ¹H-MRSIs showing significant decreases of NAA/Cr. The two patients with normal ¹H-MRSIs had extra-temporal epilepsy; one had a dysplastic lesion in the frontal lobe, and the correspondent ¹H-MRSI had artefactual voxels at the same place as the MRI visible lesion. The other patient had no visible lesion on MRI, and it is possible that the ¹H-MRSI-VOI did not cover the site of the extratemporal seizure generator.

Previous reports have described conflicting findings in their studies of the presence²⁷² or absence^{159,273} of remote NAA reduction in patients with localization-related epilepsy. Our series of patients with intractable seizures, showed that patients with TLE and extra-TLE had additional neuronal dysfunction outside of the primary epileptogenic area in about 40% and 50% respectively (see Figure 2). The additional NAA/Cr decrease in the VOI outside the seizure generator tended to be more widespread in the multilobar group (6/10 [60%] diffuse) than in the temporal lobe or extra-temporal groups (5/16 [31%] diffuse).

In patients with extra-temporal epilepsy there was a trend for significant difference in duration of epilepsy for those with and those without additional temporal lobe neuronal metabolic dysfunction. No significant difference, however, was observed for age of seizure onset, seizure-frequency (either of partial or secondarily generalized types), or clustering. In patients with temporal lobe epilepsy there was no difference in any of these factors for those with or without additional extra-temporal lobe decreases in NAA/Cr.

Figure 2

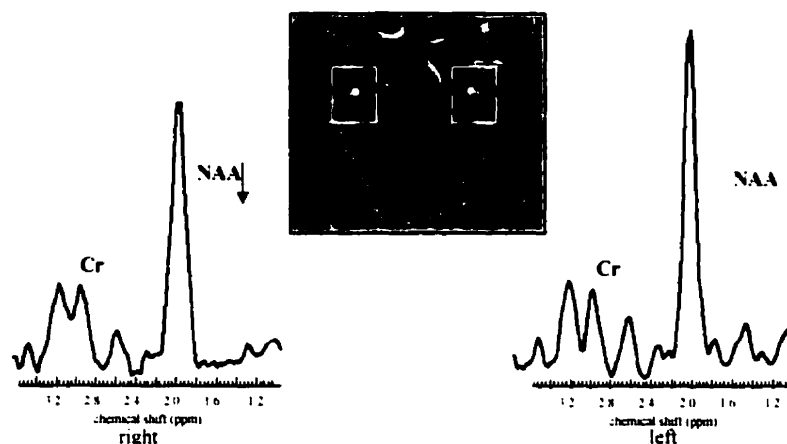


Figure 2: ^1H -MRSI of temporal regions showed significant NAA/Cr reduction in the right medial temporal region of a patient with right fronto-central focus and normal amygdala and hippocampal volumes.

The finding that the frequency of clinical seizures was not a significant factor suggests that factors other than seizures themselves might be associated with additional neuronal dysfunction seen in the temporal lobe. One possibility would be the nature of the epileptic lesion, which could cause disruption of neuronal network over time with consequent neuronal dysfunction in vulnerable interconnected areas. This hypothesis is, in part, supported by two observations: 1) NAA/Cr recovery in patients after successful temporal lobe resection^{161,232}, and 2) NAA/Cr reduction in seizure-free patients²⁴². The NAA/Cr recovery following removal of an epileptogenic area can occur as early as two months after surgery²³³ and cannot be explained solely by the absence of seizures for two months, since NAA/Cr does not recover in patients who do not have successful surgery but do not have seizure for 2 months. The importance of the presence of an epileptogenic area is further supported by observation that patients with TLE who are seizure-free for at least a year with antiepileptic drug treatment, continue to have low NAA/Cr in the mesial temporal region²⁴². Other possible overlapping

explanations for patients with more extensive NAA/Cr reduction include: 1) hidden dual pathology, and 2) widespread epileptogenic areas.

Dual pathology is defined as the presence of hippocampal atrophy in the presence of an extra-hippocampal lesion⁴⁶. Surgical results in patients with dual pathology suggested that both the hippocampal atrophy and the extra-hippocampal lesion play a role in seizure generation²⁷⁴. In a previous study¹¹⁵ we showed that ¹H-MRSI can be abnormal in TLE patients with normal hippocampal volumes. Qualitative pathology demonstrated mild astrogliosis and neuronal loss of mesial temporal structures in these patients¹¹⁵. Therefore, in some patients with extra-temporal epilepsy the NAA/Cr reduction in the temporal lobes might reflect underlying potential hippocampal epileptogenicity, or 'hidden dual pathology', if so, such patients would have a distinct surgical outcome²⁷⁵. In this series 5/9 patients with normal MRI and hippocampal volumes in the extra-TLE group had abnormal temporal lobe NAA/Cr. The ¹H-MRSI of the temporal lobes added significant additional information over that available from even the most careful and quantitative MRI examinations. The significance of the temporal lobe NAA/Cr decrease in the extra-TLE group is still unclear. Nevertheless our preliminary study in patients with bilateral hippocampal atrophy and TLE showed that patients with ¹H-MRSI concordant to EEG and with absence of widespread contralateral temporal lobe NAA/Cr reduction had better surgical outcomes²⁷⁶.

In conclusion, in 40-50% of patients with localization-related epilepsy, the neuronal metabolic abnormality can extend beyond the epileptogenic zone defined by electro-clinical and MRI findings. In patients with electro-clinical manifestations suggesting a wider epileptogenic zone, the neuronal metabolic abnormality also tended to be more diffuse. There were no apparent differences in those with widespread NAA/Cr reduction in age at seizure

onset, duration of epilepsy, frequency of partial and secondarily generalized seizures, and lifetime estimated number of seizures. This extensive neuronal metabolic dysfunction appears to be related to the intrinsic nature and extent of the original epileptogenic damage. Widespread abnormalities in NAA/Cr may negatively influence outcome in patients with TLE and should be further explored in patients with other localization-related epilepsy as well.

Table 1: Syndromic classification and seizure description in 51 patients with localization related epilepsy

<i>Pt/sex/age</i>	<i>Syndrome</i>	<i>Seizure description</i>
1/m/18	Extra-TLE	CPS-stare, scream, agitated at times, has aura hard to describe
2/m/31	Extra-TLE	CPS-eyes and head deviation to the right with impairment of consciousness and tonic posturing, drop attacks
3/f/44	Extra-TLE	SPS-loss of sensation, left arm, followed by tonic posturing
4/m/30	Extra-TLE	CPS-wakes up, opens his eyes, moves his head, rocks back and forth
5/f/56	Extra-TLE	CPS-no aura => tonic posturing of right arm, flexion of the left for few seconds with impairment of consciousness
6/m/20	Extra-TLE	CPS-no aura -> looks ahead, manual, and pedal automatisms
7/f/37	Extra-TLE	CPS-aura: numbness and stiffness right hand -> loss of consciousness and SGTC
8/m/19	Extra-TLE	CPS- aura: ?dizziness -> stares, opens his mouth and SGTC
9/f/51	Extra-TLE	CPS-aura: right facial numbness and headache -> lip smacking followed by slurred speech
10/m/12	Extra-TLE	SPS- aura: sensation over the left eye => left face twitching, left side jerking, and SGTC
11/f/13	Extra-TLE	CPS-no aura => wakes up, forcefully moves both legs and arms, hypertonicity (L>R)
12/f/16	Extra-TLE	SPS-left hemibody simple motor seizures
13/f/19	Extra-TLE	SPS-paresthesia and contraction of right hand with march and involvement of right leg, with difficulty speaking
14/f/36	Extra-TLE	SPS-right upper limb motor seizures
15/f/22	Extra-TLE	SGTC-no aura, SGTC
16/f/19	Extra-TLE	SGTC-no aura -> stares, SGTC

17/f/34	Extra-TLE	SPS-left arm numbness
18/m/17	Extra-TLE	SPS-left hand sensory seizures followed by left arm tonic posturing
19/f/15	Extra-TLE	SPS-no aura => head turning, laughing
20/f/43	Extra-TLE	CPS-no aura => becomes agitated, loses urine, at times without loss of consciousness
21/m/52	Multilobar (EXTRA-TLE)	CPS-aura: epigastric sensation => speech arrest, impairment of consciousness, posturing, falls and SGTC
22/m/48	Multilobar (EXTRA-TLE)	CPS-no aura => tonic extension of right arm, flexion of the left arm. Bi-manual automatism (L>R)
23/m/13	Multilobar (EXTRA-TLE)	CPS-aura: tachycardia => bipedal automatisms with scissors-like movements.
24/f/18	Multilobar (EXTRA-TLE)	CPS-aura: sees the future, epigastric sensation => stares and orofacial automatism. SPS: R-thigh pain and clonic movement
25/f/20	Multilobar (TLE)	CPS-no aura => vocalization, trashing movements, tachypnea
26/m/25	Multilobar (TLE)	CPS-aura: dizziness+tinnitus => orofacial automatisms or head deviation with tonic posturing of upper limbs
27/f/40	Multilobar (TLE)	CPS-aura: epigastric sensation => bipedal automatisms
28/m/39	Multilobar (TLE)	CPS-aura: epigastric sensation => grimace, orofacial automatism, scream, bicycling movement.
29/m/26	Multilobar (TLE)	CPS-no aura => stares, R hand automatism
30/m/35	Multilobar (TLE)	CPS-no aura => unresponsive, swallowing, twitching R side of the face, blinking
31/m/56	TLE	CPS-aura: fear => stares, vocalization, and automatism
32/f/40	TLE	CPS-aura: déjà vu, fear => arrest of activity
33/f/17	TLE	CPS-aura: epigastric sensation => manual automatisms (l. sided seizure is associated with speech impairment)
34/m/40	TLE	CPS-aura: change in breathing => lip smacking and manual automatism
35/m/38	TLE	CPS-aura: epigastric sensation, déjà vu => R hand dystonic

36/m/26	TLE	CPS-aura: nausea and feeling of internal vibration => stiffness of right forearm
37/m/34	TLE	CPS-no aura => stares, head turns to the right, R side clonic movements, SGTC
38/f/39	TLE	CPS-aura: difficult to describe, dry throat => manual automatisms
39/m/32	TLE	CPS-aura: dizziness =>stares, l. hand automatism, swings his body from side to side
40/m/48	TLE	CPS-no aura => stares, arrest of activity
41/m/30	TLE	CPS-aura: dizziness, epigastric aura => neck flexion, extension of arms
42/m/26	TLE	CPS-aura: epigastric sensation => automatisms
43/f/19	TLE	CPS-aura: epigastric sensation, fear => vocalization, automatism, chewing
44/f/45	TLE	CPS-no aura => stares, few manual automatism
45/f/23	TLE	CPS-aura: epigastric sensation => loss of consciousness for few seconds
46/f/60	TLE	CPS-aura: feeling unwell => manual automatisms
47/m/32	TLE	CPS-aura: dizziness, epigastric sensation => SGTC
48/m/36	TLE	CPS-no aura => stares and says "Oh boy, oh boy" and automatic pose "like a bodyguard"
49/f/44	TLE	CPS-aura: epigastric sensation, déjà vu => automatisms
50/f/27	TLE	CPS-no aura =>repetitive speech "somebody at home", manual automatism, tonic head deviation to the right
51/f/28	TLE	CPS-aura: feels sick => manual automatisms

SPS=simple partial seizure, CPS=complex partial seizure, SGTC=secondary generalized tonic clonic seizure L=left, R=right, Bi=bilateral

Table 2: Interictal and ictal EEG findings in 51 patients with localization related epilepsy

<i>Pt/sex/age</i>	<i>Interictal EEG</i>	<i>Ictal EEG</i>
1/m/18	L-F-C, and less frequent R-T	Bi-F-C (L>R)
2/m/31	Bi-C-P-F, more R parasagittal, GSW	Bi-hemisphere
3/f/44	R-C-P	no visible changes
4/m/30	normal	Bi-F-C parasagittal
5/f/56	L-F	Diffuse attenuation
6/m/20	Bi-F (L>R)	SEEG: R-F
7/f/37	Bi-F	Bi-F (L>R)
8/m/19	Bi-F	Bi-F
9/f/51	L-CP, and R-T	not recorded
10/m/12	R-F-C	R-C-F
11/f/13	Bi-F	SEEG: R-F
12/f/16	R-F, rare Bi-T	R-F
13/f/19	L-C-P	Left hem, max C3
14/f/36	L-hemisphere (max. central)	Left hemispheric, max central
15/f/22	GSW, and Bi-F-C	Generalized with fronto-central accentuation
16/f/19	Bi-C-P-F, more R parasagittal, GSW	not-recorded
17/f/34	R-P	not recorded

18/m/17	L-F-C	L-FC
19/f/15	Bi-F, GSW	bilateral changes
20/f/43	normal	no changes
21/m/52	Bi-F-C-T (R>L)	SEEG: multifocal (more over the R-P)
22/m/48	Bi-F, GSW	L-hemisphere
23/m/13	Bi-F-T (R>L)	R-F-T
24/f/18	GSW, Bi-F-C	L-C, and R-T
25/f/20	Bi-F, T	SEEG: multifocal
26/m/25	Bi-T	Bi-F-C, and L-T-P
27/f/40	Bi-T (R>L)	Bi-FT with later R side predominance
28/m/39	R-F-T	R-T
29/m/26	Bi-T, GSW	Bi-hemisphere
30/m/35	R-F-C-T	R-T
31/m/56	Bi-T	L-T > R-T
32/f/40	Bi-T	Bi-onset, more R-temporal
33/f/17	Bi-T	Bi-hemisphere (max. temporal regions)
34/m/40	Bi-T	Bi-T
35/m/38	L-T	SEEG: L-hippocampus onset
36/m/26	L-F-T	L-F-T, with late L-T predominance

37/m/34	L-T-F	SEEG: L-T neocortex
38/f/39	Bi-T	Bi-T (L>R)
39/m/32	L-T	Bi-hemisphere with later L-T accentuation
40/m/48	R-T	R-T
41/m/30	R-T-C	R-T
42/m/26	R-T	not recorded
43/f/19	R-T	R-T
44/f/45	Bi-T (L>R)	Bi-hemisphere (max. L-T)
45/f/23	Bi-T	SEEG: Bi-T
46/f/60	L-T	L-T
47/m/32	L-T	L-T
48/m/36	L-T	Bi-T, L-T
49/f/44	L-T	L-T
50/f/27	R-hemisphere (max. centrottemporal)	R-hemispheric (max centrottemporal)
51/f/28	R-T	not-recorded

GSW=generalized spike and wave F=frontal, C=central, T=temporal, P=parietal SEEG=stereotaxic implanted depth EEG

Table 3: Results of MRI and MRSI of temporal and extra-temporal in 51 patients with localization related epilepsy

<i>Pt/sex/age</i>	<i>Syndrome</i>	<i>MRSI temporal region</i>	<i>MRSI extra-temporal region</i>	<i>MR imaging and MRVol</i>
1/m/18	Extra-TLE	Abnormal - Bi (L.>R)	Abnormal - L-parietal	Normal
2/m/31	Extra-TLE	Abnormal - Bi (L.>R)	Abnormal - R parietal	FCD
3/f/44	Extra-TLE	Abnormal - Bi (L.>R)	Abnormal - R-centro-parietal	FCD
4/m/30	Extra-TLE	Abnormal - Bi (L.>R)	Normal	Bi-Hc atrophy
5/f/56	Extra-TLE	Abnormal - Bi (R>L)	Abnormal - Bi-mesial-anterior-mid	Normal
6/m/20	Extra-TLE	Abnormal - Left	Abnormal - R-mid	L-Hc atrophy and R hemisphere slightly smaller
7/f/37	Extra-TLE	Abnormal - Left	Normal	Normal
8/m/19	Extra-TLE	Abnormal - Left	Normal	Bi-Hc atrophy, left smaller
9/f/51	Extra-TLE	Abnormal - L-Mid	Normal	Normal
10/m/12	Extra-TLE	Abnormal - Right	Abnormal - R-mid-central	Normal
11/f/13	Extra-TLE	Normal	Abnormal - Bi-anterior (R>L)	FCD
12/f/16	Extra-TLE	Normal	Abnormal - Bi (R-anterior-mid and L-mid)	Normal
13/f/19	Extra-TLE	Normal	Abnormal - Bi-mesial-central	Asymmetric Hc. Left smaller
14/f/36	Extra-TLE	Normal	Abnormal Diffuse (L.>R)	L-hemisphere smaller
15/f/22	Extra-TLE	Normal	Abnormal - L- mesial-central	Normal
16/f/19	Extra-TLE	Normal	Abnormal - L-parieto-central	FCD

17/f/34	Extra-TLE	Normal	Abnormal - R-centro-parietal	Asymmetric Hc. Left smaller
18/m/17	Extra-TLE	Normal	Abnormal - R-parieto-central	Normal
19/f/15	Extra-TLE	Normal	Normal	Normal
20/f/43	Extra-TLE	Normal	Normal	FCD
21/m/52	Multilobar (EXTRA-TLE)	Abnormal - Bi (L>R)	Abnormal - Bi-centro-parietal	Bi-TL + Hc atrophy
22/m/48	Multilobar (EXTRA-TLE)	Abnormal - Bi (L>R)	Abnormal - R-side	Normal
23/m/13	Multilobar (EXTRA-TLE)	Abnormal - Right	Normal	R-TL and orbito frontal CD
24/f/18	Multilobar (EXTRA-TLE)	Abnormal - Right	Normal	Normal
25/f/20	Multilobar (TLE)	Abnormal - Bi (L>R)	Abnormal - Diffuse (L-R)	Previous operation
26/m/25	Multilobar (TLE)	Abnormal - Bi (R=L)	Abnormal - Diffuse (L-R)	PNH
27/f/40	Multilobar (TLE)	Abnormal - Bi (R>L)	Abnormal - R-side	Bi-TL + Hc and R-FC atrophy
28/m/39	Multilobar (TLE)	Abnormal - R-Post	Abnormal - R-ant-mid	Normal
29/m/26	Multilobar (TLE)	Abnormal - Asymmetry (R>L)	Abnormal - R-mid-central	Normal
30/m/35	Multilobar (TLE)	Normal	Abnormal - Diffuse (L-R)	Normal
31/m/56	TLE	Abnormal - Bi (L>R)	Abnormal - Bi-mid-central	Normal
32/f/40	TLE	Abnormal - Bi (L>R)	Abnormal - Diffuse (L-R)	Bi-Hc atrophy, Left smaller
33/f/17	TLE	Abnormal - Bi (L>R)	Abnormal - R-ant-mid	Bi-Hc atrophy, Left smaller
34/m/40	TLE	Abnormal - Bi (L>R)	Abnormal - R-central	Normal
35/m/38	TLE	Abnormal - Bi (L>R)	Normal	L-Hc atrophy and R-PNH

36/m/26	TLE	Abnormal - Bi (L>R)	Normal	L-Hc atrophy
37/m/34	TLE	Abnormal - Bi (L>R)	Normal	L-Hc atrophy
38/f/39	TLE	Abnormal - Bi (R=L)	Normal	Normal
39/m/32	TLE	Abnormal - Bi (R=L)	Normal	L-T dysplasia
40/m/48	TLE	Abnormal - Bi (R>L)	Abnormal - R-central	Bi-TL+Hc atrophy
41/m/30	TLE	Abnormal - Bi (R>L)	Abnormal - Bi-central	Previous surgery
42/m/26	TLE	Abnormal - Bi (R>L)	Abnormal - R-centro-parietal	Normal
43/f/19	TLE	Abnormal - Bi (R>L)	Normal	Bi-Hc atrophy. Right smaller
44/f/45	TLE	Abnormal - Left	Abnormal - Bi-central	Normal
45/f/23	TLE	Abnormal - Left	Normal	Normal
46/f/60	TLE	Abnormal - Left	Normal	Normal
47/m/32	TLE	Abnormal - Left	Normal	L-Hc atrophy
48/m/36	TLE	Abnormal - Left	Normal	Normal
49/f/44	TLE	Abnormal - Right	Normal	Bi-Hc atrophy no asymmetry
50/f/27	TLE	Abnormal - Right	Normal	Bi-Hc atrophy, subtle change in the right inferior central sulcus
51/f/28	TLE	Abnormal - Right	Normal	Normal

Hc= hippocampus FCD= focal cortical dysplasia CD= cortical dysplasia

**Paper 3: Relation of interictal spike frequency to ¹H-MRSI-measured
NAA/Cr.**

Serles W, Li LM, Caramanos Z, Arnold DL, Gotman J.
Epilepsia; 1999;40:1821-1827.

Lippincott Williams & Wilkins

SUMMARY

Background: Whereas EEG spiking and decreases of the neuronal marker N-acetyl-aspartate (NAA) both *localize* the epileptic focus well, the significance of the *intensity* of these variables is unclear.

Objective: To investigate whether the frequency of interictal surface spikes is related to the degree of N-acetyl-aspartate/Creatine (NAA/Cr) ratio decrease as measured by proton MR spectroscopic imaging (¹H-MRSI) in patients with intractable partial epilepsy.

Patients/Methods: We retrospectively studied 14 patients, nine with temporal lobe epilepsy and five with frontal lobe epilepsy. Spikes that occurred during prolonged video-EEG monitoring from electrodes placed according to the International 10-20 system were counted blinded to the ¹H-MRSI results. Eight electrode positions (F3/4;C3/4; T3/4;T5/6) were assigned to underlying brain subregions in the ¹H-MRSI's volume of interest. We converted NAA/Cr ratios into z-scores (NAA/Cr_z) to directly compare NAA/Cr values across subregions. We calculated Spearman rank-order (ρ) and Pearson product-moment (r) correlations between spike frequency and NAA/Cr_z values overall as well as within each brain subregion.

Results: We found an overall negative relationship between spike frequency data and NAA/Cr_z data ($\rho = -.341$). When analyzing only spiking subregions, this negative relationship became slightly stronger ($\rho = -.442$; $r = -.338$). When data from the eight sites were considered separately, this negative relationship remained in most instances.

Conclusions: Our results reveal a trend toward higher interictal spike frequencies on surface EEG in regions of pronounced neuronal metabolic damage or dysfunction. This

suggests that both variables parallel an underlying pathological substrate, although the pathophysiological processes may be distinct.

INTRODUCTION

EEG still provides the gold standard parameters for localizing the epileptic focus in the presurgical evaluation of patients with intractable partial epilepsy. The distribution of spikes and the ictal EEG onset zone are strongly indicative of the site of seizure origin. In recent years, proton magnetic resonance spectroscopic imaging (^1H -MRSI) has been used to lateralize the seizure focus on the basis of localized decreases in N-acetyl-aspartate (NAA) relative to Creatine (Cr) signal intensity (NAA/Cr)^{173;268}. We, and others, have shown that low NAA is not due primarily to neuronal loss but, rather, to neuronal metabolic dysfunction as it will increase to normal levels after successful epilepsy surgery^{161;232}. To better understand the reason for this observation, we asked whether the frequent, interictal synchronized firing (*i.e.* spiking) of neurons was coupled to regional neuronal metabolic damage or dysfunction. More specifically, we were interested in those regions of NAA decrease, where spiking was present, because loss of NAA can be found in many neurologic diseases and is not specific for epilepsy^{149;150;277}. To answer this question, we examined the relationship between localized ^1H -MRSI-measured NAA/Cr values and surface-EEG-measured spike frequency in individual patients with intractable partial epilepsy.

PATIENTS AND METHODS

Patients

We retrospectively studied 14 patients (eight women, mean age = 25.1 years, range, 13–45 years), who had undergone both ^1H -MRSI of the frontal and the temporal lobes. Nine patients had temporal lobe epilepsy (TLE) and five had frontal lobe epilepsy (FLE). Diagnosis was based on a comprehensive electroclinical investigation that included depth electrodes in

five patients.

MR imaging

We acquired sagittal and coronal T₁-weighted (TR = 550 ms; TE = 19 ms) images, followed by dual spin-echo transverse proton density and T₂-weighted images (TR = 2100 ms; TE = 20 and 78 ms). In addition, a T₁-weighted gradient-echo volume acquisition of the whole brain (TR = 18 ms, TE = 10 ms, 30° angle, 1-mm-thick contiguous slice) was obtained for multiplanar reconstruction.

EEG analysis

A single observer (W.S.) who was blinded to the ¹H-MRSI results reviewed tracings from the first three days of prolonged video-EEG monitoring with automatic spike detection. To minimize any influence of seizures on the spiking rate we excluded those samples arising either 1 hour prior to, or 8 hours following a clinical attack. Interictal spikes were counted manually on the basis of morphological criteria (*i.e.* having a duration < 200 ms and being clearly distinguishable from background activity on a bipolar montage). We obtained the distribution of amplitudes using an average reference montage, choosing a 50th cut-off value compared to the maximum peak. For each patient, we counted the number of spikes that were recorded from 10:00 p.m. to 8:00 a.m. over the course of two nights (up to a maximum of 100 spikes). This was done from the following electrode sites: Fp1, F3, F7, F9, C3, T3, T5, T9, P3, P9, and O1; the homologous sites on the right; Fz, Cz, Pz; and zygomatic electrodes Zy1 and Zy2. For each patient, the mean spike frequency per hour was calculated for each electrode position.

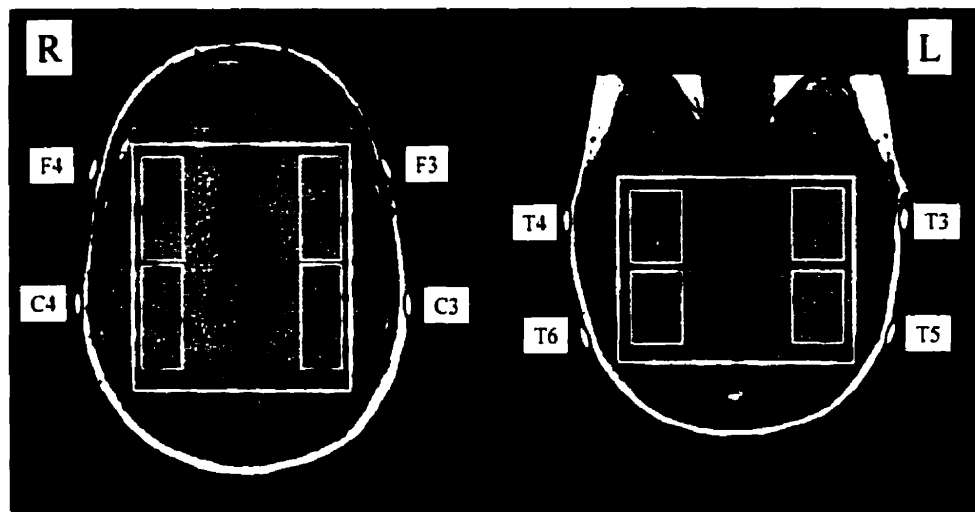
¹H-MRSI acquisition and processing

For each patient, separate ¹H-MRSI studies were carried out in the temporal lobe¹¹⁵ and the extra-temporal lobe²⁶⁸ regions using a Philips 1.5 T combined imaging and spectroscopy system (Philips Medical Systems, Best, The Netherlands). After scout images in axial and sagittal planes were acquired, a multislice transverse spin-echo MRI (TR = 2000 ms; TE = 30 ms) was obtained. The volume of interest (VOI) for the temporal lobe protocol (TLP) included part of the body and tail of the hippocampus, as well as portions of gray and white matter from the mid (Mid) and the posterior (Post) temporal lobe in both the left (Lt) and right (Rt) hemispheres. The VOI of the extra-temporal lobe protocol (ETLP) included a large portion of the frontal lobes (Front) and the central area of the parietal lobes (Cent) bilaterally. The size of the VOIs for TLP (ETLP) spectroscopy was 85-100 (75-100) mm in the left-right axis, 75-95 (75-105) mm in the antero-posterior axis, and 20 (18-20) mm in thickness. The size of the individual voxels after post-processing was approximately 1.2 cm x 1.2 cm x 1.8-2 cm.

A water-suppressed ¹H-MRSI was acquired from the VOI (TR = 2000 ms; TE = 272 ms; FOV = 250 x 250 mm, 32 x 32 phase-encoding steps). This was followed by a ¹H-MRSI without water suppression (TR = 850 ms, TE = 272 ms, FOV = 250 x 250 mm, 16 x 16 phase-encoding steps). Post-processing included zero-filling the water unsuppressed MRSI to obtain 32x32 profiles, followed by application of mild Gaussian *k*-space filter and an inverse 2D Fourier transformation to both water suppressed and unsuppressed MRSI. For the ETLP residual water signal was removed by applying the linear HSVD fitting method²⁴⁸. For the TLP the resulting time domain signal was left shifted and subtracted from itself to improve water suppression²⁶⁹. This procedure reduces the amplitude of water and nearby resonances

and results in relatively high ratios of NAA/Cr. The same process was performed for specific group control data (25 for the ETLP and 40 for the TLP).

We divided the ^1H -MRSI VOIs into subregions that would best represent the underlying brain volumes that corresponded to the surface electrode sites. Thus, spectra from the lateral frontal subregions were related to electrodes F3 and F4; spectra from the lateral centro-parietal subregions were related to C3 and C4; and spectra from the mid- and posterior-temporal subregions were related to electrodes T3, T4, T5, and T6 (Fig. 1). Resonance intensities of NAA and Cr within each subregion were determined using locally developed



software to integrate the areas under the NAA and Cr peaks in each of the individual spectra.

Fig 1. Location of electrodes in relation to volume of interest of ^1H -MRSI. R = right; L = left; F4, F3, C4, C3; T4, T3, T6, T5 = electrode positions according to the International 10-20 system.

Standardization of ^1H -MRSI data

Because of biological variability of NAA levels in different regions of the brain^{278,279} and because of differences in post-processing methods^{248,269}, we used a z -score transformation

to standardize each of our patients' NAA/Cr ratios to that of a group of normal control subjects that underwent similar $^1\text{H-MRSI}$. This allowed us to directly compare NAA/Cr values across subregions.

For each subregion, standardized values (NAA/Cr_z) were calculated for each patient by: (i) subtracting their NAA/Cr value from the mean NAA/Cr value obtained from the same region in normal control subjects, and (ii) dividing the result by the normal control subjects' NAA/Cr standard deviation (SD) for that region.

Data Analysis

Concordance of localization between EEG and $^1\text{H-MRSI}$ within a subregion was defined as either: (i) the absence of spiking and the presence of normal NAA/Cr levels (*i.e.* NAA/Cr_z less negative than -2.0); or (ii) the presence of both spiking and of abnormal NAA/Cr levels (*i.e.* NAA/Cr_z more negative than -2.0). The overall degree of concordance for each individual was expressed as the percentage of subregions that showed such concordance.

Scatter plots were used to illustrate the overall relationship between spike frequency data and NAA/Cr_z data (*i.e.* displaying together the data from all subregions in order to increase the sample size). Because the spike frequency data was positively skewed, we also examined the relationship between NAA/Cr_z values and logarithmically transformed spike frequency values. Analyzing together all regions from all patients, however, resulted in data points not being independent from one another because each patient contributed more than one data point. Thus, Spearman rank-order correlation coefficients (ρ) were calculated for these data, but only for descriptive purposes. Pearson product-moment correlations (r) were

also calculated for the relationships between the logarithmically transformed spiking frequency data and the NAA/Cr_r values but, again, only for descriptive purposes. Similar analyses were also performed within each subregion

Table 1: Patients' demographic and clinical data

Patient / Sex / Age	Epilepsy syndrome [#]	MRI/hippocampal volumetry	NAA/Cr _r values and interictal spike frequency at corresponding scalp electrodes																Concordance [*]
			Rt-Mid	T4	Lt-Mid	T3	Rt-Post	T6	Lt-Post	T5	Rt-Front	F4	Lt-Front	F3	Rt-Cent	C4	Lt-Cent	C3	
1 / f / 13	FLE	Rt frontal FCD	-1.55	0.00	-1.78	0.00	-0.85	0.00	-0.18	0.00	-2.55	3.90	*	0.00	-0.55	2.00	0.68	0.00	86%
2 / m / 18	FLE	Normal	-5.81	0.00	-3.99	14.10	-4.86	0.00	-3.64	0.40	0.70	0.00	-1.44	0.10	-0.36	0.00	-0.89	0.00	63%
3 / m / 17	FLE	Normal	1.40	0.00	0.38	0.00	-0.19	0.00	1.05	0.00	-2.35	0.40	-1.75	0.00	-1.07	1.30	-1.16	0.00	88%
4 / f / 19	FLE	Normal	-0.53	0.00	0.35	0.00	-0.75	0.00	0.33	0.00	-1.59	0.40	-2.54	2.90	-1.78	0.00	-1.32	10.20	75%
5 / m / 30	FLE	Bilateral HA	-8.46	0.00	-5.82	0.00	-2.13	0.00	-2.04	0.00	0.49	0.00	-0.40	0.00	-0.50	0.00	-0.95	0.00	50%
6 / f / 45	TLE	Normal	-1.18	0.00	-4.58	22.80	-0.48	0.00	-1.78	1.20	-2.04	0.50	-1.11	0.50	-1.85	0.10	-0.54	0.00	63%
7 / f / 19	TLE	Rt HA	-8.33	0.00	-4.53	0.00	0.12	0.00	-0.49	0.00	*	0.00	0.23	0.00	*	0.00	*	0.00	60%
8 / f / 39	TLE	Normal	-4.34	0.20	-3.43	1.60	0.02	0.10	0.06	0.10	-0.92	0.00	-0.95	0.00	-0.99	0.00	-0.63	0.00	75%
9 / f / 17	TLE	Bilateral HA	-5.52	4.10	-6.57	8.00	-1.66	0.20	-2.36	1.60	-2.51	0.10	-1.23	0.90	-1.59	0.00	-0.34	0.00	75%
10 / m / 34	TLE	Lt HA	-2.56	0.00	-6.43	37.90	-1.62	0.00	-2.58	7.60	-1.37	0.00	-0.81	0.10	-1.67	0.00	0.51	0.00	75%
11 / m / 35	TLE	Normal	-1.64	65.20	-1.28	0.00	-0.86	2.40	-0.54	0.00	-1.00	0.30	-0.25	0.00	-2.35	0.00	-0.82	0.00	50%
12 / m / 38	TLE	Lt HA and Rt PNH	-3.81	1.90	-5.75	6.80	-0.12	0.00	-0.80	0.70	-1.74	0.20	-0.88	1.40	-0.09	0.00	0.92	0.00	63%
13 / f / 23	TLE	Normal	-0.07	0.70	-4.78	0.30	-1.88	0.00	-2.38	0.00	-1.42	0.00	-0.16	0.10	-0.41	0.00	-1.47	0.00	63%
14 / f / 40	TLE	Bilateral HA	-11.63	1.10	-13.94	0.00	-8.82	0.00	-8.75	0.00	-2.77	0.00	-1.33	0.00	-2.37	0.00	-1.30	0.00	38%

f=female; m=male; NAA/Cr_r=NAA/Cr values standardized to normal control values in the homologous subregion # Based on ILAE syndromic classification - 1989²⁷¹ Bolding indicates abnormally low NAA/Cr_r values or presence of spiking FCD=Focal cortical dysplasia; HA=Hippocampal atrophy, PNH=Periventricular nodular heterotopia *=-Artifactual spectra; % of subregions that showed concordance between spiking and NAA/Cr_r values

RESULTS

The mean duration of the analyzed EEG samples for the 14 patients was 15.1 hours (hrs) (range = 4.3-19.5 hrs) and the mean interictal spike frequency at the most active electrode was 13.4 / hr (range = 0-65.2 / hr). Two patients (5 and 7) had no interictal spiking and a small number of ^1H -MRSI spectra were artifactual in two patients (1 and 7). Our patients' demographic, clinical, spike frequency, and ^1H -MRSI data are summarized in Table 1.

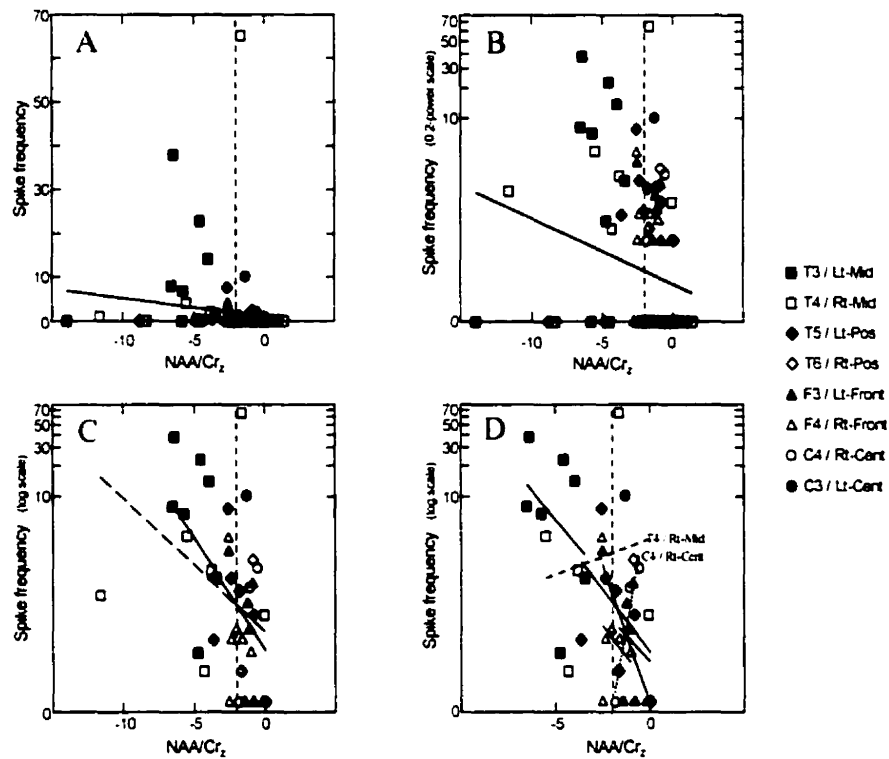


Fig. 2: Scatter plots illustrating: (A) the overall relationship between spike frequency and NAA/Cr₂ values plotted using a linear y-axis scale; (B) same as (A) but with a 0.2 power-transformed y-axis scale; (C) overall relationship between logarithmically transformed spike frequency and NAA/Cr₂ values with the NAA/Cr₂ outlier (broken line) and without the NAA/Cr₂ outlier (solid line); (D) relationship between logarithmically transformed spike frequency and NAA/Cr₂ values plotted separately for each subregion. The broken vertical line represents the NAA/Cr₂ normalcy cut-off point of -2.0. The shape and fill of the data points reflect the location at which they were acquired. NAA/Cr₂ = N-acetyl-aspartate/Creatine-z-scores; see text for abbreviations in the legend.

Fig. 2-A illustrates the overall negative relationship between spike frequency data and

their NAA/Cr_z data ($\rho = -.341$; $n = 108$). Fig. 2-B presents this exact same data but with the y-axis rescaled using a power of 0.2 in order to better illustrate the distribution of the individual data points. When data from the 8 electrode positions were considered together across the 14 patients, spiking was present in 40 instances and absent in 72. When data from the 8 ¹H-MRSI subregions were considered together across the 14 patients, abnormal NAA/Cr_z values (*i.e.* more negative than -2.0) were found in 35 subregions and normal values in 73 subregions: (i) abnormal NAA/Cr_z and non-spiking was found in 16 subregions overall; (ii) abnormal NAA/Cr_z values and spiking was found in 19; (iii) normal NAA/Cr_z and spiking was found in 21; and (iv) normal NAA/Cr_z and no spiking was found in 52. Within individuals, a mean of 66% (range = 33 - 88%) of the sites showed concordance between the presence of spiking and the abnormality of the NAA/Cr_z value in that location (Table 1).

As shown in Fig. 2-C, when the spike frequency data were logarithmically transformed (leaving only the 40 subregions with non-zero frequencies) this negative relationship became slightly stronger ($\rho = -.442$; $r = -.338$). When the one extremely low NAA/Cr_z value outlier was removed from this analysis, this negative relationship still remained ($\rho = -.456$; $r = -.499$).

Table 2: Results of Spearman rank order (rho) and Pearson product moment correlation (r) for individual subregions

Electrode/ subregion	n of subregions	rho	r
T3 / Lt-Mid	7	-0.250	-0.369
T4 / Rt-Mid	6	0.029	0.160
T5 / Lt-Post	6	-0.429	-0.505
T6 / Rt-Post	3	-0.500	-0.233
F3 / Lt-Front	7	-0.519	-0.388
F4 / Rt-Front	7	-0.270	-0.270
C4 / Rt-Cent	3	1.000	0.961
C3 / Lt-Cent	1	n.a.	n.a.

n.a. = not applicable

As shown in Fig. 2-D and Table 2, for the most part, this negative relationship between NAA/Cr_z values and spike frequency remained even when we considered data from the 8 sites separately. It should be noted that: (i) the positive relationship at T4/Rt-Mid was due mostly to the one individual who had a normal NAA/Cr_z value but a very high spiking frequency; and (ii) the positive relationship at C4/Rt-Cent was associated with very little variability in NAA/Cr_z data.

DISCUSSION

The present study attempted to investigate the relationship between the spike frequency on surface EEG and the magnitude of the decrease in NAA/Cr as measured by ¹H-MRSI in patients with intractable partial epilepsy. We addressed this specific question, because we hypothesized that enhanced epileptic activity and more severe neuronal metabolic damage or dysfunction of epileptic areas should change in parallel. Our results suggest some correlation in the overall analysis. This holds true for most of the subregions.

The focal interictal spike represents the fundamental hallmark of partial epilepsy and its experimental neuronal correlate in intracellular recording is the paroxysmal depolarization shift^{280,281}. The detection of an interictal epileptiform discharge on surface EEG requires the synchronous firing of a large number of neurons within at least 6 cm² of cortical tissue^{282,283}. Quantification of surface spikes has been used for lateralization of the epileptogenic zone in temporal lobe epilepsy patients during presurgical evaluation^{284,285}. Looking specifically at the *frequency* of interictal spiking on surface EEG, Gotman *et al.*^{185,186} have shown that this can be influenced by seizure activity. Yet, the pathophysiological significance of this measure in epilepsy has not been investigated.

In ^1H -MR spectroscopy, the amino acid NAA is well accepted as a marker of cerebral neuronal integrity²⁴⁷. NAA decrease can be detected in various neurological diseases with neuronal damage^{149;150;277} and there seems to be a correlation between NAA decrease and clinical impairment in some diseases^{286;287}. In partial epilepsy, one study reports that seizure frequency correlates with the degree of NAA decrease²⁸⁸. In a recent article investigating 82 patients with TLE, Tasch *et al.* found that NAA/Cr was negatively correlated with the duration of epilepsy and the number of generalized tonic-clonic seizures²⁸⁹. The only experimental study, which addressed a similar question to ours by comparing increased electrical brain activity and metabolic changes, using phosphorus (^{31}P)-spectroscopy in the penicillin epilepsy model in rats, was reported by McLachlan *et al.*²⁹⁰. These authors found no differences in pH, phosphocreatine or adenosine-triphosphate levels between areas of active spiking, induced by topical application of penicillin, and the contralateral unaffected hemisphere or control animals. In contrast to our approach, spectroscopic measurements in this animal study were performed after a maximum of 60 min of continuous focal spiking and more importantly, this study used ^{31}P -spectroscopy, thus detecting metabolites different from those observed by ^1H -MRS. Therefore, it remains unclear, if or how neuronal metabolic dysfunction or damage as detected by *in vivo* spectroscopic methods pathophysiologically relates to epileptic activity.

Our study comprised only nonlesional cases except for two patients. In one patient, a focal cortical dysplasia of the frontal lobe was partly included. In the other patient, a periventricular nodular heterotopia was outside both the temporal and the frontal VOI. Therefore, NAA changes due to the underlying pathology as reported in cortical developmental malformations^{1;291} can be ruled out.

Although the ^1H -MRSI in our study did not provide coverage of the entire brain, we

believe our method is a reasonable approach because in all patients most active electrodes were assigned to corresponding brain regions in the ¹H-MRSI. Furthermore, metabolic abnormalities of epileptic foci are known to be more widespread than structural changes demonstrated by conventional MRI¹⁷⁵. Similarly, although the VOI predominantly included white matter as opposed to epileptic cortex, the white matter projections from epileptic cortex are very sensitive to abnormalities in TLE¹⁷⁵. Further support for our approach is given by the considerable spatial overlap of the two measures in our patients as also found in other studies^{176,292}. Finally, as already noted, interictal spikes detected on surface EEG must involve a considerable amount of cerebral tissue^{282,283}.

In our study, we tried to rule out any sleep-induced increase in spiking between patients by sampling over the same period of time in each patient²⁹³, and to minimize seizure-induced changes by appropriate choice of sample periods^{185,186}.

¹H-MRSI in all patients was performed either before or after prolonged video-EEG monitoring. We believe that NAA measurements remain constant during such a short period of time, since Cendes *et al.* observed no significant NAA/Cr differences between the ictal, interictal, and postictal states²⁴⁹.

In conclusion, our results indicate that spike frequency on surface EEG tends to be higher in regions of pronounced neuronal metabolic damage or dysfunction. However, we also found decreases in NAA in non-spiking areas. It is possible that there may have been spiking in these regions, which was not visible from the surface EEG. It appears therefore that spikes and NAA decreases often coincide spatially and vary together in intensity possibly reflecting the severity of the epileptogenic process. We believe it is the first time that spiking frequency can be related to a measure of neuronal dysfunction.

CHAPTER III

Clinical relevance of new types of MR-based techniques

There is a small percentage of patients with partial epilepsy referred for pre-surgical evaluation in which no visible lesion is detected on MRI. This group of 'MR-negative' patients represents a major problem in defining the epileptogenic area for surgical resection. Searching for alternative imaging methods, we investigated the clinical usefulness of magnetization transfer in epilepsy.

MRVol and temporal lobe ¹H-MRSI have proven to be useful in the lateralization of seizures. We sought alternative, more sophisticated, mathematical analyses of these MR data sets. Linear discriminant analyses were applied in order to predict video-EEG lateralization and to discriminate TLE from extra-TLE. These analyses test multivariate differences among groups and explore which variables alone and in combination are most useful for discriminating among groups, and which groups are most alike and most different.

¹H-MRSI is very sensitive to neuronal metabolic dysfunction and useful in lateralization of TLE, however, the prognostic value of this technique is unknown. We investigated this issue by analyzing ¹H-MRSI results and surgical outcome in a group of patients with bilateral hippocampal atrophy and TLE.

Paper 4: Magnetization transfer contrast in the lateralization of temporal lobe epilepsy.

Li LM, Narayanan S, Pike B, Andermann F, Dubeau F, Arnold DL.
Submitted.

SUMMARY

Background: A preliminary report of magnetization transfer ratio (MTR) measurement in three patients with temporal lobe epilepsy (TLE) and two controls has shown promising results.

Objective: To assess the clinical use of magnetization transfer ratio (MTR) for lateralizing patients with refractory temporal lobe epilepsy (TLE).

Patients/Methods: We compared the MTRs of amygdalae and hippocampi in 10 patients with unilateral TLE versus 10 normal control subjects.

Results: Three out of 10 patients had MTR values two standard deviation below the normal mean, and in only one of the three was the MTR abnormality concordant with electro-clinical lateralization.

Conclusion: MTR of amygdalae and hippocampi are not useful for the lateralization of TLE.

INTRODUCTION

MR imaging of brain produces images that reflect the distribution of water among various chemical environments. Hydrogen nuclei associated with various semi-solid (macro-molecular) components have extremely short T₂s (<~100 μs) and are not directly detectable with MRI since minimum echo times on clinical scanners are typically 2-orders of magnitude longer. However, interaction between semi-solid and bulk water protons results in a continuous exchange of magnetization, referred to as cross-relaxation or magnetization transfer^{188,189}. Magnetization transfer (MT) imaging detects this exchange by selectively saturating the semi-solid magnetization pool, and measuring the resulting decrease in the bulk water signal due to transfer of this saturation in regions undergoing exchange¹⁹⁰⁻¹⁹⁴. The biological meaning of magnetization transfer is still unclear, though abnormal MTR has been shown to correlate with low NAA in some other pathologies¹⁹⁵. A preliminary report of MT measurement in three patients with temporal lobe epilepsy (TLE) and two controls has shown promising results². We further investigated whether MT measurement could be of clinical utility in lateralizing patients with refractory TLE.

PATIENTS AND METHODS

Subjects

We selected 10 consecutive patients (7 women, mean age = 38 years, range 26 to 54) with unilateral non-foreign tissue lesional TLE referred for pre-surgical evaluation. The side of seizure origin was defined after comprehensive work-up, including prolonged video monitoring for seizure recording. Controls were mainly composed of research staff (7 men,

mean age = 32 years, range 19 to 51). All were in good health and none were taking any medication at the moment of scanning. There was no significant difference in age between patients and controls (t test, $p=0.18$)

MT acquisition and data analysis

MT imaging was acquired using a Philips Gyroscan ACS-III with a field strength of 1.5T. Fifty slices (3mm) T1-weighted and MT images was obtained using a pair of gradient echo acquisitions, without (No Saturation) and with (Saturation) MT saturation pulses respectively, using a TR= 1000 ms TE = 20ms. Semi-solid spin saturation was achieved using 1.2ms on -resonance $|2|$ binomial pulses ($|B_1| = 19 \mu\text{T}$) placed just prior to each slice selective excitation. Percentage difference ($100 \times [\text{No Sat} - \text{Sat}] / \text{No Sat}$) MT images were calculated after thresholding above the noise background.

Amygdalae and hippocampi were outlined on 1-mm thick contiguous T1 weighted images using a previously described protocol^[45,27].

After registration of the MT images with the 1 mm T1 image volume²⁹⁴, mean MT values for the outlined structures were computed using locally developed software.

MTR values below 2 standard deviation from the normal mean were considered abnormal.

RESULTS

Clinical information and MT ratios are shown in the Table. Volumetric measurements of amygdalae and hippocampi showed abnormal values in seven of 10 patients and these were concordant to the side of seizure origin. MT ratios in controls were very symmetrical and had

a relative narrow variation for amygdalae and hippocampi (see Table). MT ratios were more than 2SD below normal mean in three patients (Table: patients 1, 8 and 10), and were concordant to electro-clinical diagnosis in patient 1 only.

DISCUSSION

The results indicate that MT ratio measurements in amygdalae and hippocampi are not useful in the lateralization of temporal lobe epilepsy. We do not believe that the low sensitivity observed could be due to the MT acquisition and processing, because it is currently in use for studying multiple sclerosis with good results. The coefficient of variation in our control for hippocampus was larger than reported previously², which is not surprising in view of the very small sample size in that report. Even if we considered a 5% difference to be abnormal for hippocampus, we would have detected only one more patient (Table: pt. 6) with abnormal MT ratio.

The reasons why MTR was not low in cases with severely abnormal hippocampus are not clear. It could be that while in hippocampal sclerosis there is neuronal loss with astrogliosis causing volume decrease, the relative cell density in the outlined MR imaging ROI might not change enough to cause a significant drop in MT ratio. Although MTR is very sensitive to white matter lesion of multiple sclerosis, in epileptic lesion this appeared not to be the case, which might reflect different underlying pathophysiological mechanism of neuronal *vs.* axonal damage.

Table: Summary of clinical information, MTR and volumetric data

Subjects	Side of seizures	Age (years)	sex	Amygdalae			Hippocampi			Volumes (L-R)/(L+R)	
				Left	Right	(L-R)/(L+R)	Left	Right	(L-R)/(L+R)	Amygdalae	Hippocampi
TLE-1	Left	45	f	22.42	25.18	-0.06	26.07	25.43	0.01	-0.02	-0.03
TLE-2	Left	38	m	28.97	28.34	0.01	28.44	27.34	0.02	-0.03	-0.21
TLE-3	Left	38	f	27.04	28.53	-0.03	25.73	25.46	0.01	-0.06	-0.07
TLE-4	Left	40	f	28.32	26.93	0.03	28.13	26.88	0.02	-0.10	-0.27
TLE-5	Left	54	f	28.70	27.62	0.02	26.03	26.53	-0.01	-0.19	-0.11
TLE-6	Left	26	m	27.09	27.17	0.00	24.66	26.61	-0.04	0.01	-0.09
TLE-7	Right	41	m	30.41	28.32	0.04	27.28	26.76	0.01	0.03	-0.02
TLE-8	Right	39	f	21.24	18.48	0.07	19.21	21.21	-0.05	-0.01	0.17
TLE-9	Right	34	f	26.29	28.04	-0.03	27.23	27.57	-0.01	-0.03	0.10
TLE-10	Right	28	f	23.99	24.82	-0.02	22.30	21.65	0.01	-0.02	0.00
Control-1	-	25	m	28.24	26.96	0.02	26.98	27.43	-0.01	0.00	-0.04
Control-2	-	34	m	29.51	29.02	0.01	29.16	28.15	0.02	-0.03	-0.03
Control-3	-	35	m	28.31	30.56	-0.04	28.22	30.38	-0.04	-0.05	-0.01
Control-4	-	25	m	28.94	25.71	0.06	28.03	27.56	0.01	-0.05	-0.05
Control-5	-	46	m	27.31	28.12	-0.01	25.48	25.64	0.00	-0.04	-0.04
Control-6	-	19	m	28.39	26.58	0.03	25.33	26.11	-0.02	-0.01	-0.04
Control-7	-	51	f	25.72	24.10	0.03	23.91	22.10	0.04	-0.04	0.01
Control-8	-	34	f	27.83	25.31	0.05	25.38	24.61	0.02	-0.01	-0.01
Control-9	-	23	f	25.95	26.76	-0.02	24.51	22.71	0.04	-0.01	-0.01
Control-10	-	34	m	27.23	24.98	0.04	23.45	22.63	0.02	0.00	0.00
		Mean (control)		27.74	26.81	0.02	26.04	25.73	0.01	-0.03	-0.02
		SD (control)		1.22	1.97	0.03	1.95	2.73	0.02	0.02	0.02
		Mean - 2SD (control)		25.31	22.87	-0.05	22.15	20.28	-0.04	-0.06	-0.06
		Mean + 2SD (control)		30.18	30.75	0.08	29.94	31.19	0.05	0.01	0.02

Highlighted numbers are below 2 SD from the mean of controls

Paper 5: Lateralization of temporal lobe epilepsy (TLE) and discrimination of TLE from extra-TLE using pattern recognition on MR spectroscopic and volumetric data.

Li LM, Caramanos Z, Cendes F, Andermann F,
Antel S, Dubeau F, Arnold DL.
Epilepsia 2000 (in press).

Lippincott Williams & Wilkins

SUMMARY

Background: The results obtained with both MR volumetric (MRVol) and proton MR spectroscopic imaging ($^1\text{H-MRSI}$) for the lateralization of patients with temporal lobe epilepsy (TLE) are consistent with results derived from prolonged video-EEG monitoring.

Objective: We examined whether or not pattern analysis of MR volumetric (MRVol) and proton MR spectroscopic imaging ($^1\text{H-MRSI}$) data would enable (i) the accurate lateralization of temporal lobe epilepsy (TLE) and (ii) the discrimination of TLE from extra-temporal epilepsy (E-TLE).

Patients and Methods: For the *lateralization* analysis we used data from 150 non foreign tissue lesional TLE patients [88 left-sided (L-TLE), 46 right-sided (R-TLE), and 16 bilateral (Bi-TLE)]. For the *discrimination* of TLE from E-TLE we used data from 174 patients [145 with unilateral TLE, 14 with unilateral E-TLE, and 15 with widespread epileptogenic zones involving both the TL and extra-TL regions – multilobar epilepsy (Multi-L)]. A series of 'leave-one-out' cross-validated linear discriminant analyses were performed using the MRVol and $^1\text{H-MRSI}$ data sets in order to lateralize TLE and discriminate it from E-TLE.

Results: *Lateralization:* the 'leave-one-out' linear discriminant analyses were able to correctly lateralize (with a posterior probability > 0.50) 120 of the 134 (90%) L- and R-TLE patients. Imposing higher posterior probability (> 0.95) increased accuracy of lateralization to 98%, with only two discordant cases who underwent surgery on the side of EEG and both had bad outcome. *Discrimination:* the 'leave-one-out' linear discriminant analyses were able to correctly classify (with a posterior probability > 0.50) 142 of the 159 (89%) TLE and E-TLE patients. Accuracy increased slightly as higher posterior probability cut-offs were imposed,

with fewer patients being classified.

Conclusion: We have shown that pattern analysis of ^1H -MRSI and MRVol data can accurately lateralize TLE. Discriminating TLE from E-TLE was less accurate, probably due to presence of temporal lobe damage in some patients with E-TLE reflecting dual pathology.

INTRODUCTION

In the general population of developed countries, approximately 50 to 75 individuals out of every 100,000 experience non-provoked recurrent seizures every year.^{4,5} Current anti-epileptic drugs can control seizures in only 80% of individuals with epilepsy. Surgical treatment is an effective therapeutic option for those individuals who have medically-intractable epilepsy, especially those with well-localized temporal lobe epilepsy (TLE). It is important to note, however, that the success of surgical treatment in controlling an individual's seizures depends largely on the accurate localization, and subsequent resection, of the epileptogenic area^{66,67,69}. Unfortunately, in most cases, this is not easily determined.

At the present time, results from an individual's clinical and neurophysiological examinations which are both interpretable and congruent are regarded as the 'gold standard' for localizing the epileptogenic area. This usually involves a combination of video-monitoring and electroencephalographic (EEG) recording that is generally performed in a hospital setting: often for a prolonged period of time and under the reduction of medication. The duration of such video-EEG monitoring is dictated by the number of recorded seizures required for an unequivocal diagnosis. Furthermore, in some patients with no clear localization or lateralization of the epileptogenic area, an invasive neurophysiological approach is required for further clarification. This is often the case in those patients who are either diagnosed with bilateral TLE or who have shown conflicting clinical- and EEG-localizing features. Unfortunately, such a procedure increases the overall risk, cost, and complexity of the investigation.

Magnetic resonance (MR) imaging can often reveal underlying epileptogenic lesions in many patients with refractory epilepsy⁴⁵ and, thus, is continuing to play a more important role in the pre-surgical evaluation of such individuals. Moreover, the clinical utility of MR imaging in localizing individuals' epileptogenic lesions increases as other pre- and post-processing techniques such as FLAIR⁸⁰⁻⁸², volumetric measurement^{83-85;295;296}, and T₂ relaxometry⁸⁹⁻⁹¹ are used. For example, MR volumetric (MRVol) analyses have been shown to possess high sensitivity in detecting hippocampal sclerosis^{87;113;297;298}, the most common underlying pathology seen in surgical specimens removed from operated-TLE patients^{39;299}.

Proton MR spectroscopic imaging (¹H-MRSI) is another technique that is increasingly being used in the clinical study of epilepsy. ¹H-MRSI allows for the non-invasive, *in vivo* quantification of certain metabolites that are visible in the ¹H spectrum. The most intense signal which is visible in ¹H-MRSI of brain tissue arises from N-acetyl groups – mostly from the N-acetyl-aspartate (NAA)²⁴⁷. NAA has been demonstrated to be found exclusively in neurons and neuronal processes of mature brain^{124;247} and, thus, areas of decreased NAA signal intensity have been interpreted as reflecting either neuronal loss or dysfunction²⁴⁷. Creatine and phosphocreatine (Cr) are also readily visible in ¹H-MRSI of the brain. Cerebral Cr is stable or undergoes only minor changes in patients with epilepsy and, thus, tissue Cr intensity has been used as an internal standard against which to compare the relative changes in NAA intensity^{157-161;177}. ¹H-MRSI studies in our lab, as well as in those of other researchers, have found reduced NAA/Cr in the temporal lobes of patients with refractory TLE. Importantly, the maximum reduction in NAA/Cr is often lateralized to the side of seizure origin as defined by prolonged video-EEG monitoring^{115;116;157-159;174;176;178}.

An appropriate combination of these MRVol and ¹H-MRSI techniques should allow

us to non-invasively acquire structural and metabolic measurements of temporal lobe structures in a quick, safe, and repeatable manner. Indeed, the results of such MRV_{ol} and ¹H-MRSI studies have already been shown to be highly concordant with the results of prolonged video-EEG recordings in patients with TLE^{115,116}. In the present study, we examined whether or not pattern analysis of MRV_{ol} and ¹H-MRSI data would allow us to: (i) provide accurate lateralizations in patients with either left, right, or bilateral TLE; and/or (ii) provide accurate discrimination between patients with either TLE, extra-TLE, or multilobar epilepsy.

PATIENTS AND METHODS

Subjects

Patients with medically refractory epilepsy were recruited from the Epilepsy Service of the Montreal Neurological Institute and Hospital during their pre-surgical investigation. In order to define the epileptogenic area in each patient, prolonged video-EEG monitoring was performed using an International 10-20 System electrode placement, with additional electrodes if required. Classification of patients' epileptic syndromes was based on the system proposed by the International League Against Epilepsy in 1989²⁷¹. Seizure lateralization was defined as follows: predominately left or predominantly right when > 70% of recorded seizures were from that side; or bilateral when < 70% of recorded seizures were from any one side. We chose this lateralization cut-off of > 70% to reflect the fact that patients who have > 70% of seizures arising from one side often have good surgical results following resection of tissue from that side³⁰⁰.

Data from 150 non-foreign tissue lesional TLE patients were included in the lateralization analysis: 86 females and 64 males ranging between 12 and 64 years of age (mean age = 35 years). These 150 patients were divided into three groups: (i) 88 with predominantly

left-sided seizure onset (L-TLE); (ii) 46 with predominantly right-sided seizure onset (R-TLE); and (iii) 16 with bilateral seizure onset (Bi-TLE). None of these patients showed evidence of foreign tissue lesions.

Data from 174 lesional and non-lesional patients with localization-related epilepsy were included in the discrimination of TLE from extra-TLE (E-TLE) analysis: 97 females and 77 males ranging between 12 and 64 years of age (mean age = 35 years). These 174 patients were divided into three groups: (i) 145 with unilateral TLE (TLE); (ii) 14 with unilateral extra-TLE (E-TLE); and (iii) 15 with widespread multilobar epilepsy involving either only extra-temporal-lobe regions or both temporal-lobe and extra-temporal-lobe regions (Multi-L). Of the 145 TLE patients, 11 (7%) had foreign tissue lesions in their temporal lobes that were visible on MRI: 6 with cortical developmental malformations, 3 with vascular malformation, and 2 with tumors. Of the 14 E-TLE patients, 8 (57%) had lesions outside their temporal lobe that were visible on MRI: 6 had cortical developmental malformations and 2 had a focal atrophy. Of the 15 Multi-L patients, 3 (20%) had lesions outside their temporal lobe which were visible on MRI: 1 had cortical developmental malformation and 2 had bilateral posterior quadrant atrophy.

MRVol acquisition and data analysis

MRVol studies were performed using a Philips ACS II or III combined imaging and spectroscopy system (1.5 T, Philips Medical Systems, Best, The Netherlands). Because of changes in clinical practice at our institute, two MRVol protocols were used over the course of this study. Initially, we used 3-mm thick, contiguous slices which were perpendicular to the plane of the Sylvian fissure and which were acquired with a three-dimensional fast-field echo or inversion recovery sequence. Subsequently, we used global MR images obtained with an

interpulse delay (TR) of 18 ms, a spin-echo refocusing time (TE) of 10 ms, a 30° angle, and 1 mm isotropic voxels. The MRI data were exported to a SunSparc workstation and the volumes of the left and right amygdaloid and hippocampal formations were calculated using locally-developed software and the anatomical protocol developed by Watson and colleagues²⁷⁰. For each individual, left-right asymmetry indices were computed separately for the amygdaloid and the hippocampal formations ($asy = \text{left-right} / [(\text{left} + \text{right}) / 2]$).

Each individual patient's six MRVol values were compared to those obtained similarly in a group [mean (standard deviation)] of healthy normal control subjects [$n = 30$ for the first protocol, amygdaloid volume: left = 2812.33 mm³ (255.23), right = 2843.95 mm³ (265.54), left-right asymmetry = -0.01 (0.04); hippocampal volume: left = 4563.6 mm³ (257.9), right = 4670.76 mm³ (275.26), left-right asymmetry = -0.02 (0.02); $n = 22$ for the second protocol, amygdaloid volume: left = 2452.87 mm³ (150.76), right = 2483.92 mm³ (146.59), left-right asymmetry = -0.01 (0.04); hippocampal volume: left = 4014.48 mm³ (163.03), right = 4040.62 mm³ (182.35), left-right asymmetry = -0.01 (0.02)].

¹H-MRSI acquisition and data analysis

¹H-MRSI studies were performed using the same Philips ACS II or III combined imaging and spectroscopy system (1.5 T, Philips Medical Systems, Best, The Netherlands) as for the MRVol. Scout images were obtained in the axial and sagittal planes. These were followed by the acquisition of a multi-slice transverse spin-echo MRI using a TR of 2000 ms and a TE of 30 ms. The temporal lobe ¹H-MRSI volume of interest (VOI) included part of the head, body, and tail of the left and right hippocampi, as well as portions of gray and white matter in the mid and posterior portions of the temporal lobes. The size of this VOI was approximately 85-100 mm in the left-right axis, 75-95 mm in the antero-posterior axis, and 20

mm in thickness. After post-processing, individual voxels within the VOI were approximately 12 mm x 12 mm x 20 mm in size.

A water-suppressed ^1H -MRSI was acquired from the VOI [TR = 2000 ms, TE = 272 ms, 250 x 250 mm field of view (FOV), and 32 x 32 phase-encoding steps], followed by a ^1H -MRSI without water suppression (TR = 850 ms, TE = 272 ms, 250 x 250 mm FOV, and 16 x 16 phase-encoding steps). Post-processing included zero-filling the non-water-suppressed ^1H -MRSI to obtain 32 x 32 profiles, followed by application of a mild Gaussian k -space filter and an inverse 2D Fourier transformation to both water-suppressed and non-suppressed ^1H -MRSI scans. The resulting time domain signal was left-shifted and subtracted from itself to improve water suppression ²⁶⁹.

^1H -MRSI spectra were excluded from the analyses if they were artifactually broadened (*i.e.* full width at half maximum >10 Hz). For each subject, locally-developed software was used to calculate the average NAA/Cr values for the mid and posterior regions of interest (ROI) in both the left and right medial temporal lobes. The mid temporal ROI included tissue from the head and body of the hippocampus, whereas the posterior temporal ROI included tissue from the tail of the hippocampus. Both ROIs also included surrounding portions of gray and white matter. All ^1H -MRSI analyses were done “blind” as to the side of the seizure focus. For each individual, left-right asymmetry indices were computed separately for the mid and the post ROIs ($\text{asy} = \text{left-right}/[(\text{left}+\text{right})/2]$).

Two raters (LML and FC) analyzed the ^1H -MRSI, and each individual patient’s six ^1H -MRSI-NAA/Cr values were compared to those obtained similarly in a group of healthy normal control subjects [LML control group values, $n = 40$, mid temporal: left = 4.13 (0.17), right = 4.16 (0.16), left-right asymmetry = -0.01 (0.03); posterior temporal: left = 4.33 (0.21),

right = 4.38 (0.21), left-right asymmetry = -0.01 (0.04); FC control group values, $n = 21$ for other group control, mid temporal: left = 4.17 (0.25), right = 4.26 (0.22), left-right asymmetry = -0.02 (0.03), posterior temporal: left = 4.54 (0.23), right = 4.57 (0.21), left-right asymmetry = -0.01 (0.03)].

Statistical analyses

All statistical analyses were performed using SYSTAT 7.01 for Windows.

STANDARDIZED SCORES

In order to directly compare the findings across the two types of MR imaging techniques (MRVol and ¹H-MRSI) and between the two MRVol protocols (3 mm and 1 mm), each of the patients' six ¹H-MRSI and six MRVol measures were converted into z-scores relative to the appropriate normal control group. Thus, for any MR measure, a patient's score represents the difference of that patient's MR value from the mean value of the appropriate normal controls on that measure; this difference in means was expressed in units of the appropriate normal control group's standard deviation on that measure.

GROUP DIFFERENCES

One-way multivariate analysis of variance (MANOVA) was used to determine if the groups differed in their pattern across the twelve MR values. Subsequent one-way univariate analyses of variance (ANOVA) followed by Tukey's HSD *post hoc* pairwise comparisons were used in order to determine which groups differed from which on the various individual MR-based measures. For these analyses, differences were assumed to be significant with $p < 0.05$.

CLASSIFICATION OF INDIVIDUAL PATIENTS

A series of cross-validated linear discriminant analyses were performed in order to

classify: (i) patients with L- vs. R-TLE; (ii) patients with L-, vs. R-, vs. Bi-TLE; (iii) patients with TLE vs. E-TLE; and (iv) patients with TLE vs. E-TLE vs. Multi-L. A series of 'leave-one-out' linear discriminant analyses based on the patients' profiles across the 12 MR values was used in the two-group classifications [*i.e.* (i) L- vs. R-TLE and (iii) TLE vs. E-TLE]. A slightly different two-step process was used for the three-group classifications [*i.e.* (ii) L- vs. R- vs. Bi-TLE and (iv) TLE vs. E-TLE vs. Multi-L]. For example, for the L- vs. R- vs. Bi-TLE classifications, the set of linear discriminant functions based on the 12 MR features that best separated the L- and R-TLE patients were also applied to the Bi-TLE patients. Each L-, R-, and Bi-TLE patients' resulting pair of Mahalanobis distances were then used in a 'leave-one-out' linear discriminant analysis approach in order to classify the patients as having L-, R-, or Bi-TLE. An analogous procedure was used to discriminate between patients with TLE, E-TLE, and Multi-L.

For the two sets of lateralization analyses [*i.e.* (i) L- vs. R-TLE and (ii) L- vs. R- vs. Bi-TLE], each individual's data were categorized as arising from either their left or their right hemisphere. On the other hand, for the two sets of differential diagnosis analyses [*i.e.* (iii) TLE vs. E-TLE and (iv) TLE vs. E-TLE vs. Multi-L], each individual's data were expressed in terms of arising from either the hemisphere ipsilateral or contralateral to the side of their epileptogenic disturbance.

The posterior probability associated with each classification indicated its degree of prediction strength and Cohen's Kappa statistic was used to evaluate the degree of agreement between each set of predicted classifications and the actual results from the patients' prolonged video-EEG recordings (Kappa < 0.4 = poor agreement, 0.4 < Kappa < 0.6 = fair, 0.6 < Kappa < 0.75 = good, 0.75 < Kappa < 0.90 = strong, Kappa > 0.90 = very strong).

Graphical Representation

GROUP DIFFERENCES

Box-and-whiskers plots superimposed with dot plots were used to show the range and central tendencies of the patient groups' standardized MR data. In these plots, the horizontal lines within the boxes mark the median value of the group and the edges of the boxes, called hinges, mark the first and third quartiles: the central 50% of the group data falls within the range of the box. The whiskers are the lines which extend vertically from the boxes and show the range of the values that fall within 1.5 spreads of the hinges. Outliers are plotted with asterisks and far outliers are marked with open circles. The dot plots show the individual data points in order to better illustrate the distribution of the data.

CLASSIFICATION OF INDIVIDUAL PATIENTS

Line plots were used to show the results of the leave-one-out linear discriminant analyses as a function of increasing level of associated posterior probability.

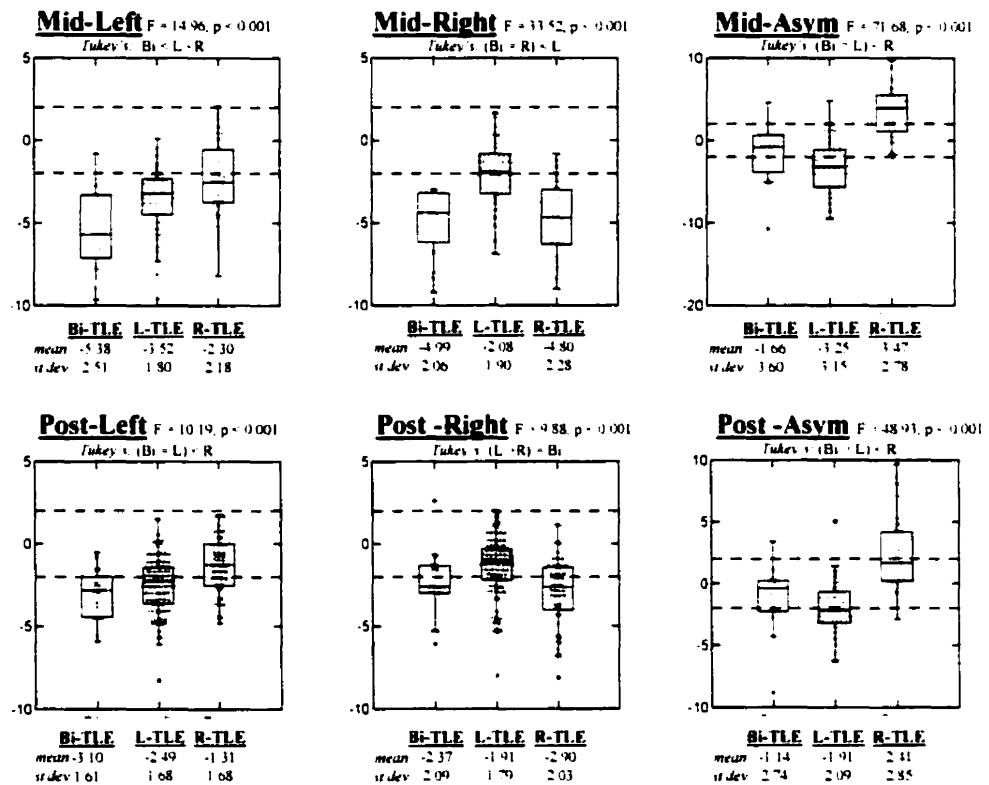
RESULTS

Lateralization

MANOVA found a significant difference among the L-, R-, and Bi-TLE groups' profiles across the 12 MR-based features (Wilk's $\lambda = 0.292$, $F_{24, 274} = 79.655$, $p < 0.001$).

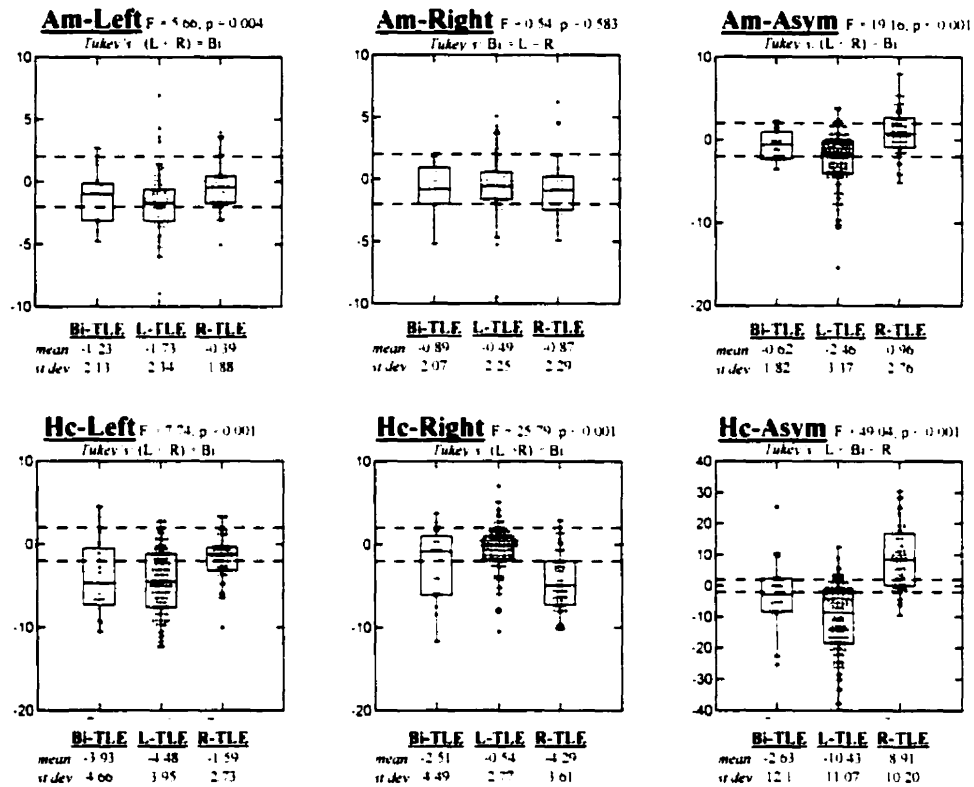
Subsequent ANOVAs found significant differences on 11 of the 12 MR measures. These findings are summarized in Figure 1.

Figure 1a: Box-and-whiskers plots of ^1H -MRSI for Bi- (n=16), L- (n=88) and R-(n=46) TLE. Results of one-way ANOVA (2, 147), and Tukey's HSD *post hoc* pairwise comparisons are displayed assuming significance when $p < .05$.



Units in y axis are NAA/Cr z-scores, the two horizontal dashed lines across the boxes represent z-scores of 2 and -2.

Figure 1b: Box-and-whiskers plots of MRVol for Bi- (n=16), L- (n=88) and R-(n=46) TLE. Results of one-way ANOVA (2, 147), and Tukey's HSD *post hoc* pairwise comparisons are displayed assuming significance when $p < .05$.



Units in y axis are structure's volume z-scores, the two horizontal dashed lines across the boxes represent z-scores of 2 and -2.

In the two-group linear discriminant analyses, 120 of the 134 patients (90%) were classified in agreement with the results of their video-EEG recording with a posterior

probability > 0.50: 78 of the 88 L-TLE (89%) and 42 of the 46 R-TLE patients (91%). This agreement increased as higher posterior probability cut-offs were imposed (see Figure 2a and Table 1), imposing a posterior probability of 0.95 we were able to accurately classify 98% of the patients, with only two patients with discordant classification. Importantly, these two patients underwent surgery on the side of EEG lateralization and had bad outcome. In the three-group linear discriminant analyses, 117 of the 150 patients (78%) were classified in agreement with the results of their video-EEG recording with a posterior probability > 0.33: 72 of the 88 L-TLE (82%), 39 of the 46 R-TLE patients (84%), and 6 of the 16 Bi-TLE patients (37%). Again, agreement increased as higher posterior probability cut-offs were imposed; this time however, fewer patients were capable of being classified (see Figure 2b and Table 2).

Figure 2: 'Leave-one-out' linear discriminant functions show a strong predictive value in lateralizing patients with temporal lobe epilepsy

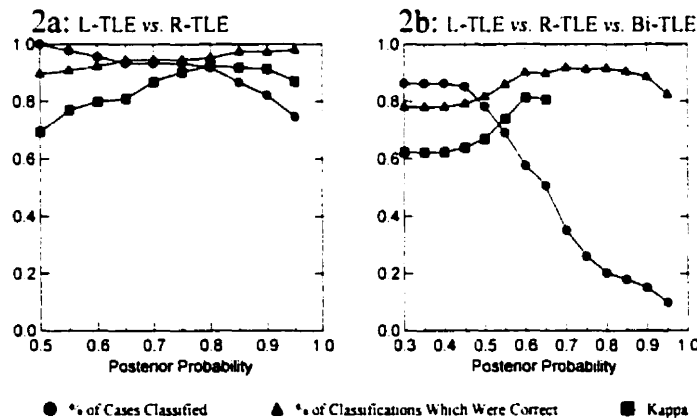


Table 1: 'Leave-one-out' discriminant analyses of ¹H-MRSI and MRVol profiles in L- and R-TLE patients provide very strong predictions of TLE lateralization based on prolonged video-EEG monitoring

Posterior Probability	L-TLE Predicted		R-TLE Predicted		Classified		Cohen's	
	L-TLE	R-TLE	L-TLE	R-TLE	Classified	Correct	Kappa	Agreement
>0.50	78	4	10	42	134 (100%)	120 (90%)	0.69	good
>0.55	78	4	8	41	131 (98%)	119 (91%)	0.77	very good
>0.60	78	4	6	40	128 (96%)	118 (92%)	0.80	strong
>0.65	78	3	4	40	125 (93%)	118 (94%)	0.81	strong
>0.70	78	3	4	40	125 (93%)	118 (94%)	0.87	strong
>0.75	78	3	4	40	125 (93%)	118 (94%)	0.90	very strong
>0.80	78	2	4	39	123 (92%)	117 (95%)	0.92	very strong
>0.85	76	0	3	37	116 (87%)	113 (97%)	0.92	very strong
>0.90	74	0	3	33	110 (82%)	107 (97%)	0.91	very strong
>0.95	70	0	2	28	100 (75%)	98 (98%)	0.87	strong

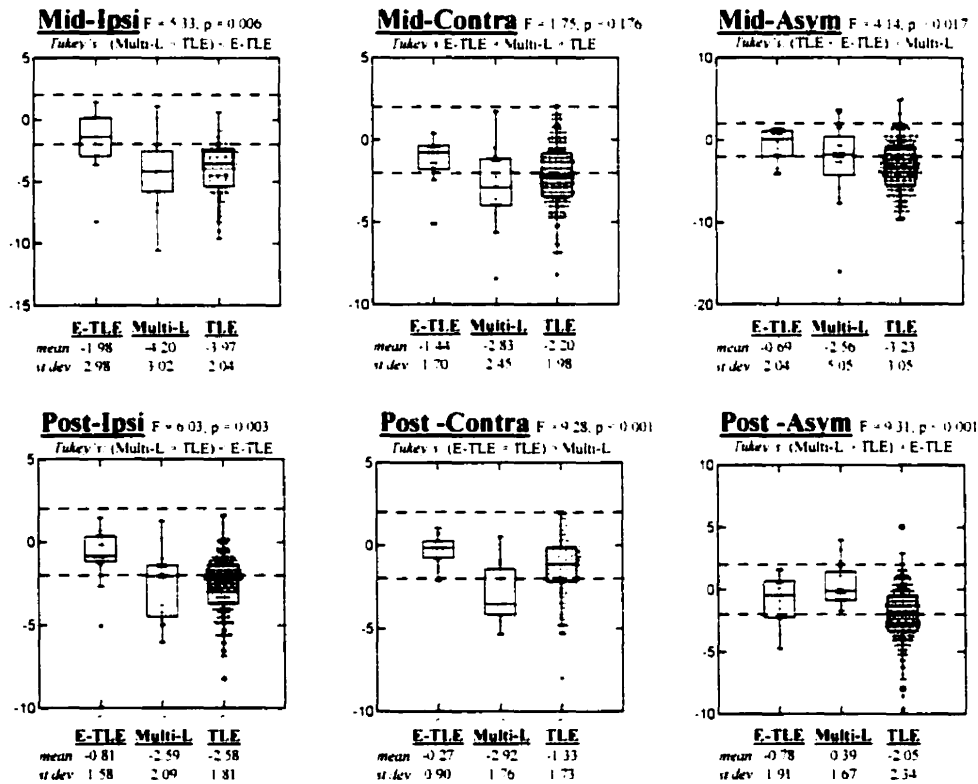
Table 2: 'Leave-one-out' discriminant analyses on ¹H-MRSI and MRVol profiles provide strong predictions of the TLE lateralization based on prolonged video-EEG monitoring, even with addition of patients with bilateral TLE

<u>Posterior Probability</u>	<u>Bi-TLE Predicted</u>			<u>L-TLE Predicted</u>			<u>R-TLE Predicted</u>			<u>Classified (%)</u>	<u>Classified Correct (%)</u>	<u>Cohen's Kappa</u>	<u>Agreement</u>
	<u>Bi-TLE</u>	<u>L-TLE</u>	<u>R-TLE</u>	<u>Bi-TLE</u>	<u>L-TLE</u>	<u>R-TLE</u>	<u>Bi-TLE</u>	<u>L-TLE</u>	<u>R-TLE</u>				
>0.30	6	13	7	6	72	0	4	3	39	150 (100%)	117 (78%)	0.62	good
>0.35	6	13	7	6	72	0	4	3	39	150 (100%)	117 (78%)	0.62	good
>0.40	6	13	7	6	72	0	4	3	39	150 (100%)	117 (78%)	0.62	good
>0.45	6	12	6	6	72	0	4	3	39	148 (99%)	117 (79%)	0.64	good
>0.50	4	10	3	5	70	0	4	3	37	136 (91%)	111 (82%)	0.67	good
>0.55	3	4	1	5	64	0	4	3	36	120 (80%)	103 (86%)	0.74	very good
>0.60	2	2	0	4	53	0	2	2	35	100 (67%)	90 (90%)	0.81	strong
>0.65	0	1	0	4	45	0	2	2	34	88 (59%)	79 (90%)	0.81	strong
>0.70	0	0	0	2	25	0	1	2	31	61 (41%)	56 (92%)	0.00	--
>0.75	0	0	0	1	13	0	1	2	28	45 (30%)	41 (91%)	0.00	--
>0.80	0	0	0	0	6	0	1	2	26	35 (23%)	32 (91%)	0.00	--
>0.85	0	0	0	0	2	0	1	2	26	31 (21%)	28 (90%)	0.00	--
>0.90	0	0	0	0	1	0	1	2	22	26 (17%)	23 (88%)	0.00	--
>0.95	0	0	0	0	0	0	1	2	14	17 (11%)	14 (82%)	0.00	--

Discrimination of TLE from E-TLE and Multi-L

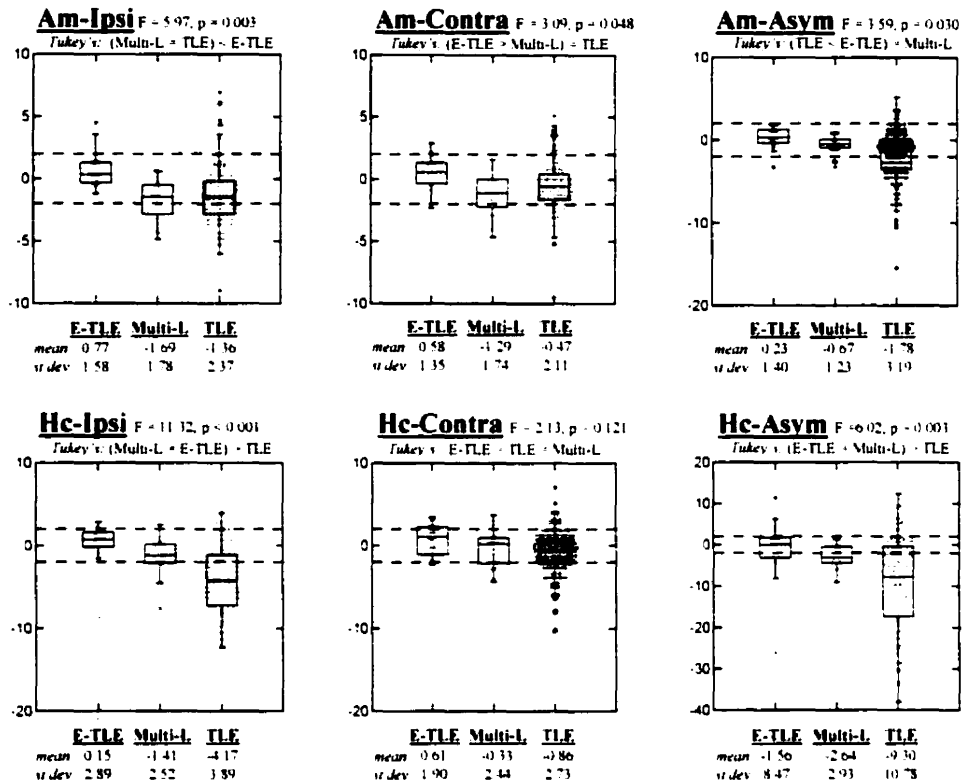
MANOVA found a significant difference among the TLE, E-TLE, and Multi-L groups' profiles across the 12 MR-based features (Wilk's $\lambda = 0.649$, $F_{24, 322} = 3.212$, $p < 0.001$). Subsequent ANOVAs found significant differences on 10 of the 12 MR measures. These findings are summarized in Figure 3.

Figure 3a: Box-and-whiskers plots of ¹H-MRSI E-TLE (=14), Multi-L (n=15) and TLE (n=145). Results of one-way ANOVA (2, 171), and Tukey's HSD *post hoc* pairwise comparisons are displayed assuming significance when $p < .05$.



Units in y axis are NAA/Cr z-scores, the two horizontal dashed lines across the boxes represent z-scores of 2 and -2.

Figure 3b: Box-and-whiskers plots of MRVol for E-TLE (=14), Multi-L (n=15) and TLE (n=145). Results of one-way ANOVA (2, 171), and Tukey's HSD *post hoc* pairwise comparisons are displayed assuming significance when $p < .05$.



Units in y axis are structure's volume z-scores, the two horizontal dashed lines across the boxes represent z-scores of 2 and -2.

In the two-group linear discriminant analyses, 142 of the 159 patients (89%) were classified in agreement with the results of their video-EEG recording with a posterior probability > 0.50: 131 of the 145 TLE patients (90%) and 11 of the 14 E-TLE patients (79%). Agreement increased slightly as higher posterior probability cut-offs were imposed but, again, fewer patients were classified overall (see Figure 4a and Table 3). In the three-group linear discriminant analyses, only 105 of the 174 patients (60%) were classified in agreement with the

results of their video-EEG recording with a posterior probability > 0.33 : 90 of the 145 TLE patients (62%), 12 of the 14 E-TLE patients (85%), and only 3 of the 15 Multi-L patients (20%). Moreover, in this set of analyses, imposing a higher posterior probability cut-off did not increase the accuracy of classification (see Figure 4b, Table 4).

Figure 4: ‘Leave-one-out’ linear discriminant functions show a poor differential diagnosis predictive value in patients with localization-related epilepsy

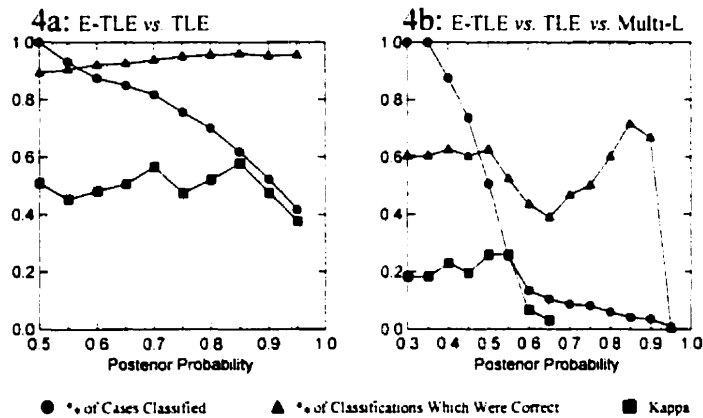


Table 3: 'Leave-one-out' discriminant analyses of ¹H-MRSI and MRVol profiles of patients with TLE and E-TLE provide fair predictions of epileptic anatomical localization based on prolonged video-EEG monitoring

Posterior Probability	E-TLE Predicted		TLE Predicted		Classified		Cohen's	
	E-TLE	TLE	E-TLE	TLE	Classified	Correct	Kappa	Agreement
>0.50	11	14	3	131	159 (100%)	142 (89%)	0.51	fair
>0.55	7	11	3	127	148 (93%)	134 (91%)	0.45	fair
>0.60	6	8	3	122	139 (87%)	128 (92%)	0.48	fair
>0.65	6	7	3	119	135 (85%)	125 (93%)	0.51	fair
>0.70	6	5	3	116	130 (82%)	122 (94%)	0.57	fair
>0.75	3	3	3	111	120 (75%)	114 (95%)	0.47	fair
>0.80	3	2	3	103	111 (70%)	106 (95%)	0.52	fair
>0.85	3	2	2	91	98 (62%)	94 (96%)	0.58	fair
>0.90	2	2	2	77	83 (52%)	79 (95%)	0.48	fair
>0.95	1	1	2	62	66 (42%)	63 (95%)	0.38	poor

Table 4: 'Leave-one-out' discriminant analyses of ¹H-MRSI and MRVol profiles, with addition of patients with multilobar epilepsy, provide poor predictions of epileptic anatomical localization based on prolonged video-EEG monitoring

Posterior Probability	E-TLE Predicted			Multi-L Predicted			TLE Predicted			Classified	Classified Correct	Cohen's Kappa	Agreement
	E-TLE	Multi-L	TLE	E-TLE	Multi-L	TLE	E-TLE	Multi-L	TLE				
>0.30	12	3	20	1	3	35	1	9	90	174 (100%)	105 (60%)	0.18	poor
>0.35	12	3	20	1	3	35	1	9	90	174 (100%)	105 (60%)	0.18	poor
>0.40	12	3	15	1	3	30	1	7	80	152 (87%)	95 (63%)	0.23	poor
>0.45	11	2	11	1	1	29	1	7	65	128 (74%)	77 (60%)	0.19	poor
>0.50	11	2	8	0	0	17	1	5	44	88 (51%)	55 (63%)	0.26	poor
>0.55	11	2	5	0	0	10	0	4	12	44 (25%)	23 (52%)	0.26	poor
>0.60	10	2	5	0	0	3	0	3	0	23 (13%)	10 (43%)	0.07	poor
>0.65	7	2	5	0	0	2	0	2	0	18 (10%)	7 (39%)	0.03	poor
>0.70	7	2	5	0	0	1	0	0	0	15 (9%)	7 (47%)	0.00	--
>0.75	7	2	4	0	0	1	0	0	0	14 (8%)	7 (50%)	0.00	--
>0.80	6	2	2	0	0	0	0	0	0	10 (6%)	6 (60%)	0.00	--
>0.85	5	1	1	0	0	0	0	0	0	7 (4%)	5 (71%)	0.00	--
>0.90	4	1	1	0	0	0	0	0	0	6 (3%)	4 (67%)	0.00	--
>0.95	0	0	1	0	0	0	0	0	0	1 (1%)	0 (0%)	0.00	--

DISCUSSION

In the present study we examined whether or not pattern analysis of MRVol and ¹H-MRSI data would allow us to accurately lateralize TLE and discriminate TLE from E-TLE. We found that a leave-one-out linear discriminant analysis approach allowed us to accurately lateralize TLE, but not to discriminate TLE from other non-TLEs. Moreover, we believe our approach added information to the conventional approach of using a cutoff of two standard deviations from the means of normal controls for characterizing findings as normal or abnormal. By imposing higher posterior-probability cut-off we increase accuracy of our lateralization from 90% to 98% (Table 1). Our discriminant function takes into consideration the differences across the 12 features at once and each individual's predicted group membership is associated with posterior-probability, that provides physicians, not only the lateralization/localization of seizures, but also with a degree of certainty associated with MR-based diagnosis which should aid in defining the subsequent steps of clinical investigation strategy.

Lateralization. Very few disagreements were found between individuals' video-EEG diagnoses and our MR-based predictions in the two-group analyses (*i.e.* L- vs. R-TLE). It should be noted that surgical results in patients with discordant MR results and EEG findings have, thus far, been unsatisfactory ¹¹⁵. In our previous study ¹¹⁵, such discordance between MRI and EEG was seen in three patients (3%), all three were operated on the side of maximal EEG abnormality with no major improvement ¹¹⁵. On the other hand, a higher number of disagreements were found in the three-group analysis (*i.e.* L- vs. R- vs. Bi-TLE). Most of these involved individuals with unilateral TLE being diagnosed as having Bi-TLE and vice-versa.

Discrimination of TLE from E-TLE and multi-L. A fair-sized agreement was found

between our predictions and the actual video-EEG findings in the two-group analysis (*i.e.* TLE vs. E-TLE). There was poor agreement, however, in the three-group analysis (*i.e.* TLE vs. E-TLE vs. Multi-L): with most disagreements involving the TLE and Multi-L patients. This might be expected since both of these patient types had some degree of temporal lobe involvement. Interestingly, the medial temporal-lobe ¹H-MRSI results in patients with E-TLE tended to be more abnormal than their hippocampal MRVol results (compare figures 3a:Mid-Ipsi and 3b:Hc-Ipsi). For instance, four (28%) E-TLE patients with normal hippocampal volumes had significant NAA reduction. Thus, it appears that the neuronal metabolic disturbances we found using ¹H-MRSI may be less specific than the structural abnormalities we found using MRVol, and that these ¹H-MRSI abnormalities may be present in the temporal lobes of some patients with E-TLE. Several different mechanisms might be responsible for this distant and/or widespread underlying neuronal dysfunction. These might include: (i) the effect of prolonged seizures; (ii) the presence of ‘hidden dual pathology’; and (iii) the presence of an unseen, widespread epileptogenic area. The first hypothesis is supported by finding in animal kindling model^{301,302}. The two last assumptions have implications in surgical strategy, in which the extent of surgical removal is important. It has been demonstrated that in some patients, NAA reduction in normal hippocampal volumes might represent subtle hippocampal sclerosis¹¹⁵. In our previous study on patients with dual pathology, the best results were seen when both the extra-hippocampal lesion and atrophic hippocampus were removed²⁷⁵. Furthermore, the degree of hippocampal atrophy did not influence the result, suggesting that even small degree of hippocampal atrophy accounted for poor surgical outcome²⁷⁵.

Our limited ability to discriminate TLE from E-TLE and Multi-L can, in part, be explained by: (i) the limited sample sizes of our E-TLE and Multi-L groups; (ii) our lack of ¹H-MRSI coverage of extra-TL regions; and (iii) the mathematical limitations of our linear

discriminant technique. These last two limitations can be overcome by: (i) the use of multi-slice ^1H -MRSI covering extra-TL regions combined with other MR quantification techniques of extra-TL regions such as gray/white matter ratio analysis of the whole brain³⁰³; and (ii) the use of non-linear neural-network or machine-intelligence analytical approaches to increase our computational power and, thus, possibly improve our diagnostic accuracy.

The survey on worldwide epilepsy surgery programs conducted by the Commission of the International League Against Epilepsy showed that only approximately 30% of patients who undergo extensive pre-surgical video-EEG investigations will eventually go on to have surgery⁷⁰. This is particularly the case in patients with no identifiable MR abnormality, in whom the chance of proceeding to surgery, even after invasive intracranial recording, is very low³⁰⁴. Therefore, a cost-effective epilepsy surgery program would therefore benefit from a means to select those patients who are most suitable for such neurophysiological investigation and, eventually, for such a surgical intervention. In this study, pattern analysis of MRVol and ^1H -MRSI data was shown to be a strong predictor of the epileptogenic area in patients with TLE. Moreover these MR techniques are safe, easy, and non-invasive and they have been shown to be strong predictors of surgical outcome^{70,201,203-205}. Acquisition and interpretation of prolonged video-EEG monitoring compared to MRVol and ^1H -MRSI, is more laborious, time consuming, and presents some risks for the patients. For these reasons, we propose that the pre-surgical investigation of seizure patients should start with routine outpatients EEGs and MR-based techniques that, if necessary, could be complemented with prolonged video-EEG monitoring.

Paper 6: Prognostic value of proton MR spectroscopic imaging in surgical outcome of patients with intractable temporal lobe epilepsy and bilateral hippocampal atrophy.

Li LM, Cendes F, Antel S, Andermann F,
Dubeau F, Serles W, Olivier A, Arnold DL.
Annals of Neurology 2000;47:195-200.

Lippincott Williams & Wilkins

SUMMARY

Background: Patients with intractable temporal lobe epilepsy (TLE) and bilateral hippocampal atrophy have less satisfactory surgical results than patients with unilateral hippocampal atrophy.

Objective: To assess which features of temporal lobe proton MR spectroscopic imaging ($^1\text{H-MRSI}$) are associated with satisfactory surgical outcome in patients with intractable temporal lobe epilepsy (TLE) and bilateral hippocampal atrophy.

Patients/Methods: We studied 21 patients with intractable TLE and bilateral hippocampal atrophy defined by MRI volumetric measurements who underwent surgical treatment. $^1\text{H-MRSI}$ was used to determine the relative resonance intensity ratio of the neuronal marker N-acetyl-aspartate to creatine+phosphocreatine (NAA/Cr) for mid and posterior temporal lobe regions of the left and right hemisphere, as well as an asymmetry index. Values lower than 2 standard deviations below the normal mean were considered abnormal. We used Engel's classification to assess surgical outcome with respect to seizure control.

Results: Eleven patients (52%) were in class I-II and ten (48%) were in class III-IV. All 21 were operated on the side of maximal EEG lateralization. Concordant lateralization of decreases in NAA/Cr to the side of surgery and normal NAA/Cr values in the contralateral posterior-temporal region were significantly associated with good surgical outcome: 11/16 (69%) patients with $^1\text{H-MRSI}$ abnormalities concordant with EEG lateralization and none of the 5 patients with non-concordant $^1\text{H-MRSI}$ had good outcome (class I-II); 10/13 (77%) patients with normal NAA/Cr contralateral to the EEG lateralization versus 1/8 (12.5%) of

those with NAA/Cr reduction contralateral to EEG lateralization were in class I-II (Fisher's exact test, 2-tailed $p < 0.05$). Regression-correlation analysis showed significant linear correlation between the mid-temporal NAA/Cr relative symmetry ratio and surgical outcome; the greater the asymmetry the better the outcome ($p=0.007$).

Conclusion: Discriminant ^1H -MRSI features associated with favorable surgical outcome in patients with TLE and bilateral hippocampal atrophy were: 1) concordant ^1H -MRSI lateralization, 2) greater side to side asymmetry of NAA/Cr, and 3) absence of contralateral posterior NAA/Cr reduction.

INTRODUCTION

MR volumetric studies (MRVol) of mesial temporal structures have proven useful in the pre-surgical evaluation of patients with non-lesional intractable temporal lobe epilepsy (TLE)^{83-85,93}. In addition to the ability to lateralize seizures, MRVol provide prognostic information^{201-204,305,306}. We and others have shown that different patterns of hippocampal atrophy in patients with intractable TLE yield distinct surgical results^{201,204,305,307}. The best outcome is seen in patients with unilateral hippocampal atrophy^{201,202}. On the other hand, patients with normal hippocampal volume or those with bilateral hippocampal atrophy have less satisfactory outcome with approximately 50% achieving good seizure control (Engel's class I-II)^{201,203}.

Proton MR spectroscopic imaging (¹H-MRSI) allows measurement of the neuronal marker N-acetyl-aspartate (NAA), the main contributor to the N-acetyl group signal seen at 2.02 ppm of the brain spectrum²⁴⁷. The side of maximal NAA reduction shows very good concordance to the side of seizure origin in patients with TLE^{115,116,157,176-178}. The metabolic abnormality seen ¹H-MRSI is at times more extensive than the epileptogenic area defined by EEG and/or structural imaging^{115,178,268}. For instance, bilateral relative NAA to creatine+phosphocreatine (NAA/Cr) reduction is seen in 18%¹⁷⁶ to 50%¹⁷⁸ of patients with unilateral TLE, and the NAA/Cr decreases are found beyond EEG focus in extra-temporal lobe epilepsy patients²⁶⁸. Whether a widespread metabolic abnormality might also indicate a widespread underlying epileptogenic process, with a distinctly worse prognosis in surgical result remains uncertain.

The objective of this study was to assess which features of temporal lobe ¹H-MRSI are associated with good surgical outcome in patients with bilateral hippocampal atrophy and

intractable TLE.

PATIENTS AND METHODS

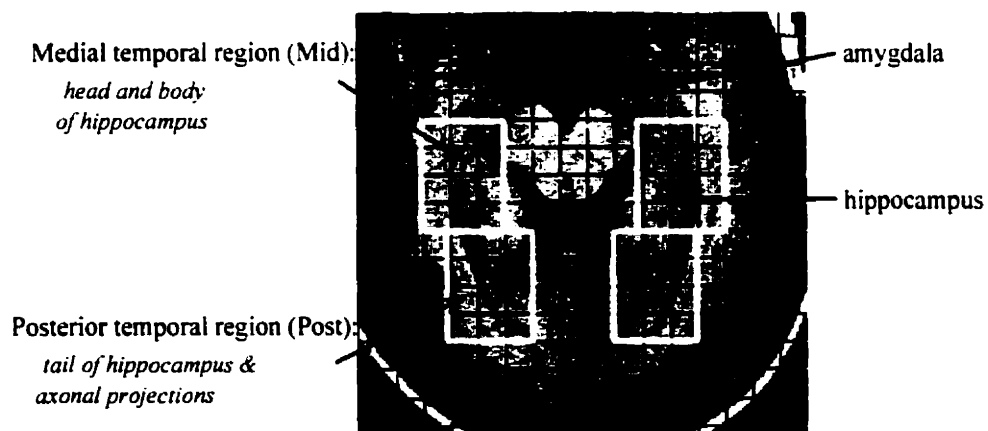
We studied twenty-one patients with bilateral hippocampal atrophy (12 women) with a mean age of 37 years (range 16 - 62 years) who underwent surgical treatment for intractable TLE. The mean post-operative follow-up was 34 months (range 12 - 60 months).

All patients had electro-clinical manifestations of TLE. Sixteen had temporal-limbic auras. The mean age of habitual seizure onset was 14 years (range from few weeks of life to 31 years). Five patients had febrile convulsions in early childhood, four had meningitis or encephalitis, two had a history of head trauma, and the remaining 10 had no identified risk factors. Six patients had a family history of epilepsy.

All 21 patients had diagnostic MR imaging using a Philips 1.5 T combined imaging and spectroscopy system (Philips Medical Systems, Best, The Netherlands). The protocol consisted of sagittal and coronal T1 weighted (TR 550, TE 19 ms) images, followed by axial proton density (TR 2000, TE 20 ms), and T2 weighted (TR 2100, TE 78 ms) images. T1 weighted 1mm thick contiguous slices gradient-echo volume acquisition of the whole brain (TR 18, TE 10 ms, 30° angle, isotropic voxel) was acquired for subsequent multiplanar reconstruction and volumetric study of mesial temporal structures. Details of volumetric protocol and previous results have been published elsewhere^{35,270}. Hippocampal volumes were corrected for variation of total brain volume to allow for detection of bilateral atrophy. Asymmetry index $(\text{left-right})/(\text{left+right})/2$ was obtained and compared to values from normal controls. All 21 patients had corrected hippocampal volumes 2 standard deviations (SD) below the normal mean on both sides.

¹H-MRSI of temporal lobes was performed in a separate examination using the same scanner. After scout images in axial and sagittal planes, a multislice transverse spin-echo MRI (TR 2000, TE 30) was obtained. The volume of interest (VOI) included part of the head, body and tail of the hippocampus and portions of gray and white matter from mid and posterior temporal lobe (Figure 1). The size of the VOI was 85-100mm in the left-right axis, 75-95mm in the antero-posterior axis, and 20mm in thickness. A water suppressed ¹H-MRSI was acquired from the VOI (TR 2000 ms, TE 272 ms, 250x250 mm FOV, 32x32 phase-encoding steps), followed by a ¹H-MRSI without water suppression (TR 850 ms, TE 272 ms, 250x250 mm field of view, 16x16 phase-encoding steps). Post-processing included zero-filling the water unsuppressed ¹H-MRSI to obtain 32x32 profiles, followed by application of mild Gaussian *k*-space filter and an inverse 2D Fourier transformation to both water suppressed and unsuppressed ¹H-MRSI. The resulting time domain signal was left shifted and subtracted from itself to improve water suppression²⁶⁹. The same process was performed for specific group control data (30 subjects). Resonance intensities in individual spectra were determined by integration of peak areas using locally developed software.

Figure 1: The four sub-regions of temporal lobe ¹H-MRSI:



The number of spectra averaged for each sub-region (mid and posterior temporal regions) within the VOI was 10 ± 2 . The size of the individual voxel after post-processing was approximately 1cc. Voxels on the edge of the VOI that were affected by chemical shift artifact and voxels that were artifactually broadened were excluded from the analyses. The resonance intensity of NAA was normalized to intravoxel Cr. It is assumed that in epilepsy Cr is stable or undergoes minor changes that do not significantly influence the NAA/Cr ratio^{157,158,160,161,177}. Changes in NAA/Cr reflect neuronal loss or dysfunction, and NAA/Cr ratios below 2 SD from the normal mean were considered abnormal. Asymmetry index (left-right)/(left+right)/2 was also obtained and compared to values from normal controls

All patients underwent prolonged video-EEG monitoring. Four patients had additional invasive neurophysiological studies with depth electrodes for lateralization. The EEG was classified as unilateral, when $>90\%$ of ictal EEG onsets were on one side, and bilateral when $< 90\%$ of seizures started from one side.

We used Engel's classification to assess surgical outcome with respect to seizure control²⁶⁷. Class I (excludes early postoperative seizures in the first 2 weeks): a) completely seizure free since surgery, b) auras only since surgery, c) less than 3 complex partial seizures after surgery, but free of complex partial seizures for at least two years, d) generalized convulsion with antiepileptic drug withdrawal only. Class II: a) initially free of complex partial seizures and less than 3 seizures per year, b) less than three seizures per year, c) more than three seizures per year after surgery, but now less than three seizures for at least two years, d) nocturnal seizures only. Class III: a) seizure reduction of more than 90%, b) prolonged seizure-free intervals amounting to greater than half the follow-up period, but not less than two years. Class IV: a) seizure reduction of less than 90%, b) no appreciable change, c)

seizures worse

Fourteen patients had a selective-amygdalo-hippocampectomy (SAH) and seven had anterior temporal resection (ATL). There were no significant differences between SAH and ATL for ¹H-MRSI, MRVol, EEG, age, sex, follow-up, and surgical outcome ($p > 0.05$, independent t-test for numerical data and Chi-square for categorical data)

Fisher's exact test was used to assess probability of association between temporal lobe ¹H-MRSI features and surgical outcome. Regression and correlation analyses were used to assess significance of correlation between surgical outcome and either the asymmetry of NAA/Cr or the asymmetry of hippocampal volume. For this analysis, we used a simple ratio obtained by dividing the value ipsilateral to operation by the value contralateral to operation, as this allowed a simple correlation for patients regardless of the side of operation.

RESULTS

Eleven patients (52%) were in class I-II and ten (48%) in class III-IV.

Results of ¹H-MRSI, MRVol studies, EEG, type of surgery and outcome are displayed in the Table.

All 21 patients were operated on the side of EEG lateralization, including three who had discordant hippocampal asymmetry index and EEG lateralization (Table: pts. 1, 2, and 12). One patient with discordant MRVol and EEG findings had seizures only on medication reduction, and the other two were in class IV.

Temporal lobe ¹H-MRSI NAA/Cr measures showed that:

Concordant lateralization of temporal region NAA/Cr reduction to the side of major

EEG abnormality and surgery was significantly associated with good surgical outcome: 11/16 (69%) patients with concordant MRSI and none of the 5 patients with non-concordant MRSI were in class I-II (Fisher's exact test, 2-tailed $p = 0.012$). Odds ratio was zero ($0 < 95\%$ confidence limits < 0.75).

Lateralization of NAA/Cr reduction from the mid-temporal sub-region to the side of major EEG abnormality and of surgery was significantly associated with good surgical outcome: 9/12 (75%) patients with concordant MRSI and 2/9 (22%) patients with non-concordant MRSI were in class I-II (Fisher's exact test, 2-tailed $p = 0.03$). Odds ratio was 0.10 ($0.01 < 95\%$ confidence limits < 0.99) and relative risk was 0.30 ($0.08 < 95\%$ confidence limits < 1.05).

Absence of NAA/Cr reduction in the contralateral posterior-temporal sub-region $^1\text{H-MRSI}$ was significantly associated with good surgical outcome: 10/13 (77%) patients without and 1/8 (12.5%) with contralateral NAA reduction were in class I-II (Fisher's exact test, 2-tailed $p = 0.008$). Odds ratio was 23.33 ($1.56 < 95\%$ confidence limits OR < 1152.71), and relative risk was 6.15 ($0.96 < 95\%$ confidence limits RR < 39.43). Regression-correlation analysis showed significant linear correlation between contralateral posterior NAA/Cr z-scores (CtrPostZ) and surgical outcome, with the correlation coefficient (r^2) = 0.203, $F(1, 19) = 4.850$, $p = 0.040$, with slope expressed as 'surgical outcome = $0.387 \times \text{CtrPostZ} + 1.253$ '.

Hippocampal asymmetry lateralized 16 patients to the same side as the EEG, three patients to the side opposite the EEG. Two patients had an asymmetry index within 2 standard deviations of normal mean and were not lateralized. There was no difference in surgical outcome of patients in whom MRI volumetry lateralization was concordant with EEG lateralization and patients in whom MRI volumetry was non-concordant with EEG

lateralization, 10/16 (62%) vs. 1/5 (20%) of patients in Engel's class I-II, Fisher's exact test, $p = 0.12$, 1 tailed.

Regression-correlation analysis between mid-temporal ^1H -MRSI ratio (MidR = ipsi/contralateral NAA/Cr to the side of operation) showed significant linear correlation to surgical outcome, with the correlation coefficient (r^2) = 0.321, $F(1, 19) = 8.995$, $p = 0.007$, with slope expressed as 'surgical outcome = $0.0918 \times \text{MidR} - 6.374$ '.

Regression-correlation analysis between hippocampal asymmetry ratio (HcR = ipsi/contralateral hippocampus to the side of operation) showed significant linear correlation to surgical outcome, with the correlation coefficient (r^2) = 0.219, $F(1, 19) = 5.342$, $p = 0.032$, with slope expressed as 'surgical outcome = $0.0516 \times \text{HcR} - 2.385$ '.

Unilateral EEG foci were not significantly associated with good surgical outcome in this series of patients with bilateral hippocampal atrophy: 4/7 (57%) patients with unilateral and 7/14 (50%) with bilateral EEG seizure onsets were in class I-II (Fisher's exact, 2-tailed $p = 1$).

DISCUSSION

In this series, the surgical outcome is similar to what has been reported in other series of patients with bilateral hippocampal atrophy and intractable TLE^{201,202}, with about 50% achieving good surgical outcome (Engel's class I-II).

MR-based techniques have demonstrated distinct features associated with good surgical results. In terms of hippocampal volumetric studies, these results are in keeping with previous reports, with better surgical results in those with greater hippocampal asymmetry^{201,202,305,306}. Temporal lobe NAA/Cr values measured by ^1H -MRSI showed many

interesting outcome features. Concordant lateralization according to either one region (mid) or two (mid and posterior) provided a significant difference in surgical outcome, with better results seen in those who had NAA/Cr reduction lateralized to the same side as the EEG. This finding would suggest that single voxel ¹H-MRS could also provide prognostic guidance. In addition, our ¹H-MRSI results showed that the presence of contralateral posterior NAA/Cr reduction, reflecting a widespread metabolic abnormality, was a powerful predictor of less satisfactory surgical outcome. In our study, patients with contralateral posterior quadrant NAA/Cr reduction had a relative risk six times higher of having poor surgical outcome compared to those who did not have contralateral metabolic abnormality. The degree of NAA/Cr asymmetry was also important, and better results correlated with greater side to side asymmetry.

In our series, all patients were operated on the side of EEG lateralization. Classification of ictal electrographic onsets into unilateral or bilateral did not discriminate further between patients with good and those with poor surgical outcome. In the three patients (Table: pts. 1, 2, and 12) with discordant MRV_{ol} and EEG, only one patient had good outcome. This patient had concordance between ¹H-MRSI and EEG, while in the other two, one had no ¹H-MRSI lateralization and the other had discordance between ¹H-MRSI and EEG lateralization.

In conclusion, both MRV_{ol} and ¹H-MRSI of temporal lobes provided discriminant features associated with favorable surgical outcome in patients with intractable TLE and bilateral hippocampal atrophy. In pre-surgical evaluation of patients with TLE, neuroimaging findings can help not only to lateralize and to localize the seizure focus, but may also help to define prognosis on an individual basis. Our ¹H-MRSI results show that indicators for good

surgical outcome are: greater asymmetry of NAA/Cr from the mid-temporal region (MidR < 0.80), and absence of contralateral posterior temporal NAA/Cr reduction.

Table: Intractable TLE and bilateral hippocampal atrophy: summary of MRSI, MRVol, EEG, type of surgery and outcome

p/sex/age	Mid		# Mid	*Mid		*Post		MRSI	Diagnosis	Hc		# Hc	*Hc		EEG	Surgery	Follow-Up (months)	Outcome		
	Mid-Lt	Mid-Rt	Ipsi/contra	Mid-Lt-Z	Mid-Rt-Z	Asym-Z	Post-Lt-Z			Post-Rt-Z	Asym-Z	Hc-Lt	Hc-Rt	Ipsi/contra					Hc-Lt-Z	Hc-Rt-Z
1/f/44	3.33	3.36	1.01	-3.42	-4.07	0.31	-2.60	-2.78	0.01	Bilat	3046	3658	1.20	-5.94	-2.10	-9.53	DP-Right	R-SAH	35	IVa
2/f/38	3.76	3.16	0.84	-2.17	-6.36	5.53	1.62	-3.56	7.21	R>L	3243	3562	1.10	-4.73	-2.63	-4.72	Right	R-SAH	14	Id
3/m/39	3.38	3.66	1.08	-3.20	-2.73	-1.75	-3.58	-6.63	5.25	R>L	3496	3478	0.99	-3.18	-3.09	0.63	Right	R-ATL	38	IVa
4/f/38	3.63	3.30	0.91	-2.18	-4.33	3.52	-1.13	-3.71	3.99	R>L	2661	2577	0.87	-6.46	-8.03	7.83	Right	R-SAH	49	Ia
5/m/36	3.22	3.21	1.00	-3.86	-4.76	0.71	-1.58	-2.21	0.82	R>L	3465	3011	0.87	-3.37	-5.65	7.91	DP-R>L	R-ATL	29	IIIa
6/m/34	4.30	4.07	0.95	0.51	-0.84	2.27	-0.73	-1.88	1.66	Right	3680	3133	0.85	-2.05	-4.98	9.02	R>L	R-SAH	42	Ic
7/f/34	3.53	3.55	1.01	-2.60	-3.21	0.45	-1.60	-1.28	-0.65	Bilat	2922	2486	0.85	-6.70	-8.53	9.05	R>L	R-ATL	28	IVa
8/f/52	3.55	2.96	0.83	-3.39	-7.67	5.82	-1.99	-1.41	-0.83	R>L	3233	2714	0.84	-4.79	-7.27	9.77	R>L	R-ATL	19	Ib
9/f/19	3.35	2.86	0.85	-4.53	-8.33	5.15	-0.49	0.12	-0.82	R>L	3046	2542	0.83	-5.94	-8.22	10.08	R>L	R-SAH	12	Ia
10/f/42	3.16	3.31	1.05	-4.10	-4.30	-0.80	-2.67	-2.92	0.12	Bilat	2294	1901	0.83	-10.55	-11.73	10.46	R>L	R-SAH	33	IVa
11/m/44	3.70	2.94	0.79	-2.51	-7.81	7.33	-0.76	-1.77	1.43	R>L	3605	2594	0.72	-2.51	-7.93	17.96	R>L	R-SAH	26	Ia
12/f/21	3.60	3.45	1.05	-2.30	-3.68	1.99	-1.76	-2.75	1.38	R>L	3815	3254	1.17	-2.90	-5.15	8.71	DP-L>R	L-SAH	13	IV b
13/m/27	4.05	4.56	0.89	-0.49	1.36	2.95	-1.61	0.20	-2.81	Left	3636	3662	0.99	-2.32	-2.08	-0.04	Left	L-SAH	36	IVa
14/m/42	2.58	3.88	0.70	-9.01	-3.08	-10.74	-2.97	-1.36	-2.39	L>R	2924	3284	0.89	-6.69	-4.15	-5.92	L>R	L-SAH	20	Ia
15/f/47	3.61	3.49	1.03	-2.27	-3.48	1.65	-4.62	-5.32	0.73	Bilat	2956	3560	0.83	-6.23	-4.04	-7.79	L>R	L-SAH	61	IV b
16/m/24	3.38	3.71	0.91	-3.19	-2.50	-2.15	-3.77	-2.58	-2.41	L>R	2788	3601	0.77	-6.89	-3.89	-11.09	DP-L>R	L-ATL	51	IIIa
17/f/34	3.06	4.15	0.74	-4.50	-0.50	-8.56	0.14	-0.83	1.40	Left	2466	3237	0.76	-9.50	-4.41	-14.28	Left	L-SAH	49	Ic
18/f/46	2.16	2.77	0.78	-8.13	-6.72	-6.94	-8.28	-8.00	-1.92	L>R	2543	3376	0.75	-9.03	-3.64	-14.87	L>R	L-ATL	31	IV a
19/m/44	3.67	3.63	0.98	-2.45	-2.86	0.11	-3.07	-0.80	-3.85	L>R	2401	3522	0.68	-9.90	-2.84	-20.12	L>R	L-SAH	36	Ia
20/f/49	3.65	3.72	0.98	-2.10	-2.43	0.06	-3.07	-1.62	-2.63	L>R	2214	3589	0.62	-9.11	-3.93	-21.60	Left	L-ATL	50	Ib
21/m/16	3.06	3.48	0.88	-4.50	-3.53	-3.28	-4.05	-4.52	0.38	L>R	2196	3671	0.60	-11.15	-2.03	-26.82	L>R	L-SAH	50	Ia

= ipsi and contralateral to the side of the operation. This ratio was used only for correlation and regression analysis, and was not used for the lateralization. * = (L-R)/(L+R)/2, this asymmetry index was used for interpretation of lateralization of MRSI and hippocampal volume. DP = depth electrode results. Mid = mid temporal region of VOI. Post = posterior temporal region of VOI. Rt = right, Lt = left. Z = z-scores (number of standard deviations from the mean of normal control subjects), values 2SD below the normal mean were considered abnormal. Hc = hippocampal volume. SAH = selective amygdalo-hippocampectomy, ATL = anterior temporal resection. Outcome = Engel's modified classification, see text for explanation. MRSI diagnosis = this was based on the results derived from the 4 subregions (left and right mid and posterior temporal regions), and asymmetry index.

CHAPTER IV

Dynamic changes in lesions underlying epilepsy

There has been considerable debate over the occurrence of progressive neuronal damage and its relationship to seizures. The ideal way to assess this issue is to perform a longitudinal study in a cohort of patients with epilepsy with serial measurements of neuronal integrity. However, the time necessary to detect neuronal damage is unknown, and could be years. An alternative way is to perform a cross sectional study in a large group of patients with the same epileptic syndrome. This approach can provide evidence for progressive neuronal damage, and if so, indicate the magnitude of neuronal damage in relation to time and to seizure burden.

NAA recovery has been reported after successful removal of the temporal lobe epileptogenic area. There has been report of NAA recovery as early as two months post-operatively. However, the exact time course of NAA recovery is unknown. This piece of information is important for understanding of the dynamics of NAA recovery in other types of anti-epileptic treatments.

Patients with chronic refractory TLE often have temporal lobe neuronal damage, but we do not know if patients with newly diagnosed epilepsy also have neuronal damage in the early stages of their condition, and if this can be improved with AED treatment.

Paper 7: Neuroimaging evidence of progressive neuronal loss and dysfunction in temporal lobe epilepsy.

Tasch E, Cendes F, Li LM, Dubeau F, Andermann F, Arnold DL.
Annals of Neurology 1999;45:568-576.

Lippincott Williams & Wilkins

SUMMARY

Background: There is debate whether temporal lobe epilepsy (TLE) is the result of an isolated, early injury or if there is ongoing neuronal dysfunction or loss due to seizures.

Objective: We attempted to address this issue using magnetic resonance techniques. Proton magnetic resonance spectroscopic imaging (MRSI) can detect and quantify focal neuronal dysfunction or loss based on reduced signals from the neuronal marker N-acetylaspartate (NAA), and magnetic resonance imaging (MRI)-based measurements of hippocampal volumes (MRIVol) can quantify the amount of atrophy in this structure.

Patients/Methods: We performed MRSI and MRIVol in 82 consecutive patients with medically intractable TLE to determine whether there was a correlation between seizure frequency, type or duration of epilepsy with NAA to creatine (NAA/Cr) values or hippocampal volumes. Volumes and spectroscopic resonance intensities from the temporal lobe were categorized as ipsilateral or contralateral to the predominant EEG focus.

Results: Ipsilateral and contralateral NAA/Cr was negatively correlated with duration of epilepsy. Hippocampal volumes were negatively correlated with duration ipsilaterally but not contralaterally. Frequency of complex partial seizures was not correlated with any of the MR techniques. However, patients with frequent generalized tonic-clonic seizures had lower NAA/Cr bilaterally and smaller hippocampal volumes ipsilaterally than patients with none or rare generalized tonic-clonic seizures.

Conclusion: The results suggest that although an early, fixed injury may cause asymmetric temporal lobe damage, generalized seizures may cause progressive neuronal dysfunction or loss.

INTRODUCTION

Mesial temporal sclerosis (MTS) is a common pathological finding associated with temporal lobe epilepsy (TLE) as demonstrated at autopsy^{179;213;308} and in tissue resected during surgery^{39;309-312}. The etiology and pathogenesis of MTS remain poorly understood, and have been a source of controversy. Some authors have suggested that hippocampal sclerosis arises from injuries early in life resulting in a brain lesion, which is therefore static and non-progressive^{313;314}. Suggested etiologies include birth trauma, cerebral infections, and prolonged convulsions^{313;314}. This is consistent with the commonly observed clinical pattern of prolonged febrile seizures of childhood followed by habitual temporal lobe epilepsy after an intervening latent period^{40;42;219;313-316}.

Seizures themselves are also capable of causing neuronal damage. Status epilepticus is often followed by extensive neuronal damage involving the hippocampus, as well as other limbic, neocortical and subcortical structures³¹⁷⁻³¹⁹. It is still unclear to what extent MTS associated with TLE may arise from progressive injury due to the intractable seizures. Animal models have shown progressive neuronal loss associated with repetitive kindled seizures^{309;312}. On the other hand, studies of the pilocarpine model, failed to show such a relationship between recurrent spontaneous seizures and hippocampal neuronal loss²¹¹. Human autopsy studies³²⁰ have shown a correlation of neuronal loss with duration of epilepsy, but the population studied included a group of patients who had had severe generalized epilepsies and the distribution of neuronal loss was not characteristic of classical MTS. Pathological study of surgical specimens from patients with temporal lobe epilepsy has revealed a correlation between hippocampal cell loss and duration, but this was also not in the same distribution as classical MTS and accounted for a relatively small amount of the total hippocampal cell

loss^{214,216}.

Conventional magnetic resonance imaging (MRI) can detect abnormalities in TLE which include atrophy or abnormal T2-weighted signals in the hippocampus, amygdala, or both^{85,115,201,311,321,322}. Volumetric analysis (MRIVol) can detect reduced volume of mesial temporal lobe structures in most patients with MTS, correlated with subsequent histopathology^{311,323}. Case reports have suggested that mesial temporal lobe atrophy can follow acute, prolonged seizure activity^{324,325}. Trenerry et. al., found an association of hippocampal atrophy with duration of epilepsy, but this relationship appeared to be accounted for in large part by the age of onset³²⁶. Recent studies by Saukkonen et. al.,³²⁵ and Salmenpera et. al.³²⁷ have found an association between seizure frequency and decreased hippocampal volumes in patients with TLE. On the other hand, a previous study by our group failed to show evidence for a causal relationship between duration or seizure frequency and mesial temporal atrophy in a heterogeneous group of patients¹⁵⁹. Furthermore, there remains a significant proportion of patients with TLE in whom MRI changes cannot be detected³²³.

Unlike conventional MRI, which provides structural information based on signals from water, proton magnetic resonance spectroscopic imaging (MRSI) provides chemical information, allowing for noninvasive assessment of regional chemical composition. N-acetylaspartate (NAA) is a compound localized exclusively in neurons, detectable by proton magnetic resonance spectroscopy^{124,125}. Several studies have shown reduced signals from NAA in temporal lobes of patients with TLE. This presumably reflects focal neuronal dysfunction or loss^{115,157,175,176,201,321}. MRSI can also detect acute chemical changes in the temporal lobes of TLE patients and is a more sensitive indicator of neuronal dysfunction than MRIVol¹¹⁵. MRSI and MRIVol are often concordant and are an effective combination in the

presurgical evaluation of patients with TLE^{115;116}. Whether the temporal-lobe metabolic abnormalities detected by MRSI are progressive is unknown. One study has shown a correlation between reduced temporal-lobe NAA and seizure frequency, but not with duration of epilepsy²⁸⁸.

We studied a series of patients with non-foreign-tissue lesional TLE evaluated for seizure surgery using MRSI and MRIVol, in an attempt to determine whether repeated seizures, longer duration of epilepsy, or the presence of secondary generalization of seizures correlate with: 1) the amount of hippocampal formation atrophy or 2) reduced intensity of the temporal-lobe NAA signal measured by MRSI.

PATIENTS AND METHODS

We studied 82 consecutive patients (mean age: 35, SD: 11) with medically refractory TLE who had no mass lesion on high quality conventional MRI. Identification of the type and localization of the seizures was determined by comprehensive evaluation including a detailed history and neurological examination, serial EEGs with sphenoidal electrodes, and intensive video-EEG telemetry for recording of seizures. Patients with mass lesions or non-TLE were excluded from the study.

Informed consent was obtained from all subjects. This study is part of a research project approved by the Ethics Review Committee of the Montreal Neurological Institute and Hospital.

Estimation of the duration and frequency of seizures was based on a review of medical records and seizure calendars, and specific questioning of the patient and family members. Age of onset of epilepsy was defined as the age at which the patient developed habitual and

recurrent seizures. The duration, or number of years of epilepsy, was defined as the interval between the age of onset and the time of the examination. Prolonged febrile convulsions (PFC) were defined as seizures lasting 30 minutes or more. The history of PFC was based on detailed accounts from parents and other relatives at the time of hospital admission as well as on a review of the patients' medical records of early childhood hospitalization.

EEG Investigation

Prolonged EEG recordings, using the International 10-20 system including sphenoidal electrodes, and long term video-EEG monitoring were performed to record at least three habitual seizures in all patients. If discrepancies arose between the localization of ictal and interictal abnormalities, if EEG seizure discharges could not be localized due to movement or muscle artifacts, or if ictal behavioral manifestations suggested a possible seizure generator in extratemporal structures, patients underwent intracranial EEG recordings with stereotaxically implanted depth electrodes (SEEG). Eighteen patients required SEEG investigation in order to confirm seizure onsets in the temporal lobe.

Patients were classified according to the localization of the majority of EEG seizure onsets preceding the first clinical manifestations as either Left (L) or Right (R). For the purposes of this study, "majority" was defined as over 50% of seizure onsets. The electroencephalographers were unaware of the MRSI and MRIVol results.

Proton Magnetic Resonance Spectroscopic Imaging

Conventional MRI as well as two-dimensional proton MRSI scans were acquired by using either a 1.5-T ACS II or III imaging/spectroscopy system (Phillips Medical Systems, Best, The Netherlands).

After scout images in axial and sagittal planes, multislice spin echo MRIs (repetition time [TR] 2,000 msec, echo time [TE] 30 msec) were obtained in the transverse plane along the axis of the temporal lobes and in the coronal plane perpendicular to the axis of the Sylvian fissure. A large region of interest (ROI) behind the clivus, including both temporal lobes and excluding bone, was defined for selective excitation before phase encoding for the proton MRSI. The ROI was oriented in a similar position for all examinations to cover the entire extent of both hippocampi (85-100 mm left-right x 75-95 mm anteroposterior x 20 mm thickness), as shown in Fig 1.

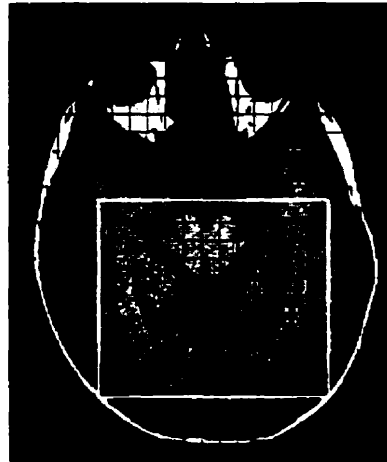


Figure 1: T1-weighted MRI showing the location of the voxels used for the MRSI analysis. Each small box on the grid is a voxel from which a spectrum is obtained. Several voxels from each temporal lobe are chosen to obtain an average temporal-lobe spectrum. Each temporal lobe was classified as either ipsilateral or contralateral to the predominant EEG focus and analyzed separately.

A water-suppressed proton MRSI was obtained from that ROI by using a 90-180-90 pulse sequence with a 2-second interpulse delay (TR 2,000 msec, TE 272, 250 x 250-mm field of view (FOV), 32 x 32 phase-encoding steps), followed by a proton MRSI without water suppression (TR 850, TE 272, 250 x 250-mm FOV, 16 x 16 phase-encoding steps). After zero-filling the latter to 32 x 32 profiles, the water suppressed MRSI was divided by the non-

water suppressed MRSI to correct for artifacts resulting from magnetic field inhomogeneity. The resulting time domain signal was left shifted and subtracted from itself to improve the water suppression²⁶⁹. This reduces the amplitude of the creatine (Cr) as well as water and results in relatively high ratios of NAA/Cr; however, this is consistent for all control and patient data. To enhance the resolution of the spectral peaks a Lorentzian-to-Gaussian transformation was applied before Fourier transformation in three dimensions. The nominal voxel size in plane was approximately 8 x 8 mm and 12 x 12 mm after K-space filtering.

Resonance intensities on MRSIs were determined from peak areas by integration, using locally developed software. The values for NAA, choline (Cho), Cr, and NAA/Cr were determined for each temporal lobe by averaging 24 +/- 3 spectra in each region (Fig 1). Spectra were excluded from the analyses if they were artifactually broadened (i.e., full width at half maximum > 10 Hz) or if Cho and Cr peaks were not resolved.

The intensity ratio NAA/Cr for each temporal lobe was calculated and classified as either ipsilateral (NAA/Cr-*ipsi*) or contralateral (NAA/Cr-*contra*) to the EEG lateralization. Cr is homogeneously distributed throughout the brain, and it is reasonable to assume that Cr is stable or not significantly deranged in brain regions associated with epileptic damage^{157;158;164;177}. Therefore the decreases in the ratio of NAA/Cr can be interpreted in terms of neuronal dysfunction or loss, which is useful for understanding the pathogenesis of TLE^{158;164;173;175-177;328;329}.

Patient average NAA/Cr values for each side were compared with each other as well as with the values obtained in 21 healthy normal controls (12 men and 9 women; mean age, 28.2 years; SD = 4.5). Values less than two standard deviations below the normal control group were considered abnormal. In the normal control group, NAA/Cr values were not

statistically significantly different between left and right temporal lobes. Patient values were categorized as to whether they were ipsilateral or contralateral to the EEG focus without further reference to side.

MRI Volumetric Studies

The MRI volumetric studies were performed using two acquisition protocols. For the first 34 patients, we acquired 3-mm contiguous slices perpendicular to the plane of the Sylvian fissure, with a three-dimensional (3D) fast-field echo (FFE) or an inversion recovery (IR) sequence. For the subsequent 48 patients, we acquired 1-mm thick slices by using a 3D FFE sequence with isotropic voxels. The images were transferred to a computer workstation and the ROIs were outlined, using a locally developed interactive software program^{85,270}. Watson and colleagues have described the anatomical guidelines used for identification of the HF²⁷⁰.

Volumes were compared with age matched healthy volunteers who had the same MRI acquisition protocol (n = 30 for 3-mm-thick [17 men and 13 women; mean age, 32.4 years, SD = 11.3] and n = 22 for 1-mm thick slices [12 men and 10 women; mean age, 29.5 years, SD = 10.2]). In order to standardize the two different protocols, absolute HF volumes were converted into a Z-score (HF volume-mean/SD) using the appropriate control group for each temporal lobe (left or right) for each protocol. Comparison of the Z-score results derived from the two protocols show no statistical difference between them (t = -0.004, p = 0.997). We analyzed the hippocampal formation Z-scores (HFZ) and, as with the MRSI, classified them as ipsilateral (HFZ-*ipsi*) or contralateral (HFZ-*contra*) to the EEG lateralization.

Statistical Analysis

We performed simple biserial Pearson correlation analyses between NAA/Cr-*ipsi*,

NAA/Cr-*contra*, HF-*ipsi*, and HF-*contra*, and the duration, age of onset, and frequency of complex partial and secondarily generalized seizures. In addition, partial correlation coefficients were computed between the spectroscopic/volumetric measurements and age of onset, controlling for the duration of epilepsy; and duration of epilepsy while controlling for age of onset, in order to determine the association of each with the neuroimaging measurement while controlling for the effect of the other.

Linear regression analysis was used to further illustrate the relationship between the neuroimaging measurements and the clinical parameters. Student's t-test was used to test for differences between group means. The statistical software package SPSS was used to perform these calculations.

RESULTS

Patient characteristics are summarized in Table 1.

Magnetic Resonance Spectroscopic Imaging

Simple correlations were performed between the NAA/Cr intensities and the independent predictor variables. Although the absolute magnitude was modest, there was a statistically significant negative correlation between the duration of epilepsy and both NAA/Cr-*ipsi* ($r = -.286$, $p = 0.010$) and NAA/Cr-*contra* ($r = -.312$, $p = 0.005$). There was no significant correlation between duration and the left-right asymmetry ratio of NAA/Cr or the left-right difference. Likewise, there was no significant correlation of either NAA/Cr-*ipsi* or NAA/Cr-*contra* with the age of onset. Figure 2 shows the least-squares regression analysis for the relationship between duration and NAA/Cr.

Partial correlations revealed that after controlling for the patient's age at onset of

epilepsy, there was still a significant correlation between duration and NAA/Cr-*ipsi* ($r = -0.302$, $p = 0.006$) and NAA/Cr-*contra* ($r = -0.316$, $p = 0.004$). The partial correlation of the age of onset with either NAA/Cr-*ipsi* or NAA/Cr-*contra* after controlling for the duration remained non-significant.

Because of the nature of the duration variable we cannot statistically rule out that the relationship between NAA/Cr is, in fact, due to the effect of the age of the patient alone. Because age and duration are highly correlated with each other, we could not perform a partial correlation of one of them, controlling for the effect of the other. The normal control group did not show any significant correlation between age and NAA/Cr in either temporal lobe.

Table 1: Patients demographic data

Patient characteristics, n=82 (36 male, 46 female)	Mean (Standard Deviation)
Age at examination (years)	35 (11)
Age at onset (years)	14 (12)
Frequency of complex partial seizures (per month)	23 (37)
Frequency of generalized tonic-clonic seizures (per year)	12 (47)
Duration of epilepsy	20 (9)
NAA/Cr- <i>ipsi</i>	3.65 (0.35)
NAA/Cr- <i>contra</i>	4.05(0.37)
HFZ- <i>ipsi</i>	-4.70 (3.3)
HFZ- <i>contra</i>	-1.19 (2.6)

Temporal-lobe NAA/Cr vs. Duration of Epilepsy

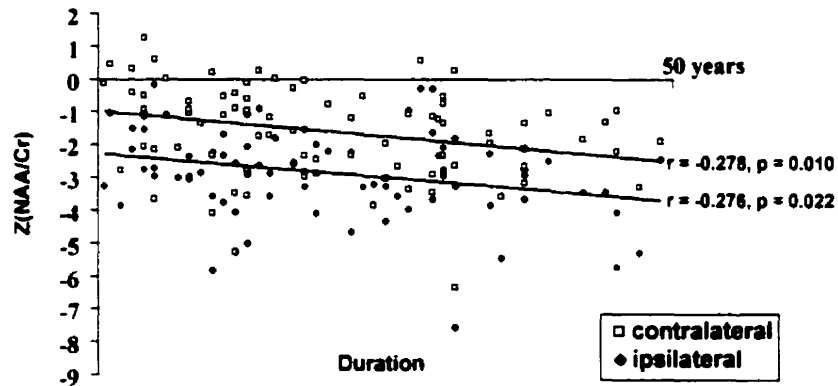


Figure 2: NAA/Cr is plotted against duration of epilepsy for each temporal lobe for each patient. Temporal lobes are ipsilateral (triangles) or contralateral (circles) to the predominant EEG focus. Least-squared regression lines are shown ($z\text{-score NAA/Cr-ipsi} = -0.03 * \text{duration} - 2.275$, $z\text{-score NAA/Cr-contra} = -0.03 * \text{duration} - 0.982$). Both ipsilateral and contralateral temporal-lobe NAA/Cr ratios are negatively correlated with duration (see text).

Compared to the normal controls, 33 (40%) patients had bilaterally reduced NAA/Cr. If NAA/Cr reduction were progressive, one might expect patients with bilaterally reduced NAA/Cr to have longer duration than those with only unilaterally reduced NAA/Cr. Student's *t*-tests revealed that these patients did not significantly differ in their age, age of onset, duration, or frequency of complex partial or generalized tonic-clonic seizures. However, patients with bilaterally reduced NAA/Cr did have significantly lower NAA/Cr-*ipsi* than patients with unilaterally reduced NAA/Cr (Table 2).

Table 2: Patients with bilaterally vs. unilaterally reduced temporal-lobe NAA/Cr

	<i>Unilateral</i>	<i>Bilateral</i>	<i>P value</i>
N	49 (60%)	33 (40%)	
Age	34	37	0.131
Age of Onset	14	15	0.867
Duration	18	20	0.144
NAA/Cr-ipsi	3.829	3.390	<0.001

Despite the relationship we found between NAA/Cr and duration, there was no significant correlation between NAA/Cr on either side and frequency of complex partial seizures. Patients with generalized tonic-clonic seizures (n = 27) had lower NAA/Cr-ipsi (t = 2.505, p = 0.015) and lower NAA/Cr-contralateral (t = 2.498, p = 0.014) than patients who had no or only rare generalized tonic-clonic seizures (n = 54) (Table 3).

Table 3 Temporal-lobe NAA/Cr and hippocampal volume (z-score) in patients with or without generalized tonic-clonic seizures

	<i>With GTC</i>	<i>None or rare GTC</i>	<i>p-value</i>
N	27	55	
NAA/Cr-ipsi	3.55	3.75	0.015
NAA/Cr-contralateral	3.96	4.12	0.032
HFZ-ipsi	-6.0	-4.0	0.010
HFZ-contralateral	-1.7	-0.9	0.232

There was no significant difference in NAA/Cr of either side between patients with and patients without a history of prolonged febrile convulsions. (Table 4)

Table 4: Neuroimaging measurements in patients with and without a history of prolonged febrile convulsions

	+PFC	No PFC	P value
N	51	31	
NAA/Cr-ipsi	3.673	3.617	0.500
NAA/Cr-contra	4.014	4.088	0.398
HFZ-ipsi	-5.773	-3.975	0.022
HFZ-contra	-1.121	-1.277	0.810

Magnetic Resonance Imaging Volumetry

As with the spectroscopic data, simple biserial correlations were performed between the standardized volumes and the independent predictor variables. A statistically significant negative correlation was found between the duration of epilepsy and HFZ-ipsi ($r = -0.399$, $p < 0.001$), but not HFZ-contra ($r = -0.047$, $p = 0.678$). Figure 3 shows the regression analysis between the duration and HFZ. As discussed above, the effects of the age of the patient cannot be adequately controlled for because of its high correlation with duration.

In contrast to the spectroscopic data, the age of onset was also found to be significantly correlated with HFZ-*ipsi* ($r = 0.219$, $p = 0.050$), but not HFZ-*contra* ($r = .005$, $p = 0.969$). The partial correlation of duration with HFZ-*ipsi* controlling for the age of onset remained significant ($r = -0.360$, $p = 0.001$). However, the partial correlation of age of onset with HFZ-*ipsi*, controlling for duration, did not remain statistically significant ($r = 0.047$, $p = 0.678$). As discussed above, the effects of the age of the patient cannot be examined independently of the duration, and there was no significant correlation of age and HF volume in either temporal lobe in the controls.

Hippocampal Volume vs. Duration of Epilepsy

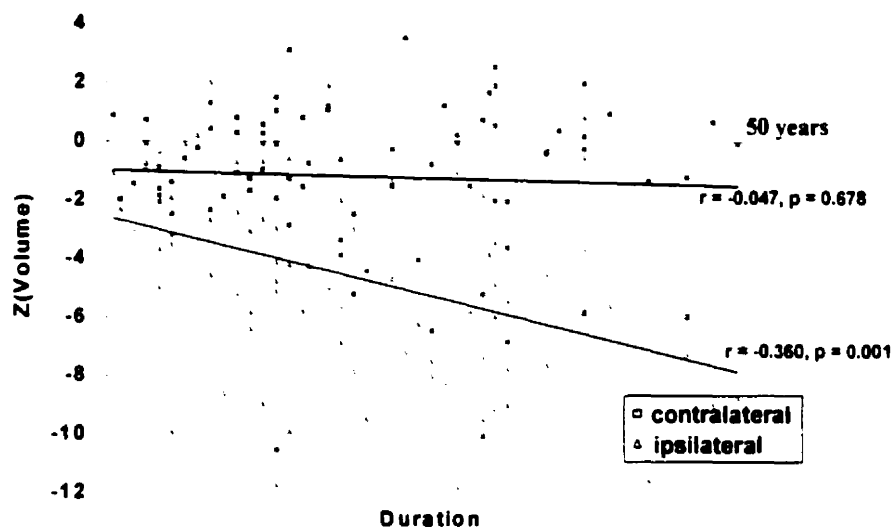


Figure 3: Hippocampal volume z-score is plotted against duration of epilepsy for each temporal lobe of each patient. Hippocampi were ipsilateral (triangles) or contralateral (circles) to the predominant EEG focus of each patient. Hippocampal volume was negatively correlated with duration ipsilaterally but not contralaterally. Least-squared regression lines are drawn ($HFZ_{ipsi} = -0.1085 \cdot \text{duration} - 2.5685$, $HFZ_{contra} = -0.0109 \cdot \text{duration} - 0.9805$).

Despite the relationship found between HFZ_{ipsi} and duration, there was no significant correlation between HFZ on either side and frequency of complex-partial seizures. Patients with generalized tonic-clonic seizures ($n = 27$) had lower HFZ_{ipsi} ($t = 2.602$, $p = 0.015$) but not lower HFZ_{contra} ($t = 1.424$, $p = 0.159$) than patients who had no or only rare generalized tonic-clonic seizures ($n = 54$) (Table 3). Patients with history of prolonged febrile convulsions had statistically significantly lower HFZ ipsilaterally ($t = 2.465$, $p = 0.16$) but not contralaterally ($t = -0.242$, $p = 0.810$) (Table 4).

Compared to normal controls, 18 (22%) of patients had bilaterally reduced hippocampal volumes. Student's t-tests revealed that these patients did not significantly differ

in age, age of onset, duration, or frequency of complex partial seizures. However, patients with bilaterally reduced volumes did have significantly lower HFZ-*ipsi* than patients with unilaterally reduced volumes (Table 5).

Table 5: Patients with bilaterally vs. unilaterally reduced hippocampal volume (z-score).

	<i>Unilateral</i>	<i>Bilateral</i>	<i>P value</i>
N	64 (78%)	18 (22%)	
Age	35	34	0.911
Age of Onset	15	14	0.712
Duration	19	21	0.576
HFZ- <i>ipsi</i>	-4.3	-6.3	0.009

DISCUSSION

It has been a matter of dispute whether or not recurrent seizures can cause neuronal loss in human temporal lobe epilepsy, and whether TLE is a progressive disease. Some studies have demonstrated that neuronal loss can be the result of seizure activity. Cavazos et al showed that hippocampal cell loss could be induced by kindled generalized seizures in rats^{219,302}. However the relevance of seizures induced by direct electrical stimulation of the perforant pathway to the habitual complex partial seizures of human TLE is not clear. Using the pilocarpine model of epilepsy in the rat, a model of spontaneous recurrent seizures that follow a period of status epilepticus, Liu et. al. failed to show any additional neuronal loss with repeated seizures, concluding that all variation in the degree of neuronal loss could be accounted for by the severity of the initial status²¹¹.

Using human autopsy material, Mouritzen-Dam demonstrated that frequent generalized tonic-clonic seizures (>2 seizures per month) were positively correlated with significant reductions in the number of neurons in fields H₁ and H_{1,2} when compared with patients who had suffered only a few such seizures (<6 per year)^{212,320}. This neuronal loss increased throughout life with the duration of the disorder. On the other hand, several retrospective neuropathological reviews have provided evidence to the contrary^{213,312,316,330}. A recent study by Mathern and Babb has taken an intermediate view, suggesting that hippocampal sclerosis is caused for the most part by an “initiating precipitating event” on top of which further progressive damage over time is superimposed^{214,216,219}.

MR-based studies in humans have emphasized mesial temporal atrophy as a cause rather than consequence of temporal lobe epilepsy. Harvey et al demonstrated hippocampal sclerosis in 57% of a series of children, suggesting that its presence at a young age was evidence against seizures as an etiology of hippocampal atrophy³³¹. Trenerry et al found that mesial temporal atrophy in patients with left, but not right, temporal lobe epilepsy is associated with early onset of recurrent seizures and not necessarily with the duration of epilepsy³²⁶. A previous study by our group investigated patients with temporal and extratemporal lobe epilepsy and showed that neither seizure frequency nor duration of epilepsy were correlated with hippocampal or amygdaloid atrophy²²⁰.

Studies using MRSI have produced seemingly conflicting results. Vermathen et al studied a group of patients with non-temporal neocortical epilepsy and showed that hippocampal NAA/Cr was not reduced, in contrast to patients with unilateral TLE. They argued that seizures did not cause secondary hippocampal damage¹⁵⁹. Garcia et al found a negative correlation between NAA and seizure frequency in patients with both frontal and

temporal epileptics, although no correlation with duration²⁸⁸.

The discrepancies among different studies may be explained, in part, by the different methods used, and at least also in part, by the fact that TLE is a heterogeneous condition, with varying degrees of pathological abnormalities. Thus depending on the patient population studied, a significant correlation between atrophy/dysfunction and duration of epilepsy may or may not be present.

Whether the MR findings we report represent irreversible neuronal loss or simply neuronal dysfunction is unclear, in part because of the cross-sectional and retrospective nature of the data. Our data show correlations that can only suggest but not prove causal relationships. Furthermore, the biological basis of the two MR techniques used is different. Although hippocampal atrophy measured by MRI is known to be correlated with hippocampal cell loss^{85,323,332} the cellular basis for the decrease in NAA/Cr measured by MRSI is less clear: NAA/Cr has been shown to recover ipsilaterally and contralaterally after resection of the ipsilateral seizure focus^{161,232}. Nevertheless, the data presented provide some evidence that the MR-findings observed in the temporal lobes of TLE patients are in part, due to progressive changes, and also represent lesions that are, in part, fixed and acquired in the remote past.

Spectroscopic data

We found a negative correlation between NAA/Cr and the duration of epilepsy in the temporal lobes ipsilateral and contralateral to the EEG focus. This suggests that progressive neuronal dysfunction may occur in both temporal lobes in patients with TLE, even when the seizures originate in only one temporal lobe. Because duration is a composite variable, consisting of both age of onset and the age of the patient, one might suspect that any change

in that variable might be due to the effect of the age of onset or the increasing age. We did not find any relationship of NAA with the age of onset itself. The relationship we found with duration remained robust even after controlling for age of onset. Given the cross-sectional and longitudinal design of this study, we could not statistically control for the effects of aging, however there was no such relationship in our normal controls. Furthermore, hippocampal cell counts in autopsy studies of normal aging individuals, fail to show significant drop-off until early in the 7th decade^{157,333}. The difficulties in dissecting out the effects of the different components of duration are consequences of the cross-sectional and retrospective nature of this study. Future, long-term prospective studies, beginning in childhood, involving serial examinations, are required to further elucidate the possible causal relationships suggested by the correlations we have found.

The rate of change of NAA/Cr (or the slope of the regression lines) was the same for both sides, implying that whatever the cause of this decline, affects both sides. Habitual, complex-partial seizures do not appear to be the cause of the progressive dysfunction given the lack of correlation between seizures and NAA/Cr in either temporal lobe. However, generalized tonic-clonic seizures *were* associated with lower NAA/Cr *bilaterally*, suggesting that they are more importantly related to the metabolic dysfunction we are detecting. Whether they are the cause or effect of this metabolic dysfunction remains unknown. This association of generalized tonic-clonic seizures with temporal lobe neuronal dysfunction echoes Mouritzen-Dam's autopsy results that showed increased hippocampal cell loss in patients with frequent generalized tonic-clonic seizures^{212,334}.

Figure 1 shows that ipsilateral NAA/Cr is more reduced than contralateral NAA/Cr, an observation that confirms previous work from our group and others^{115;157;158;173;175-177;201;321}.

This relationship is maintained even when the two regression lines are extrapolated back to time zero, suggesting that ipsilateral NAA/Cr is lower than contralateral NAA/Cr even at a very early age. This is consistent with the notion that the neuronal dysfunction or loss in the temporal lobes of patients with mesial TLE is acquired early, in agreement with clinical, pathological, and MR studies in children^{217,331}.

Despite the relationship between duration and NAA/Cr, patients with bilaterally abnormally low NAA/Cr do not tend to have longer duration than those with unilaterally low NAA/Cr. Thus, even though longer duration is associated with lower NAA/Cr on one or both sides, the data do not suggest that an individual with unilateral spectroscopic abnormality could progress over time to become bilaterally abnormal. The fact that the basic side-to-side asymmetry of the NAA/Cr ratios does not progress suggests that this asymmetry may be the result of an initial, remote injury. Therefore, the spectroscopic data are consistent both with the concept that neuronal dysfunction or loss in TLE is an early, acquired condition and also with the notion that progressive neuronal dysfunction or loss may occur.

MRI volumetry

In contrast to the spectroscopic data, there was a marked difference between ipsilateral and contralateral hippocampal volumes in our analysis. Progressively smaller volumes were correlated with longer duration for the ipsilateral but not for the contralateral hippocampus. The discrepancy between the two neuroimaging modalities may lie in the fact that they are measuring quite different things. Due to limits in its resolution, the spectroscopic images include large portions of white matter as well as small amounts of neocortex whereas the volumetric studies include just allocortical structures. In addition, MRS is more sensitive than MRI volumetry in detecting abnormalities as shown by the fact that bilateral abnormalities are

more common in MRS than MRIVol¹¹⁵. Neuronal dysfunction (measured by MRS) may be more widespread than can be detected with anatomical measures.

Unlike the spectroscopic data, the age of onset is negatively correlated with the ipsilateral hippocampal volume. This raises the possibility that early injuries may be relatively more responsible for the anatomic changes seen in ipsilateral mesial temporal lobe structures, whereas the more subtle functional changes over both temporal lobes, detected by MRS, are gradually progressive. Hippocampal volumes were also independently correlated with duration, since, as for the spectroscopic data, duration remained correlated with ipsilateral hippocampal volume even after controlling for age of onset, while the correlation of age of onset with duration failed to remain statistically significant after controlling for the duration.

Febrile seizures were associated with smaller ipsilateral hippocampal volumes but not with MRS abnormalities on either side. This may be an indication that, although MRS is more sensitive than MRIVol, it may be less specific.

Similar to the spectroscopic data there was no correlation with the frequency of complex partial seizures. Thus, hippocampal atrophy does not appear to be due to the recurrent complex partial seizures themselves, although the failure to find such a correlation may be related to the unreliability of a patient's estimate of the frequency of complex-partial seizures.

Generalized tonic-clonic seizures seem to be correlated with the progressive decline in volume, and were associated with lower ipsilateral volumes. Thus, both the spectroscopic and volumetric data show that generalized tonic clonic seizures are associated with increased MRI abnormality only on the side where there is also a negative correlation with duration. This

suggests that generalized tonic clonic seizures may be a causal factor of progressive neuronal dysfunction or loss in TLE. Again, our ability to detect stronger correlations of NAA/Cr and hippocampal volume with the frequency of generalized as opposed to partial seizures may be because they are more damaging to neurons, but also because patients may more reliably estimate the frequency of generalized, rather than partial, seizures.

The correlation of duration with hippocampal volume contradicts previously published work by our group²²⁾. Several differences between that and the present analysis may explain this discrepancy. First, our previous study included patients with temporal and extratemporal lobe epilepsy, a more heterogeneous group of patients. Secondly, 58% of the patients reported here were studied using a newer, more precise, MRIVol acquisition protocol using 1 mm slices, as opposed to the 3 mm slices of the previous protocol. The current protocol may have a lower threshold for detecting subtle cell loss. Thirdly, for the present study we used Z-scores for correlation analyses, and in the previous paper²²⁾ we have used absolute hippocampal volumes corrected for variation of intracranial volume. The fact that Z-scores represent the variation in SD, thus reducing the skewness of the values across patients, may explain the significant correlation found in the present study. Finally, the patients in the current study tended to be older, and had longer duration of epilepsy and lower ipsilateral volumes than in the previous study.

CONCLUSION

This study suggests that temporal lobe epilepsy, which begins with an early injury, occurs asymmetrically, and is followed by a gradual and progressive course of further neuronal loss and dysfunction. The etiology of the progression remains uncertain. Generalized tonic-clonic seizures are associated with signs of progressive neuronal loss and/or dysfunction as

measured by magnetic resonance spectroscopy and volumetry. Despite the statistically significant outcomes in this study, the majority of the variability in the data remains unexplained. This may be due to, in part, the unreliability of estimates of seizure frequency and onset of epilepsy. Longitudinal studies are likely to be more robust in fully exploring the effects of age, age of onset, repeated seizures, and duration of epilepsy. A prospective, multimodal neuroimaging study based on MR technology has the potential of gaining further insights into the natural history of temporal lobe epilepsy.

Paper 8: Time course of postoperative recovery of N-acetyl-aspartate in temporal lobe epilepsy.

Serles W, Li LM, Antel S, Cendes F, Gotman J,
Olivier A, Andermann F, Dubeau F, Arnold DL.
Submitted.

SUMMARY

Background: NAA/Cr, which can be measured noninvasively using proton MR spectroscopic imaging (^1H -MRSI), provides a surrogate marker of neuronal integrity. After successful surgical treatment of TLE, initially low NAA can return to normal values in regions outside the resected focus.

Objective: To assess the time course of increases in N-acetyl-aspartate/Creatine (NAA/Cr) after surgery in patients with intractable non-lesional temporal lobe epilepsy (TLE).

Patients/Methods: We performed pre- and postoperative ^1H -MRSI in 16 seizure-free (*SF*) patients and 16 not seizure-free (*NSF*) TLE patients. We calculated a mixed design ANOVA between *SF* and *NSF* groups, ipsi- and contralateral to the side of operation and pre- and postoperative NAA/Cr measurements. We applied non-linear regression between pre- and postoperative NAA/Cr differences and the time interval between ^1H -MRSI scans to fit a negative exponential model to NAA recovery.

Results: Mixed design ANOVA revealed that (i) postoperative NAA/Cr was significantly higher in *SF* than in *NSF* patients ($p = 0.02$) and that (ii) the *SF* group had significantly higher postoperative NAA/Cr values compared to their preoperative values ($p < 0.05$) which were within the normal range in most patients. According to our nonlinear regression-model, in *SF* patients, there was a 50% increase relative to preoperative NAA/Cr values after 5.8 months, and an improvement of 95% after 25 months.

Conclusion: Our results extend preliminary observations of postoperative NAA recovery of *SF* patients by characterizing the time course of recovery as an exponential

function with a half time of approximately 6 months. The reversal of neuronal metabolic dysfunction remote from the epileptic focus may underlie the clinical observation of improvement of cognitive function after successful epilepsy surgery.

INTRODUCTION

Brain proton magnetic resonance spectroscopic imaging (1H-MRSI) allows in vivo quantification of N-acetyl-aspartate (NAA), which is the major contributor for the N-acetyl group MR signal seen at 2.02 ppm. In mature brain, NAA is found exclusively in neurons and neuronal processes, thus, a decrease in the NAA signal reflects neuronal loss or dysfunction¹¹⁸. Neuronal damage in the temporal lobes as measured by 1H-MRSI is present virtually in all patients with intractable temporal lobe epilepsy (TLE). NAA signal loss is often seen bilaterally, with maximal reduction on the side of seizure origin defined by prolonged video-EEG monitoring^{115:157:176-178}. We and others have shown that neuronal damage and dysfunction of the temporal lobes in patients with intractable TLE can improve after successful surgical removal of the epileptogenic area^{161:231-233}. The improvement is seen both in the remaining ipsilateral temporal tissue¹⁶¹, behind the resection, and contralateral to the side of surgery²³¹⁻²³³. Neuronal recovery has been reported to occur as early as two months after operation contralaterally²³³ and five months ipsilaterally¹⁶¹. However, the dynamic changes of postsurgical recovery are not entirely clear. Better characterization of postoperative NAA increase in these patients can shed light on the factors important for recovery, such as presence or absence of seizures or adequate surgical removal of the epileptic area. Moreover, knowledge of the temporal profile of recovery might prove useful in guiding clinical management of surgically treated patients. Therefore, we evaluated the time course of neuronal recovery in the temporal lobe ipsi- and contralateral to the side of resection by means of 1H-MRSI in a series of patients with intractable TLE who underwent surgical treatment.

PATIENTS AND METHODS

Patients

We performed pre- and postoperative 1H-MRSI in 32 patients with intractable TLE (19 women, mean age = 36.4 years, range = 16 – 62 years) who had no foreign tissue lesions on MRI. All patients underwent a comprehensive evaluation for localization of the epileptogenic area. 1H-MRSI was performed within two weeks before operation. Thirteen patients had right and 19 had left-sided operations. Fourteen patients had been part of a previously published study¹⁶¹. Five of the remaining 18 patients were selected based on the fact that they were returning for routine postoperative follow-up. Thirteen patients were selected based on the fact that they had preoperative 1H-MRSI investigation, were able and willing to return for a postoperative follow-up exam and the requirement that the final groups have equal numbers of seizure-free (SF) and not seizure-free (NSF) patients. We used Engel's outcome classification with respect to seizure control²⁶⁷. Class I (excludes early postoperative seizures in the first two weeks): a) completely seizure free since surgery, b) auras only since surgery, c) less than three complex partial seizures after surgery, but free of complex partial seizures for at least two years, d) generalized convulsion with antiepileptic drug withdrawal only. Class II: a) initially free of complex partial seizures and has less than three seizures per year, b) less than three seizures per year, c) more than three seizures per year after surgery, but now less than three seizures for at least two years, d) nocturnal seizures only. Class III: a) seizure reduction of more than 90%, b) prolonged seizure-free intervals amounting to greater than half the follow-up period, but not less than two years. Class IV: a) seizure reduction of less than 90%, b) no appreciable change, c) seizures worse.

¹H-MRSI acquisition and data analysis

1H-MRSI studies were performed on a Philips 1.5 T ACS III combined imaging and spectroscopy system (Philips Medical Systems, Best, The Netherlands). After scout images in

axial and sagittal planes were acquired, a multislice transverse spin-echo MRI (TR 2000 ms, TE 30 ms) parallel to the axis of the hippocampus was obtained. The volume of interest (VOI) of the temporal lobe 1H-MRSI included part of the head, body and tail of the hippocampus and portions of gray and white matter from the mid and posterior temporal lobes. The size of the VOI for temporal lobe protocol spectroscopy was approximately 85-100mm in the left-right axis, 75-95mm in the antero-posterior axis, and 20mm in thickness. A water suppressed 1H-MRSI was acquired from the VOI (TR 2000 ms, TE 272 ms, 250x250 mm field of view, 32x32 phase-encoding steps), followed by a 1H-MRSI without water suppression (TR 850 ms, TE 272 ms, 250x250 mm FOV, 16x16 phase-encoding steps). Post-processing included zero-filling the water unsuppressed 1H-MRSI to obtain 32x32 profiles, followed by application of a mild Gaussian k-space filter and an inverse two-dimensional Fourier transformation to both water suppressed and unsuppressed 1H-MRSI. The resulting time domain signal was corrected for artifacts resulting from magnetic field inhomogeneity, and left shifted and subtracted from itself to improve water suppression²⁶⁹. This procedure was also applied to 61 control subjects. To enhance the resolution of the spectral peaks, a Lorentzian-to-Gaussian transformation was applied prior to Fourier transformation in the spectral domain. The effective voxel size was approximately 12 x 12 x 22 mm after k-space filtering.

For data analysis, locally developed software was used for baseline and peak fitting of the spectra. Analysis of the last 18 patients employed a more sophisticated baseline correction and peak fitting routine to determine metabolite resonance intensities of NAA, creatine + phosphocreatine (Cr), choline-containing compounds (Cho), and the ratio of NAA over Cr (NAA/Cr). Spectra were excluded from the analyses if they were artifactually broadened (i.e. full width at half maximum >10 Hz). The position of the postoperative VOI was matched to the preoperative one within individual patients. The region of analyzed voxels was outside the

tissue resected, usually starting behind the middle of the brainstem on an axial image, thus allowing comparison of pre- and postoperative data on both the operated and non-operated side (Figure 1A).

It is assumed that, in epilepsy, cerebral Cr is stable or undergoes minor changes that do not influence the NAA/Cr ratio significantly^{158;160;177}. Moreover, in our previous study¹⁶¹, we had performed a normalization procedure based on brainstem values of Cr as well, which should be unaffected in TLE. We showed a significant postoperative increase in brainstem-corrected NAA resonance intensities in seizure-free patients, but no significant changes in the brainstem-corrected Cr signal intensities.

Statistical analysis

Differences in baseline and peak fitting methods between the initial 14 patients and 21 controls and the 18 subsequently analyzed patients and 40 controls necessitated the use of NAA/Cr Z-scores (NAA/Crz), which allowed us to compare NAA/Cr values across groups. For each analyzed region, standardized values were calculated for each patient by: (i) subtracting their NAA/Cr value from the mean NAA/Cr value obtained from the same region in normal control subjects, and (ii) dividing the result by the normal control subjects' NAA/Cr standard deviation (SD) for that region. NAA/Crz below -2SD (i.e. below 95% of the sample distribution) compared to control data were considered to be abnormal.

We used unpaired t-tests to compare follow-up periods between the seizure-free and the not seizure-free patients. We performed a three factor, mixed design analysis of variance (ANOVA) between the seizure state (i.e. SF vs. NSF = between subject factor), the side with respect to operation (i.e. ipsi- vs. contralateral = between subject factor), and the time with

respect to operation (i.e. pre- vs. postoperative = within subject factor).

Recovery model. For each side, the postoperative NAA/Cr_z was subtracted from the preoperative one, normalized to the preoperative value and denoted as Z-score-difference ($Z_{Pre} - Z_{Post} / Z_{Pre} = ZSD$). This corrects for the different Z_{Pre} values in each patient and represents a percentage change relative to the Z_{Pre} . Furthermore, we applied non-linear regression between the ZSD and time interval to follow-up 1H-MRSI scans to fit a negative-exponential model of the time course of NAA recovery as follows: $ZSD = 1 - e^{-k * interval}$. This was done separately for the data of the SF group (contra- and ipsilateral) and the NSF group (contra- and ipsilateral), k being the calculated time-constant for each data set. This model assumes that, as the interval approaches infinity (and therefore ZSD approaches 1, i.e. 100% recovery), Z_{Post} approaches zero, which by definition is the average NAA/Cr_z for normal controls (suggesting a return to normal NAA/Cr values). The amount of time for Z_{Post} to reach a certain percentage of normalcy can be calculated by the formula: $t = \ln \{100 / (100 - x)\} / k$, where x is the desired percentage. Rationales for our model and further details are provided in the Appendix. Clinical data, NAA/Cr_z and Z-score-differences of 16 NSF and 16 SF patients are provided in the Table.

In order to test whether the ipsi- and contralateral models for the SF patients were significantly different, we performed chi-square tests for goodness-of-fit for each of the models on both the contralateral data and the ipsilateral data. For each set of data (contralateral and ipsilateral), we then used the ratio of the chi-square statistic from the two models to perform an F test³³⁵.

We used the statistical software packages of DATASIM for Macintosh, version 1.2 (Bradley DR, Department of Psychology, Bates College, Lewiston, ME, 1998) for calculating

the ANOVA and SYSTAT for Windows, version 7.01 (SPSS Inc., Chicago, IL) for calculating the non-linear regression.

RESULTS

There was no statistical significant difference between the mean time interval to the follow-up 1H-MRSI for the SF group (22 months; range 3 - 59) and for the NSF (21.2 months; range 6 - 37) ($p = 0.85$). The mean clinical postoperative follow-up period was 31.5 months (range 10 - 59) and 29.9 months (range 12 - 46), respectively ($p = 0.70$).

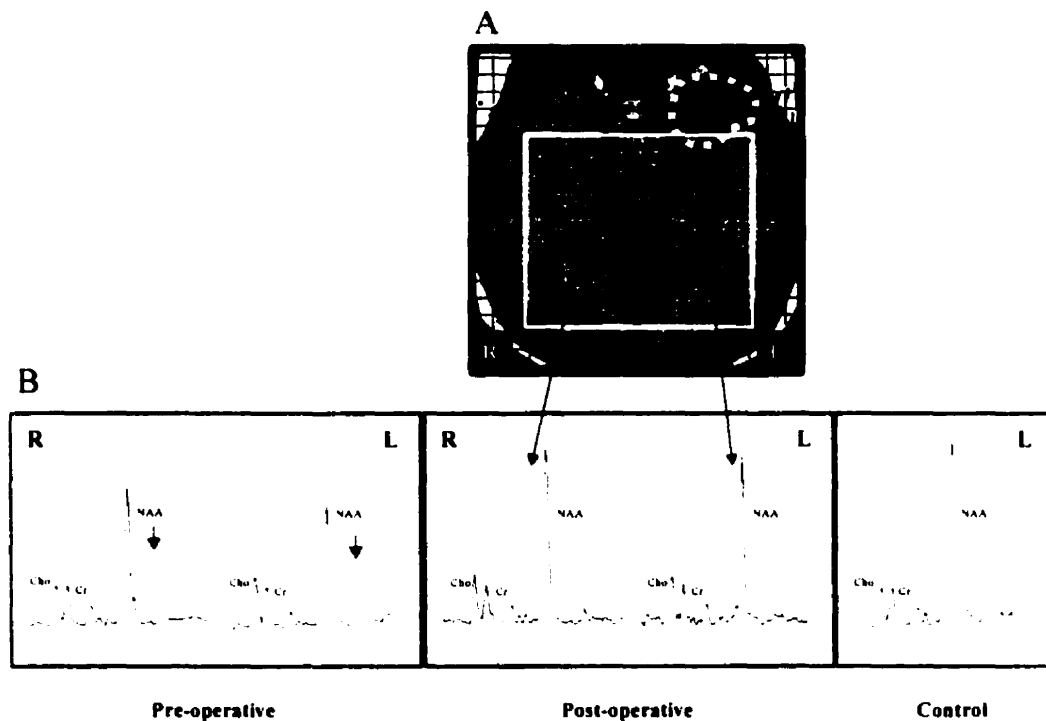


Figure 1: A: Postoperative ^1H -MRSI volume of interest (white box) and regions of analyzed voxels ipsilateral and contralateral to the side of resection. The NAA/Cr ratio was obtained by averaging the voxels of each region. Note that on the operated side, analyzed voxels are behind the resected area (broken line). B: Spectrum of a patient with left sided TLE preoperatively (i) and postoperatively after 40 months (ii) (patient 15 SF). For comparison, a spectrum of the left temporal lobe of a normal control is depicted (iii).

Mixed design ANOVA. NAA/Crz were lower on the ipsilateral side than contralateral ($F(1, 60) = 10.21; p < 0.01$). Because of a significant interaction between the factors, seizure state and time with respect to operation, a simple main effects test was calculated. This analysis revealed no significant difference for preoperative NAA/Crz between SF and NSF patients ($F(1, 120) = 0.15, p = 0.69$). However, postoperative NAA/Crz were significantly higher in SF patients than in the NSF group ($F(1, 120) = 6.55, p = 0.02$). Furthermore, in the SF group, postoperative NAA/Crz were significantly higher than preoperative values ($F(1, 60) = 5.03, p < 0.05$) and returned to the normal range in most patients (mean postoperative NAA/Crz-contralateral: -1.47 ; mean postoperative NAA/Crz-ipsilateral -1.95) (Figures 1B and 2). In contrast, in the NSF group, NAA/Crz did not change significantly between pre- and postoperative measurements ($p = 0.35$) (Figure 3). In the SF group, there were four patients who did not show improvement after surgery. Three of them started with ipsilateral NAA/Crz less than $-2SD$ below the normal control group mean and showed a further decrease postoperatively (patients 11, 12 and 14 SF, see Table). One patient however, had ipsilateral and contralateral normal NAA/Crz preoperatively and showed bilateral abnormal NAA/Crz values after surgery (patient 10 SF). Although they were considered seizure-free at the clinical follow-up interview at 10 and 26 months, patient 11 (two complex partial seizures after four and eight months) and patient 12 (one generalized tonic clonic seizure because of medication withdrawal after 11 months) retrospectively did not have class IA outcome. Furthermore, patient 14 had several normal postoperative EEG's during suspected recurrent seizures. His postoperative attacks were considered psychogenic in the context of his preexisting schizophreniform disorder and his neuroleptic medication was maintained. The one patient with bilateral decrease of NAA/Crz postoperatively (patient 10) had outcome class IA after more than 3 years of follow-up on reduced medication.

Figure 2: Box-and-whiskers plots of pre- and postoperative NAA/Cr_z in 16 seizure-free patients for the ipsi- and contralateral side (see text).

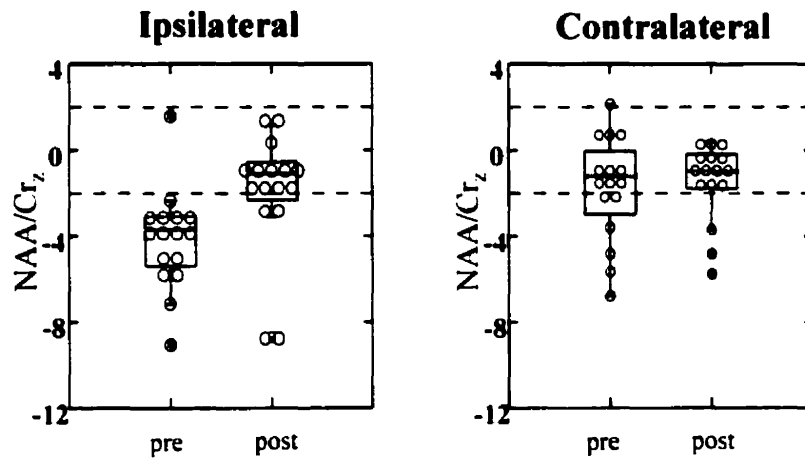


Figure 3: Box-and-whiskers plots of pre- and postoperative NAA/Cr_z in 16 not seizure-free patients for the ipsi- and contralateral side (see text).

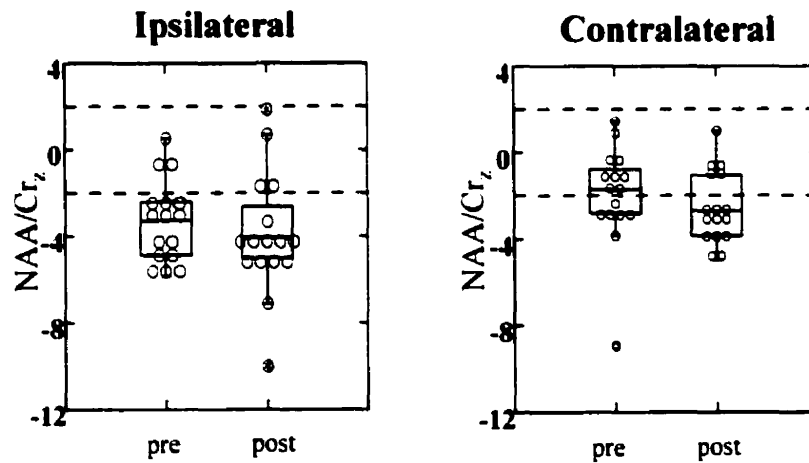


Figure 4: Combined data of the ipsi- and contralateral Z-score-differences (ZSD) over time (months) in 16 seizure-free patients.

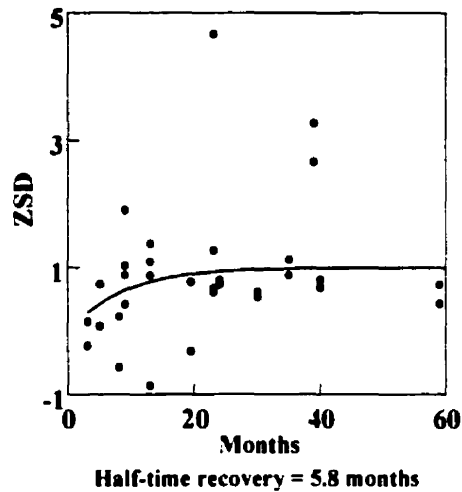


Figure 4: Fitted negative exponential function with r^2 -value of 0.47.

Recovery model. Fitting our model to the data, nonlinear regression in SF patients yielded $k = 0.08$ for the ipsilateral and $k = 0.15$ for the contralateral side with raw r^2 -values of 0.6 and 0.42, respectively. Since the F-test on the chi-square statistics of the contralateral and ipsilateral models failed to reveal a significant difference between the two models, we combined the data and repeated the nonlinear regression, which yielded $k = 0.12$ and r^2 -value = 0.47. According to our model, following surgery, there was a 50% increase relative to the preoperative NAA/Crz after 5.8 months, while an improvement of 95% was reached after 25 months (Figure 4).

Our model is designed to track NAA recovery from pathologically low values and therefore may not be applicable to patients for whom ZPre is above 0. The five instances in which a patients' ZPre was greater than zero for one or both hemispheres (patients 8, 9 (contra), 10 (contra & ipsi) and 16 SF (contra)) were all outliers with respect to our model.

Patients 11, 12, 13, and 14 SF also appeared to deviate somewhat from our model.

Examination of the ZPre and ZPost values for these patients revealed that their NAA did not recover, but in fact decreased following surgery (ipsilateral in patients 11, 12 and 14 and contralateral in patient 13, see table). Excluding the data points which did not fulfill the criteria of our model (leaving 23 data points for analysis), we found an excellent fit for our model with a r^2 -value of 0.86, yielding the same half time as for the overall data ($k = 0.12$; Figure 5).

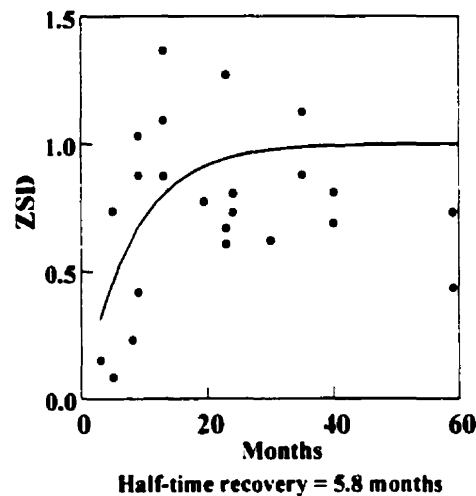


Figure 5: Combined data of the ipsi- and contralateral Z-score-differences (ZSD) over time (months) after removing ZSD's with Z_{Pre} greater than zero or not improved Z_{Post} (r^2 -value of 0.86).

In contrast, when the model was applied to the NSF group, the raw r^2 -value for the ipsilateral side was 0.01 ($p = 0.15$). Non-linear regression on the contralateral data as well as the combined contralateral and ipsilateral data did not converge.

DISCUSSION

The present study demonstrates postoperative NAA/Cr increase and eventual normalization in successful surgically treated patients that was not seen in patients who were not seizure-free. Our data confirm postoperative NAA recovery in a larger sample of operated TLE-patients than previously reported^{161,231-233}. Most importantly, however, we provide for the first time estimates of the postoperative time course of NAA recovery in *SF* patients. According to our negative exponential model, we determined a half time for NAA normalization of approximately 6 months after surgery. In addition, we found that, according to our model, dynamic postoperative NAA changes are not significantly different between the ipsilateral and contralateral side to operation. The finding of early NAA recovery in *SF* patients may serve as an early index of successful surgical treatment, which often can be fully ascertained only after two years of follow-up²⁶⁷. Potentially, this might prove useful for guiding drug withdrawal postoperatively.

In the *SF* group, there were four patients who did not show an increase in their postoperative NAA ipsilateral to the operation, although there was some increase on the contralateral side. This may be related to seizure recurrence in two (patients 11 and 12 *SF*) and concomitant psychiatric disease³³⁶ in another (patient 14 *SF*). In the remaining patient (patient 10 *SF*) the cause of NAA decrease in both temporal lobes after surgery is unclear.

The choice of our mathematical model for postoperative recovery was based on the fact that NAA normalization should occur asymptotically, starting from variably low NAA values at $t = 0$ (see Appendix). The negative exponential function provided a reasonable fit to the *SF* data. A linear model would have assumed a continuous increase to infinity, which is inappropriate.

The aim of our study was not to predict seizure-free outcome by means of ^1H -MRSI in an individual patient. Therefore, applicability of our data for predicting successful postoperative drug withdrawal in individual patients must be viewed cautiously, and future studies should address this issue. However, restricting the data to the criteria of our model, we were able to provide a more accurate estimate of NAA recovery in the *SF* group for the individual patient, which did not differ from the overall recovery.

The cause of NAA/Cr recovery is not entirely clear. The possible factors include: (i) NAA increase within individual neurons, e.g. secondary to reversal of neuronal metabolic damage; (ii) increase in relative neuronal volume within the VOI due to a) increase in cell size, dendritic arborization or both; b) increase in cell numbers through replacement of lethally damaged neurons by neurogenesis or c) resolution of cerebral edema induced by epileptic activity; and (iii) changes in the relaxation time of NAA.

It is unlikely that changes in relaxation time would occur in *SF* but not in *NSF* patients and that these changes would affect NAA differently from Cr. It is also unlikely that changes in the water content occur after surgery, since no alterations of T2-signals are observed.

We believe that the first and, in part, the second factors above are the most likely explanations for the increase in NAA. NAA recovery as a result of reversible metabolic impairment, *i.e.* after removal of metabolic stress, has been demonstrated *in vitro*^{155,156} and *in vivo* after treatment of amyotrophic lateral sclerosis with anti-glutamatergic drugs¹⁵² or after the acute phase in demyelinating lesions¹⁵¹. It is also conceivable that neuronal plasticity during the postoperative period could generate an increase in relative NAA secondary to synaptogenesis and dendritic sprouting. Finally, recent studies have demonstrated that neurogenesis can be seen not only in the adult brain of rodents^{337,338} and primates³³⁹ but also in

the adult human hippocampus³⁴⁰. Therefore, in seizure free patients after surgery, recovery of neuronal integrity could involve both neuronal plasticity *and* neurogenesis, both of which could contribute to the increase in the NAA signal.

The mechanisms by which epilepsy could cause metabolic stress, or changes in neuronal volume are unclear. Clinical seizure frequency correlates with decreases in NAA^{288,289}. It is also possible that ongoing abnormal neuronal firing (Serles *et al.*, unpublished data) or other mechanisms such as the expression of immediate-early genes and subsequent neuromodulators²²⁴ could be responsible for decreases in NAA.

It has been shown in animals that acute neuronal injuries can cause transient NAA reduction trans-synaptically¹⁸¹. Similarly, acute plaques in multiple sclerosis patients can induce transient NAA decreases in contralateral homotopic regions³⁴¹. The phenomenon of reversible decreases of NAA remote from lesion may reflect important changes in the brain secondary to, but not co-localized to the epileptic area. These reversible changes in NAA may be indicating reversible neuronal dysfunction underlying improvement in cerebral function as measured by neuropsychological testing^{234,236,238}. For instance, Jokeit and Ebner recently showed an improvement of psychometric intelligence based on full scale intelligence quotients six months postsurgically only in temporal lobe epilepsy patients who became seizure-free²³⁴.

In conclusion, our results confirm postoperative NAA/Cr recovery in *SF* patients. NAA/Cr recovery can be modeled as an exponential function with a half time of approximately 6 months. NAA/Cr recovery is seen in areas close and remote from the resected epileptic area, which may reflect improvement of cerebral function in addition to seizure control.

APPENDIX A: RECOVERY MODEL

RATIONALE FOR MODEL

Recall that we measured NAA/Cr recovery in terms of Z-score difference (ZSD).

where Z_{Pre} and Z_{Post} represent NAA/Cr_Z pre- and post-surgically, respectively:

$$ZSD = \frac{Z_{Pre} - Z_{Post}}{Z_{Pre}} \quad (1)$$

Physiological realities place 2 conditions on the recovery of NAA/Cr following surgery:

1. at $t = 0$, $Z_{Post} = Z_{Pre}$. No time has elapsed \therefore no time for recovery to occur.

$$\therefore \text{ at } t = 0, ZSD = \frac{Z_{Pre} - Z_{Pre}}{Z_{Pre}} = 0.$$

2. As $t \rightarrow \infty$, $Z_{Post} \rightarrow 0$. NAA/Cr should not recover above normal levels (recall that NAA/Cr_Z = 0 represents the average for normal controls, by definition).

$$\therefore \text{ as } t \rightarrow \infty, ZSD \rightarrow \frac{Z_{Pre} - 0}{Z_{Pre}} = 1.$$

These two restrictions led us to select a model that is commonly used for simulating time-dependent phenomena, namely, a negative-exponential function of the form $ZSD = a - e^{-kt}$. Setting $a=1$ fulfills our requirements, as outlined below, and sets our model as $ZSD = 1 - e^{-kt}$. Non-linear regression was used to determine the value of k .

At $t=0$:

$$\begin{aligned} ZSD &= 1 - e^{-kt} \\ ZSD &= 1 - e^0 \\ ZSD &= 1 - 1 \\ ZSD &= 0 \end{aligned}$$

As $t \rightarrow \infty$:

$$ZSD \rightarrow 1 - e^{-kt}$$

$$\begin{aligned} \text{ZSD} &\rightarrow 1 - 1/e^{kt} \\ \text{ZSD} &\rightarrow 1 - 1/e^{\infty} \\ \text{ZSD} &\rightarrow 1 - 0 \\ \text{ZSD} &\rightarrow 1 \end{aligned}$$

Calculation of time needed for recovery

To mathematically formulate an expression to calculate the time necessary to recover X percent towards normalcy, we first need to rewrite our model to express Z_{Post} in terms of Z_{Pre} :

$$\text{ZSD} = \frac{Z_{\text{Pre}} - Z_{\text{Post}}}{Z_{\text{Pre}}} = 1 - e^{-kt}$$

$$1 - \frac{Z_{\text{Post}}}{Z_{\text{Pre}}} = 1 - e^{-kt}$$

$$\frac{Z_{\text{Post}}}{Z_{\text{Pre}}} = e^{-kt}$$

$$Z_{\text{Post}} = Z_{\text{Pre}} * e^{-kt}$$

Recall that for our application, improvement means going from a negative Z_{Pre} to a less-negative Z_{Post} , i.e., towards 0. Thus, an X percent improvement implies

$Z_{\text{Post}} = \left(\frac{100 - X}{100}\right) * Z_{\text{Pre}}$. We set Z_{Post} to represent an X percent improvement relative to

Z_{Pre} and solve for t.

$$\left(\frac{100 - X}{100}\right) * Z_{\text{Pre}} = Z_{\text{Pre}} * e^{-kt}$$

$$\left(\frac{100 - X}{100}\right) = e^{-kt}$$

$$\log\left(\frac{100 - X}{100}\right) = -kt$$

$$t = \frac{\log\left(\frac{100 - X}{100}\right)}{-k}$$

$$t = \frac{\log\left(\frac{100}{100 - X}\right)}{k}$$

For example, the time necessary to achieve a 50% recovery towards normalcy is:

$$t = \frac{k}{\log\left(\frac{100}{100 - 50}\right)}$$

$$t = \frac{k}{\log(2)}$$

Table Clinical data, NAA/Cr-Z-scores (NAA/Cr_z) and Z-score-differences of 16 not seizure-free (NSF) and 16 seizure-free (SF) patients

Patient no.	Sex	Age (y)	Outcome class	Side of Surgery	Type of Surgery	Postop. follow-up (mo)	Duration of epilepsy to 1st MRSI (y)	Interval between OP/postoperative MRSI (mo)	Preoperative NAA/Cr _z		Postoperative NAA/Cr _z		Z-score-difference (ZSD)	
									contra	ipsi	contra	ipsi	contra	ipsi
1 NSF	F	49	IIB	L	ATL	33	49	13	-2.376	-3.283	-1.159	-3.859	0.512	-0.175
2 NSF	F	40	IIB	R	ATL	40	18	21	-3.063	-5.534	-2.746	-4.487	0.104	0.189
3 NSF	F	46	IIB	L	SAH	34	30	19	-1.053	-2.864	-0.630	-3.335	0.402	-0.165
4 NSF	M	48	IIIA	L	ATL	46	35	31	-2.746	-3.283	-3.011	-4.016	-0.096	-0.223
5 NSF	M	25	IIIA	R	SAH	34	22	21	-1.847	-4.592	-2.640	-4.120	-0.430	0.103
6 NSF	F	47	IIIA	L	SAH	28	25	13	-3.857	-5.848	-4.968	-5.429	-0.288	0.072
7 NSF	F	30	IIIA	L	SAH	30	27	30	-2.852	-0.927	-3.804	-4.016	-0.334	-3.333
8 NSF	M	25	IIIA	R	ATL	21	6	21	1.439	-0.433	-3.261	-10.018	3.266	-22.116
9 NSF	M	52	IVC	L	SAH	33	37	27.5	-2.787	-5.112	-0.644	0.682	0.769	1.133
10 NSF	F	62	IB	R	ATL	19	53	17	0.892	-4.631	1.005	-4.908	-0.127	-0.060
11 NSF	M	39	IVA	R	ATL	38	33	37	-1.312	-5.808	-0.984	-1.611	0.249	0.723
12 NSF	M	32	IVA	L	ATL	20	4	12	-0.157	-2.480	-2.513	1.835	-15.049	1.740
13 NSF	M	35	IIIA	R	ATL	29	15	28	-1.312	-3.078	-4.056	-4.169	-2.092	-0.354
14 NSF	F	18	IVB	R	ATL	33	8	19	-0.551	-4.261	-4.503	-7.121	-7.179	-0.671
15 NSF	M	34	IVA	L	SAH	12	15	6	-8.943	-2.344	-2.660	-1.937	0.703	0.174
16 NSF	F	40	IIIA	L	ATL	29	37	24	-1.592	0.516	-3.955	-5.142	-1.485	10.969
1 SF	F	31	IA	L	SAH	29	17	9	-1.899	-3.387	0.058	-1.974	1.031	0.417
2 SF	F	32	IA	R	ATL	55	12	35	-0.894	-4.592	0.111	-0.560	1.124	0.878
3 SF	F	16	IA	L	ATL	43	3	24	-1.159	-2.864	-0.312	-0.560	0.731	0.804
4 SF	F	27	IA	L	SAH	43	21	23	-1.741	-3.021	-0.577	-1.188	0.669	0.607
5 SF	M	31	IA	L	SAH	59	4	59	-2.376	-3.702	-1.345	-0.994	0.434	0.731
6 SF	F	22	IA	L	ATL	24	5	5	-1.265	-3.702	-1.159	-0.979	0.084	0.736
7 SF	F	33	IA	L	SAH	30	20	13	-0.788	-3.597	-0.101	0.330	0.872	1.092
8 SF	F	47	IA	R	ATL	36	37	30	0.858	-5.290	0.391	-2.011	0.545	0.620
9 SF	F	19	IA	R	SAH	16	11	9	0.791	-6.049	-0.711	-0.754	1.898	0.875

10	<i>SF</i>	F	19	IA	L	SAH	39	13	39	2.133	1.576	-4.843	-2.609	3.270	2.656
11	<i>SF</i>	M	50	IIA	L	SAH	10	37	3	-6.813	-7.164	-5.791	-8.779	0.150	-0.225
12	<i>SF</i>	M	48	ID	R	SAH	26	21	19.5	-3.608	-2.338	-0.824	-3.084	0.772	-0.319
13	<i>SF</i>	F	35	IA	R	SAH	19	7	13	-0.617	-3.152	-1.145	1.151	-0.854	1.365
14	<i>SF</i>	M	56	IA	R	SAH	13	37	8	-4.837	-5.500	-3.728	-8.625	0.229	-0.568
15	<i>SF</i>	F	33	IA	L	ATL	40	10	40	-5.671	-9.069	-1.772	-1.740	0.687	0.808
16	<i>SF</i>	M	44	IA	L	SAH	23	42	23	0.498	-4.107	-1.826	1.108	4.668	1.270

NSF = not seizure-free group, *SF* = seizure-free group; y = years, mo = months; outcome class - see method section; OP = operation; contra = contralateral, ipsi = ipsilateral to operation; F = female, M = male; L = left, R = right; ATL = anterior temporal lobectomy, SAH = selective amygdalo-hippocampectomy; bold figures indicate calculated ZSD's with $Z_{Pre} > \text{zero}$ or not improved Z_{Post} (see text)

Paper 9: Proton MR spectroscopic imaging studies in patients with newly diagnosed partial epilepsy.

Li LM, Dubeau F, Andermann F, Arnold DL
Epilepsia 2000 (in press).

Lippincott Williams & Wilkins

SUMMARY

Background: Patients with intractable temporal lobe epilepsy (TLE) have low values of NAA in their temporal lobes. Surgical treatment of patients with intractable TLE is associated with normalization of NAA in patients who become seizure-free, but not in those who continue to have seizures. If low NAA depends on the occurrence of seizures, one would expect NAA recovery also to occur in patients who become seizure-free after AED treatment.

Objective: We assessed whether the NAA to creatine ratio (NAA/Cr) is abnormally low at the onset of epilepsy and if successful treatment of seizures with anti-epileptic drugs (AED) is sufficient for normalization of NAA/Cr.

Patients/Methods: Using proton magnetic resonance spectroscopic imaging (¹H-MRSI) we measured NAA/Cr in the temporal lobes of eight patients with newly diagnosed epilepsy before or soon after starting medication. Six of the patients had follow-up ¹H-MRSI examinations seven months later. The clinical pattern of the seizures and the EEG findings suggested partial seizures in all, and TLE in five of them. None of the patients had lesional epilepsy according to MR imaging.

Results: Initial ¹H-MRSI of the temporal lobes showed significantly low NAA/Cr values in five out of the eight patients. Five of the six patients who had follow-up ¹H-MRSI were seizure-free after institution of medication; the remaining one decided not to take medication and continued to experience occasional auras. Wilcoxon rank sign comparison of the NAA/Cr on the initial ¹H-MRSI examination and the follow-up ¹H-MRSIs showed no significant difference ($Z = 135$, $p = 0.893$, 2-tailed) for the five seizure-free patients.

Conclusion: Neuronal dysfunction is present at an early stage of the epileptic process. The NAA/Cr recovery in seizure-free patients controlled with AEDs is less evident compared to successful surgical treatment. Thus, the mechanism for NAA/Cr normalization after surgical treatment of TLE appears to be related to removal or disconnection of the epileptic area.

INTRODUCTION

In brain ^1H -MRS, the most intense signal is visible at 2.02 ppm and corresponds to N-acetyl groups, mainly N-acetyl aspartate (NAA) ^{118;119}. NAA is synthesized in brain mitochondria from acetyl-CoA and aspartate by the enzyme L-aspartate N-acetyltransferase¹²⁰⁻¹²³ and is confined to neurons and neuronal processes of the mature brain^{124;125}. The NAA signal in the mature brain derives only from the neuronal pool, areas of decreased NAA signal intensity are interpreted as (i) neuronal loss and/or (ii) dysfunction. The assumption of neuronal loss is supported by both experimental ¹³⁷⁻¹⁴⁴ and clinical observations¹⁴⁵⁻¹⁵⁰. The assumption of neuronal dysfunction is supported by *in vivo* ¹⁵¹⁻¹⁵⁴ and *in vitro* ^{144;155;156} studies which showed the ability of the NAA signal to recover. De Stefano et al.¹⁵¹ reported on a series of patients with acute brain injury, multiple sclerosis or mitochondrial encephalopathy, who had significant NAA/Cr decrease and lactate increase during the acute phase of disease with NAA/Cr normalization paralleling their clinical recovery. Balm et al.,¹⁵³ performed ^1H -MRSI in 16 patients with symptomatic carotid artery stenosis before and after endarterectomy. They found that metabolic changes seen pre-operatively (\downarrow NAA, \uparrow lactate) normalized four days after endarterectomy. Matthews et al.¹⁵⁵ showed that neurons under stress conditions *in vitro* express less NAA and this reverses with optimization of the culture media, reflecting the survival of a population of viable neurons. Bates et al.¹⁵⁶ showed that inhibition of mitochondrial oxygen consumption and ATP synthesis also inhibited NAA production, suggesting that impaired neuronal mitochondria function, if not reversed, may result in irreversible neuronal death.

Since NAA can be quantified *in vivo* by proton MR spectroscopy, it has been a useful marker of neuronal integrity in the assessment of neurological disorders. The NAA signal is

often reduced in the brains of patients with intractable partial epilepsy.²⁴⁷ Although the NAA decrease can be widespread and usually involves the contralateral side as well, the maximal reduction coincides with the side of seizure origin as defined by EEG.^{115;116;157-159;176} NAA recovery was shown in patients with intractable temporal lobe epilepsy (TLE) who had undergone a surgical resection and became seizure-free.^{161;231-233} We have shown that the time course of NAA recovery in these patients can be modeled as a simple exponential function, with a post-operative recovery half-time of approximately six months.³⁴² In contrast, in patients whose epilepsy persisted despite surgery, NAA levels did not change significantly. The mechanism that leads to NAA improvement post-operatively is poorly understood. Since NAA recovery is only seen in those patients who become seizure free, it is unlikely that post-operative tissue changes and alterations in water content and metabolite relaxation time are the cause. An alternative explanation is that the NAA levels normalize following cessation of seizure activity, but if this were the case, one would also expect to see NAA recovery in the brains of patients who become seizure-free with anti-epileptic drug (AED) therapy.

The use of the newly introduced AEDs rarely leads to seizure freedom in patients refractory to conventional AEDs.^{343;344} On the other hand most patients with newly diagnosed epilepsy can become seizure-free with AEDs. However, it is not known whether patients with newly diagnosed epilepsy might have neuronal dysfunction that results in epileptogenic activity or whether neuronal dysfunction is a consequence of a long-standing epileptic process. In our previous cross sectional study of 82 patients with chronic refractory TLE, linear regression plots suggested that neuronal metabolic dysfunction is present at the time of clinical diagnosis of epilepsy.²⁸⁹

In this study we aimed: 1) to evaluate whether neuronal dysfunction, as measured by

NAA/Cr reduction, is present in patients with newly diagnosed partial epilepsy; and ii) to assess if neuronal dysfunction can improve with AED treatment.

PATIENTS AND METHODS

We studied with ^1H -MRSI eight patients with newly diagnosed partial epilepsy before or soon after starting medication (maximum 1 month). They were referred by neurologists of the Montreal Neurological Hospital, who were also consultants on call at the Emergency Service of the adjoining Royal Victoria Hospital. Inclusion criteria were: 1) patients who had at least two unprovoked stereotyped seizures, 2) absence of a foreign tissue lesion as detected by MRI, 3) patients willing to undergo serial ^1H -MRSI. The study was approved by the Ethics Committee of the Montreal Neurological Institute and Hospital. Informed consent was obtained from all patients. Six patients had a follow-up ^1H -MRSI seven months later.

^1H -MRSI studies were performed in a Philips 1.5 T ACS III combined imaging and spectroscopy system (Philips Medical Systems, Best, The Netherlands). Following scout images in both axial and sagittal planes, a multislice transverse spin-echo MRI (TR 2000 ms, TE 30 ms) was obtained. The volume of interest (VOI) within the temporal lobe ^1H -MRSI included part of the head, body and tail of the hippocampus and portions of gray and white matter from the mid and posterior temporal regions (Figure 1A-MRI). The size of the VOI for temporal lobe spectroscopy protocol was approximately 85-100mm in the left-right axis, 75-95mm in the antero-posterior axis, and 20mm in thickness. A water suppressed ^1H -MRSI was acquired from the VOI (TR 2000 ms, TE 272 ms, 250x250 mm field of view, 32x32 phase-encoding steps), followed by a ^1H -MRSI without water suppression (TR 850 ms, TE 272 ms, 250x250 mm FOV, 16x16 phase-encoding steps). Post-processing included zero-filling the water unsuppressed ^1H -MRSI to obtain 32x32 profiles, followed by application of a mild

Gaussian k -space filter and an inverse 2D Fourier transformation to both water suppressed and unsuppressed ^1H -MRSI. The resulting time domain signal was left shifted and subtracted from itself to improve water suppression.²⁶⁹

Resonance intensities in individual spectra were determined by integration of peak areas using locally developed software. Voxels on the edge of the VOI which were affected by chemical shift artifact and voxels that were artifactually broadened were excluded from the analyses. The resonance intensity of NAA was normalized to intravoxel Cr. In epilepsy, Cr is relatively stable^{157,158,160,161,177} so that changes in the NAA/Cr ratio reflect changes in NAA and neuronal loss or dysfunction. NAA/Cr for each temporal regions were expressed as z-scores ((value – normal mean) / normal standard deviation) compared to values from 40 healthy control subjects of similar age. Values 2 SDs below the normal mean were considered abnormal. Three controls had follow-up scans 2 years after their baseline scan. The repeatability coefficient¹⁴⁵ of the NAA/Cr measurement between scans was calculated for these three controls and found to be 0.22 (5%) for a 99% confidence interval. NAA/Cr differences between follow-up and baseline measurements that fell outside the range of the repeatability coefficient were considered significant.

Diagnostic MRI scans were acquired using the same scanner in a separate examination. We acquired sagittal and coronal T₁-weighted (TR 550 ms, TE 19 ms) images, followed by dual-spin echo (TR 2100 ms, TE 20ms - 78 ms) transverse proton density and T₂-weighted images. A T₁-weighted gradient-echo volume acquisition of the whole brain (TR 18 ms, TE 10ms, 30° angle, 1 mm thick contiguous slice) was used for multiplanar reconstruction.

RESULTS

Patients' data are displayed in Table. The mean age of patients at the time of diagnosis

of their epilepsy and ¹H-MRSI examination was 30 years (range 21 – 56 years). None of the eight patients had any identifiable risk factors, such as febrile convulsion, head trauma, or previous central nervous infection. Diagnostic MRI was normal in all eight patients.

The second seizure occurred within one year after the first seizure in all eight patients, three patients (Table: 1, 3, and 7) had the two seizures within a day. All eight patients described an aura. Three patients (Table: patients 1, 4 and 7) had occasional (<than 5) isolated auras for a period of one year before the clinical diagnosis of epilepsy was established and the remaining five patients had only two seizures before their baseline scan. They all had recollection of their seizures.

Routine and sleep EEGs were performed on all patients and showed epileptic activity over the temporal lobe in two patients (Table: patients 1 and 3). Five patients had clinical manifestations with well described temporo-limbic-type auras (Table: patients 1, 3, 4, 7 and 8) and in two of them their EEGs showed temporal lobe spikes (see Figure 1B), suggesting temporal lobe epilepsy. We could not establish precisely the anatomical location of the seizures in the remaining three patients (Table: 2, 5, and 6).

Table: Clinical description and ¹H-MRSI of eight patients with newly diagnosed epilepsy

patient/sex/age	Aura	Seizure description	EEG	Medication	Clinical status	Interval between scans (months)	NAA/Cr z-score of temporal lobe MRSI			
							Baseline		Follow-up	
							right	left	right	left
1/m/26	epigastric discomfort	SGTC	R-Temporal	CBZ	seizure-free	7.34	-8.91	-4.70	-6.27	-4.43
2/f/33	unwell feeling	SGTC	normal	CBZ	seizure-free	7.80	-2.56	-2.59	1.04	-1.27
3/m/56	fear, déjà vu	CPS	Bi-Temporal	CBZ	seizure-free	8.00	-1.91	-4.44	-4.66	-5.05
4/f/20	fear, déjà vu	SGTC	normal	not-treated	monthly auras	9.28	-0.86	-0.28	-2.29	-1.13
5/f/31	hard to describe, dizziness	SGTC	normal	VPA	seizure-free	7.28	-0.74	0.44	-1.81	-0.80
6/m/21	dizziness	SGTC	normal	CBZ	seizure-free	9.67	-4.92	-4.87	-5.70	-4.63
7/m/34	experiential phenomena	CPS, SGTC	normal	PHT			-0.40	-1.87		
8/f/24	experiential phenomena	CPS	normal	CBZ			-3.27	-0.94		

CPS = complex partial seizures, SGTC = secondarily generalized tonic-clonic seizure. R = right, L = left, Bi = bilateral. CBZ = carbamazepine, VPA = valproate acid, PHT = phenytoin. The mean normal control NAA/Cr ratios (SD) for the right TL is 4.28 (0.15) and for the left TL is 4.24 (0.16)

Figure 1:

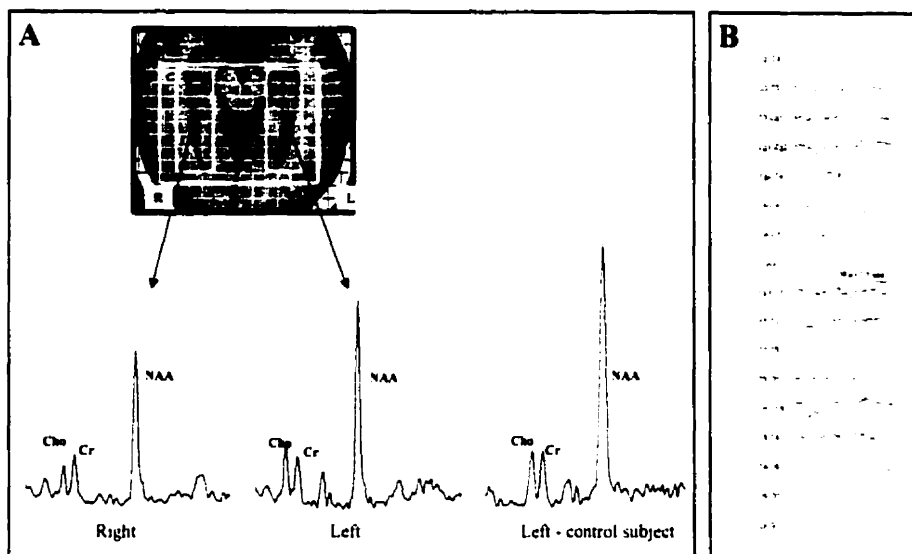


Figure 1: a 26 year-old patient with newly diagnosed temporal lobe epilepsy. A) The follow-up temporal lobe ¹H-MRSI 7 months after complete seizure control by carbamazepine still shows low NAA/Cr values in both temporal regions. B) Interictal EEG showing right temporal lobe epileptic activity.

Statistical analyses were carried out to assess (i) the difference of NAA/Cr between baseline and follow-up scans and (ii) the NAA/Cr changes in an individual patient. Temporal lobe ¹H-MRSI showed significantly low NAA/Cr values in five out of eight patients (see Table). The mean (n=8) NAA/Cr value (z-score) was 3.85 (-2.94) for the right and 3.83 (-2.40) for the left temporal region. Six patients had follow-up temporal lobe ¹H-MRSI. Five out of the six patients were seizure-free since beginning their medical treatment and the remaining one chose not to take medication and continued to experience occasional auras. Wilcoxon rank sign comparison between the baseline and the follow-up temporal lobe ¹H-MRSIs for the five seizure-free patients with alpha corrected for multiple comparison (0.025) showed no difference in NAA/Cr ratios for either side (right temporal lobe Z = 135, p = 0.893, 2-tailed; left temporal lobe Z = 135, p = 0.893, 2-tailed).

Figure 2:

Li et al

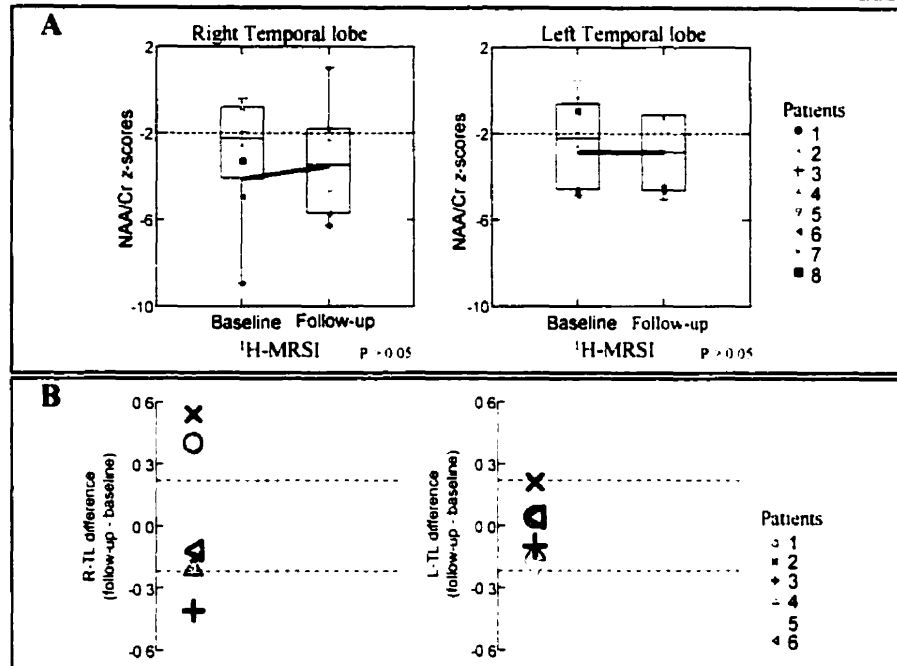


Figure 2: A) Box-and-whisker plots of $^1\text{H-MRSI}$ s NAA/Cr ratios converted into z-scores for patients with newly diagnosed partial epilepsy. The mean interval between scans was 8 months (range 7 to 10 months). The mean NAA/Cr z-score for the first $^1\text{H-MRSI}$ ($n=8$) was -2.94 (right) and -2.40 (left). The follow-up mean NAA/Cr z-score ($n=6$) was -3.28 (right) and -2.89 (left). Wilcoxon rank sign comparison between the first and the follow-up temporal lobe $^1\text{H-MRSI}$ s for the five seizure-free patients (1, 2, 3, 5, and 6) showed no difference in NAA/Cr ratios for either side (right temporal lobe $Z = 135$, $p = 0.893$, 2-tailed; left temporal lobe $Z = 135$, $p = 0.893$, 2-tailed). The baseline and follow-up NAA/Cr z-score mean values of the five seizure-free patients are linked with a line. Horizontal dashed line across represents the limits of -2 SD. B) Difference between follow-up and baseline $^1\text{H-MRSI}$ s NAA/Cr ratios are plotted in the graph with horizontal dashed lines representing the upper and lower limits (99% confidence interval) of the repeatability coefficient of NAA/Cr measurement between scans in normal controls. The patients 1 and 2 had significant improvement of NAA/Cr in the right temporal lobe, while patient 3 had significant decrease of NAA/Cr in his right temporal lobe. The remaining three patients showed no significant change.

In an individual analysis, two seizure-free patients (Table: patients 1 and 2) with bilaterally low NAA/Cr on the initial $^1\text{H-MRSI}$ had a follow-up NAA/Cr increase above the range of the repeatability coefficient, and patient 2 reached a NAA/Cr within the normal range (≥ -2 SD). Nevertheless, one other seizure-free patient (Table: patient 3) with bilaterally low NAA/Cr on the initial $^1\text{H-MRSI}$ showed a decrease in NAA/Cr in the temporal lobe below the range of the repeatability coefficient in the follow-up scan. The untreated patient (Table 1:

patient 4) had a follow-up scan showing a decrease in NAA/Cr from the normal range to < 2SD below the normal mean, but the NAA/Cr difference between baseline and follow-up scans falls within the range of the repeatability coefficient.

DISCUSSION

MR imaging abnormalities have been reported in approximately 24% of patients with newly diagnosed epilepsy²²³ and 12% of patients who had a single seizure.³⁴⁶ Fernandez et al.,³⁵ have also demonstrated that clinically asymptomatic relatives of patients with familial febrile convulsions have asymmetrical hippocampal volumes as measured by quantitative MRI. In this series of patients with no structural abnormality detected by MRI, we found that NAA/Cr was reduced in the temporal lobes early in the course of their epilepsy. It is very unlikely that the few (< 5) auras one year before the diagnosis was established were the cause of the low NAA/Cr seen in these studies. This suggests that a pre-existing underlying structural and/or functional abnormality likely facilitated the development of epilepsy. Similarly in animal models, Germano et al.³⁴⁷ demonstrated that rats with neuronal migration brain lesions had a lower afterdischarge threshold and their hippocampi would kindle more quickly than the control rats.

Normalization of NAA/Cr has been reported in patients who are seizure-free post-operatively.^{161,231-233} The normalization of NAA can be seen as early as two months after surgery.²³³ Surprisingly, in this series the two time point NAA/Cr measurements did not differ significantly in patients who became seizure-free following medical treatment. In individual patient analyses, however, the changes in temporal lobe NAA/Cr were variable: NAA/Cr went up in two patients, down in one, and did not change in the remaining two patients, though they were all seizure free. This suggests that the mechanism for NAA/Cr

normalization in the surgical series follows removal and/or disconnection of the epileptogenic area, and that seizures and neuronal metabolic dysfunction coexist but are not necessarily causally related and may represent independent variables. A mechanism by which the lesion causes local and remote neuronal dysfunction might be similar to the phenomena of diaschisis,³⁴⁸ in which acute lesions in an area of the brain leads to transitory functional impairment of interconnected areas. Rango et al.¹⁸¹ demonstrated that acute deafferentation in the central nervous system can cause transitory NAA/Cr decrease in interconnected areas. In the case of epilepsy, however, in order for sustained neuronal dysfunction to occur, there must be ongoing neuronal network disruption, which apparently is not influenced by the first line AEDs prescribed.

Explanations for not seeing neuronal improvement in this series would include 1) short follow-up, 2) sample size - group selection, and 3) type of drug. The time course of NAA/Cr normalization in drug treated patients might not follow a similar time frame to that seen in surgically treated individuals. The group of patients represented in this study are patients referred from emergency rooms and tertiary centers who usually have more severe epilepsy and do not represent the general epileptic population. Future studies with a larger sample and a community based selection will provide more power in the identification of a sub-group of patients likely to have NAA/Cr normalization. It has been suggested that gabaergic or glutamatergic action drugs can prevent epileptogenesis, while sodium, or calcium channel action drugs only alter the threshold of seizure expression.³⁰¹ There is also evidence that some of the recently developed AEDs also have neuro-protective properties,^{57,58} which might be relevant in blocking epileptogenesis^{61,349} or preventing further neuronal damage.⁵¹ If this is the case, we hypothesize that "anti-seizure" and "anti-epileptogenic" drugs have distinct NAA/Cr recovery profiles; the former shows no improvement in neuronal dysfunction, and

the latter shows improvement and normalization of the neuronal abnormality. Moreover, the presence of a structural brain abnormality is a major contributing factor for relapsing seizures,⁵³ thus patients with normal MR imaging and absence of ¹H-MRS demonstrated neuronal dysfunction would stand a higher chance of successful drug withdrawal. In that case, ¹H-MRS could be used to monitor and provide information about a patient's epileptogenic process. This, however, does not imply that patients with abnormal NAA/Cr ratios could not achieve seizure control. Mendes-Ribeiro et al.²⁴² reported single voxel temporal lobe ¹H-MRS findings in 10 seizure-free TLE patients treated with AEDs. Eight patients had normal NAA/Cr values, however, two patients had significant NAA/Cr reduction despite a long period of seizure freedom (3 years) using AEDs. Interestingly, these two patients had a past history of poor seizure control. Preliminary results from the National Institute of Health-USA²⁴⁰ in children with newly diagnosed epilepsy showed follow-up FDG-PET normalization one year later in two seizure-free patients, while in those with poor seizure control, deterioration or no change was observed on the follow-up FDG-PET examination. It is unknown, however, if glucose metabolism disturbance is a marker of poor seizure control since it is known that FDG-PET results are influenced by peri-scanning seizures²⁴¹. Unlike FDG-PET, NAA/Cr appears not to be influenced by peri-scanning seizures²⁴⁴ and in addition, NAA is a specific marker of neuronal integrity.

In conclusion, neuronal dysfunction is present at an early stage of the epileptic process, and its recovery after seizure-control with standard AEDs is less evident compared to successful surgical treatment. Thus, the mechanism for NAA/Cr normalization after surgical treatment of TLE appears to be related to removal or disconnection of the epileptic area.

Conclusion and summary

Neuronal metabolic dysfunction in relation to lesions and spikes

The results of our ^1H -MRSI study on patients with cortical developmental malformations and epilepsy are similar to a previous study¹. We found that the degree of neuronal metabolic dysfunction is different depending on the type of cortical developmental malformations (CDM), possibly reflecting the intrinsic nature of the lesion. Focal cortical dysplasia showed abnormally low NAA and in some cases a high choline signal at the lesion site. In brain tumors, an increase in the choline signal has been linked to hypercellularity^{167,350} and malignancy³⁵¹, and in the context of CDM, areas of \downarrow NAA and \uparrow choline outside the MRI visible lesion may represent microdysgenesis. Careful anatomic-pathological study of surgical FCD specimens and correlation to co-registration images using anatomical MRI, NAA and choline maps can be used to assess this issue in the future. In heterotopia, the NAA decrease was variable. Although the heterotopic neurons behave²⁵⁸ and look like normal neurons³⁵⁷, they are dysfunctional. This is additional evidence that NAA signal is a marker of neuronal cell function. A recent study³⁵² in 15 patients with CDM confirms low NAA at the site of the lesion. In addition they³⁵² found no significant association between levels of NAA/Cr and the presence of frequent runs of spikes or the seizure burden. In contrast to results seen in CDM^{1,291,352}, neuronal metabolic dysfunction and synchronized neuronal firing in non-lesional cases tend to vary together in intensity (paper 3). This was the first time we have evidence that

interictal spikes are related to neuronal dysfunction. Future study using imaging techniques to quantify neurotransmitters, such as GABA and glutamate, might yield further clarification about the relationship between the structural lesion and epileptogenicity.

The results from the second paper, which assessed the anatomical distribution of neuronal metabolic dysfunction in relation to the epileptogenic area, showed that these two variables co-localize very well, and the former often extend beyond the latter. Our results demonstrated that in addition to commonly seen contralateral homologous NAA decrease, the neuronal metabolic dysfunction also extends to non-homologous regions in ~40% of patients with partial epilepsy. These findings contrast a previous study¹⁵⁹, which using a single 2D ¹H-MRSI of the temporal lobes revealed that non-lesional E-TLE does not have decreased NAA in the hippocampus. Nevertheless, the same authors reported two preliminary studies using multislice ¹H-MRSI with conflicting findings, one showing that neuronal metabolic dysfunction exclusively localized to the seizure focus²⁷³ and the other showing that neuronal metabolic dysfunction extends beyond the seizure focus²⁷². The reasons for discrepant findings are not clear, possibilities include different types of patients (lesional *vs.* non-lesional), different brain regions (hippocampus *vs.* temporal lobe) and ¹H-MRSI techniques (2D-PRESS *vs.* multislice). Future studies should explore these issues and more important is to assess whether presence of widespread neuronal metabolic dysfunction is associated with poor surgical prognosis.

In summary, neuronal metabolic dysfunction overlaps the neuronal electrical paroxysms detected by EEG and the structural lesions displayed by MRI. The extent of neuronal metabolic dysfunction, however, tends to be wider than the MRI-visible lesion and often coincides spatially with the area of synchronized neuronal firing. We conclude that the

anatomical distribution and degree of the neuronal metabolic dysfunction reflects the intrinsic nature and extent of the original epileptogenic damage and also the severity of the epileptogenic process.

Clinical relevance of new types of MR-based techniques

Although magnetization transfer imaging is sensitive to demyelinating lesions¹⁹⁵, it was not useful for lateralizing TLE, probably reflecting distinct pathophysiological mechanisms of axonal *vs.* neuronal damage. Future studies should be performed looking for alternative imaging techniques in the investigation of MR-negative epileptic patients.

TLE patients display a spectrum of structural and metabolic abnormalities demonstrated by MR-based techniques, which allow a probabilistic prediction of TLE lateralization and discrimination between TLE and non-TLE (paper 5). An analogy of this approach towards MR data sets can be made to a weather forecast, in which case we not only predict the possibility of rain, but also its probability. The linear discriminant analyses demonstrated high accuracy for TLE lateralization using a high posterior probability cutoff, but the accuracy was not so high for discrimination of TLE from extra-TLE, mainly due to the presence of temporal lobe neuronal damage in some patients with extra-TLE, reflecting a dual pathology. Future studies using multi-slice ¹H-MRSI which provides a wider coverage, and more powerful data analysis using artificial intelligence, can overcome the limitations of our model in the task of discriminating TLE from others non-TLEs.

In terms of surgical prognosis, the results of our paper 6 showed several features associated with good outcome in a selected group of TLE patients. This contrasts with a previous study³⁵³, which failed to demonstrate a prognostic value for ¹H-MRSI. In their series,

only unilateral hippocampal atrophy was a significant factor associated with outcome. A recent report³⁵⁴ showed similar results to our paper 6, they found that the severity of contralateral neuronal metabolic abnormality was associated to surgical outcome. The discrepancy observed among these reports, including ours, on surgical prognostic value of ¹H-MRSI may be due to sample size, different types of TLE patients, i.e., NAA decreases in unilateral and bilateral hippocampal atrophy and normal hippocampal volume might have different biological meaning and impact on surgical results. It is possible that the severity of the NAA decrease in unilateral hippocampal atrophy has very little importance on outcome, while it is relevant in bilateral hippocampal atrophy patients as we have demonstrated. Since MRVol has surgical prognostic value on TLE patients^{201,203-205,353}, future studies using multivariate analysis on the various MR markers can provide us with clues about the value of these measurements. Furthermore, application of artificial intelligence on different data sets (MR-markers, EEG, neuropsychology, and clinical data) can add prognostic information to surgical outcome. In summary, MRVol and ¹H-MRSI are reliable markers of lateralization of TLE and also have surgical prognostic value, thus we conclude that these techniques should be used to streamline the presurgical evaluation. Patients with a high certainty of MR lateralization and localization plus concordant routine interictal EEG and clinical manifestations do not require prolonged video-EEG monitoring.

Neuronal damage and recovery in the epileptogenic process

In non-foreign tissue lesional TLE syndrome, the epileptogenic process is dynamic and manifests itself as seizures, cognitive impairment, and neuronal loss and dysfunction. A cross sectional study of full scale intelligence quotient (FSIQ) in a large TLE epileptic population demonstrated that there is a progressive decline of FSIQ over time²³⁴. Similarly, results of our

paper 7 showed progressive neuronal damage in a selected group of patients with non-foreign tissue lesional refractory TLE. Seizure burden did not correlate with degree of neuronal damage (paper 2 and 7). There was, however, a significant association between the presence of generalized tonic clonic seizures and neuronal damage, but no definite conclusions can be made about the causal relationship of these two variables because of the type of the study. A recent MRVol study²²² in a smaller group of patients with non-foreign tissue lesional TLE showed similar finding to our study, that the hippocampal volume declines over time and is not related to seizure burden, but history of febrile convulsion is associated with a smaller hippocampal volume. We concluded that there is progressive neuronal damage in non-foreign tissue lesional TLE patients that is not due to seizures. The slopes of NAA/Cr and hippocampal volume over time showed that the period of time needed to detect a drop of one standard deviation in these markers is 33 and nine years respectively. Seizures and neuronal damage should be regarded as distinct domains of patients' TLE process together with neuropsychological impairment or psychiatric disorder. These domains parallel each other in a given time, although their pathophysiological processes are distinct and not necessarily causally related but instead are epiphenomena of the underlying epileptogenic process.

Using a larger series of patients, we confirmed previous observations^{161,231-233} that NAA recovers after surgery. Neuronal recovery occurs only in post-operative seizure-free patients and has a recovery half time of six months (paper 8). Patients who are seizure-free on AEDs, however, do not show neuronal recovery during this timeframe (paper 9).

Based on the distinct pattern of neuronal recovery between surgically and medically treated patients, the mechanism for neuronal recovery is surgical resection or isolation of the epileptogenic area, which interrupts the ongoing neuronal network dysfunction and

consequently normalizes neuronal function, controls seizures, and improves cognitive impairment. As for medically treated patients, the available first line AEDs in most cases only control seizures by altering seizure manifestation threshold but do not improve neuronal metabolic dysfunction. Sato et al.³⁰¹ suggested that certain classes of AEDs exert a true anti-epileptic effect in kindling models, however, this has been difficult to confirm in humans. The newly marketed AEDs have shown to be neuroprotective⁵⁵⁻⁵⁹ and may prevent epileptogenesis and progression of neuronal damage and its consequences. Thus, we hypothesize that "anti-seizure" and "anti-epileptogenic" drugs would show different profiles of neuronal metabolic recovery, the former showing no effect and the latter showing improvement of the neuronal marker, NAA.

Absence of seizures did not appear to be a key factor for neuronal recovery. This supports the idea that seizures and neuronal damage co-exist but are not causally related. Mendes-Ribeiro et al.²⁴² demonstrated that patients with TLE who are seizure-free for many years may still have neuronal metabolic dysfunction. Since presence of a brain lesion is a risk factor for seizure relapse in drug withdrawal process³⁵⁵, we hypothesize that patients who are seizure-free with no structural or neuronal metabolic dysfunction would stand a higher chance of successful drug withdrawal. We add to the statement made by Walker and Sander³⁵⁶ that the final goal of drug treatment is total control of seizures and also resolution of epileptogenic process.

Epileptic State

The epileptic state, herein, refers to the patient's epileptogenic process at a given time point. Seizures, stereotyped behavioral manifestations, are the hallmark of epilepsy. The

presence of seizures denotes an active epileptogenic process, but the absence of seizures does not automatically imply an inactive epileptogenic process. This is supported by the presence of cognitive impairment²³⁵ and neuronal metabolic dysfunction in seizure-free patients²⁴² (paper 10), and seizure relapse after AED withdrawal^{357;358}. The NAA/Cr measure is closely associated with an active epileptogenic area (paper 2, 3, 5, 7-9) and its severity (paper 3). Thus we propose that the NAA/Cr measure can serve as a surrogate marker for the patient's epileptogenic state.

REFERENCE

1. Kuzniecky R, Hetherington H, Pan J, et al. Proton spectroscopic imaging at 4.1 tesla in patients with malformations of cortical development and epilepsy. *Neurology* 1997;48:1018-24.
2. Tofts PS, Sisodiya S, Barker GJ, et al. MR magnetization transfer measurements in temporal lobe epilepsy: a preliminary study. *AJNR Am J Neuroradiol* 1995;16:1862-3.
3. Hauser WA. Epidemiology of epilepsy. *Adv Neurol* 1978;19:313-39.
4. Sander JW, Shorvon SD. Epidemiology of the epilepsies [published erratum appears in *J Neurol Neurosurg Psychiatry* 1997 Jun;62(6):679]. *J Neurol Neurosurg Psychiatry* 1996;61:433-43.
5. Sander JW, Shorvon SD. Incidence and prevalence studies in epilepsy and their methodological problems: a review. *J Neurol Neurosurg Psychiatry* 1987;50:829-39.
6. MacDonald RL. Antiepileptic drug actions. *Epilepsia* 1989;30:19-28.
7. MacDonald RL, Kelly KM. Antiepileptic drug mechanisms of action. *Epilepsia* 1995;36:2-12.
8. Nashef L, Fish DR, Garner S, Sander JW, Shorvon SD. Sudden death in epilepsy: a study of incidence in a young cohort with epilepsy and learning difficulty. *Epilepsia* 1995;36:1187-94.
9. Nashef L, Fish DR, Sander JW, Shorvon SD. Incidence of sudden unexpected death in an adult outpatient cohort with epilepsy at a tertiary referral centre. *J Neurol Neurosurg Psychiatry* 1995;58:462-4.
10. Nashef L, Sander JW. Sudden unexpected deaths in epilepsy--where are we now? [see comments]. *Seizure* 1996;5:235-8.
11. Nashef L, Garner S, Sander JW, Fish DR, Shorvon SD. Circumstances of death in sudden death in epilepsy: interviews of bereaved relatives. *J Neurol Neurosurg Psychiatry* 1998;64:349-52.
12. Nashef L, Walker F, Allen P, Sander JW, Shorvon SD, Fish DR. Apnoea and bradycardia during epileptic seizures: relation to sudden death in epilepsy. *J Neurol Neurosurg Psychiatry* 1996;60:297-300.
13. Natelson BH, Suarez RV, Terrence CF, Turizo R. Patients with epilepsy who die suddenly have cardiac disease [see comments]. *Arch Neurol* 1998;55:857-60.
14. Bate L, Gardiner M. Genetics of inherited epilepsies. *Epileptic Disorders* 1999;1:7-19.
15. Berkovic SF, Scheffer IE. Genetics of the epilepsies. *Curr Opin Neurol* 1999;12:177-82.
16. McNamara JO. Emerging insights into the genesis of epilepsy. *Nature* 1999;399:15-22.
17. Annegers JF, Rocca WA, Hauser WA. Causes of epilepsy: contributions of the Rochester epidemiology project. *Mayo Clin Proc* 1996;71:570-5.

18. Scheffer IE, Bhatia KP, Lopes-Cendes I, et al. Autosomal dominant nocturnal frontal lobe epilepsy. A distinctive clinical disorder. *Brain* 1995;118:61-73.
19. Meierkord H, Fish DR, Smith SJ, Scott CA, Shorvon SD, Marsden CD. Is nocturnal paroxysmal dystonia a form of frontal lobe epilepsy? [see comments]. *Mov Disord* 1992;7:38-42.
20. Scheffer IE, Bhatia KP, Lopes-Cendes I, et al. Autosomal dominant frontal epilepsy misdiagnosed as sleep disorder [see comments]. *Lancet* 1994;343:515-7.
21. Phillips HA, Scheffer IE, Berkovic SF, Hollway GE, Sutherland GR, Mulley JC. Localization of a gene for autosomal dominant nocturnal frontal lobe epilepsy to chromosome 20q 13.2 [letter] [see comments]. *Nat Genet* 1995;10:117-8.
22. Steinlein OK, Magnusson A, Stoodt J, et al. An insertion mutation of the CHRNA4 gene in a family with autosomal dominant nocturnal frontal lobe epilepsy. *Hum Mol Genet* 1997;6:943-7.
23. Steinlein OK, Mulley JC, Propping P, et al. A missense mutation in the neuronal nicotinic acetylcholine receptor alpha 4 subunit is associated with autosomal dominant nocturnal frontal lobe epilepsy. *Nat Genet* 1995;11:201-3.
24. Kuryatov A, Gerzanich V, Nelson M, Olale F, Lindstrom J. Mutation causing autosomal dominant nocturnal frontal lobe epilepsy alters Ca²⁺ permeability, conductance, and gating of human alpha4beta2 nicotinic acetylcholine receptors. *J Neurosci* 1997;17:9035-47.
25. Dobyns WB, Andermann E, Andermann F, et al. X-linked malformations of neuronal migration. *Neurology* 1996;47:331-9.
26. Palmieri A, Andermann F, Aicardi J, et al. Diffuse cortical dysplasia, or the 'double cortex' syndrome: the clinical and epileptic spectrum in 10 patients. *Neurology* 1991;41:1656-62.
27. des Portes V, Francis F, Pinard JM, et al. doublecortin is the major gene causing X-linked subcortical laminar heterotopia (SCLH). *Hum Mol Genet* 1998;7:1063-70.
28. Gleeson JG, Allen KM, Fox JW, et al. Doublecortin, a brain-specific gene mutated in human X-linked lissencephaly and double cortex syndrome, encodes a putative signaling protein. *Cell* 1998;92:63-72.
29. Sossey-Alaoui K, Hartung AJ, Guerrini R, et al. Human doublecortin (DCX) and the homologous gene in mouse encode a putative Ca²⁺-dependent signaling protein which is mutated in human X-linked neuronal migration defects. *Hum Mol Genet* 1998;7:1327-32.
30. Barkovich AJ, Kuzniecky RI, Dobyns WB, Jackson GD, Becker LE, Evrard P. A classification scheme for malformations of cortical development. *Neuropediatrics* 1996;27:59-63.
31. Dubeau F, Tampieri D, Lee N, et al. Periventricular and subcortical nodular heterotopia. A study of 33 patients. *Brain* 1995;118:1273-87.
32. Huttenlocher PR, Taravath S, Mojtahedi S. Periventricular heterotopia and epilepsy. *Neurology* 1994;44:51-5.
33. Eksioglu YZ, Scheffer IE, Cardenas P, et al. Periventricular heterotopia: an X-linked dominant epilepsy locus causing aberrant cerebral cortical development. *Neuron* 1996;16:77-87.

34. Fox JW, Lamperti ED, Eksioglu YZ, et al. Mutations in filamin 1 prevent migration of cerebral cortical neurons in human periventricular heterotopia. *Neuron* 1998;21:1315-25.
35. Fernandez G, Effenberger O, Vinz B, et al. Hippocampal malformation as a cause of familial febrile convulsions and subsequent hippocampal sclerosis [see comments]. *Neurology* 1998;50:909-17.
36. VanLandingham KE, Heinz ER, Cavazos JE, Lewis DV. Magnetic resonance imaging evidence of hippocampal injury after prolonged focal febrile convulsions [see comments]. *Ann Neurol* 1998;43:413-26.
37. Cendes F, Lopes-Cendes I, Andermann E, Andermann F. Familial temporal lobe epilepsy: a clinically heterogeneous syndrome. *Neurology* 1998;50:554-7.
38. Kobayashi E, Cendes F, Guerreiro C, Guerreiro MM, Lopes-Cendes I. MRI abnormalities in familial temporal lobe epilepsy. *Neurology* 1999;52:A545(Abstract)
39. Babb TL, Brown WJ. Pathological findings in epilepsy. In: Engel J, Jr., ed. *Surgical treatment of the epilepsies*. First ed. New York: Raven Press, 1987:511-540.
40. Kuks JB, Cook MJ, Fish DR, Stevens JM, Shorvon SD. Hippocampal sclerosis in epilepsy and childhood febrile seizures [see comments]. *Lancet* 1993;342:1391-4.
41. Abou-Khalil B, Andermann E, Andermann F, Olivier A, Quesney LF. Temporal lobe epilepsy after prolonged febrile convulsions: excellent outcome after surgical treatment. *Epilepsia* 1993;34:878-83.
42. Cendes F, Andermann F, Dubeau F, et al. Early childhood prolonged febrile convulsions, atrophy and sclerosis of mesial structures, and temporal lobe epilepsy: an MRI volumetric study. *Neurology* 1993;43:1083-7.
43. Free SL, Li LM, Fish DR, Shorvon SD, Stevens JM. Bilateral hippocampal volume loss in patients with a history of encephalitis or meningitis. *Epilepsia* 1996;37:400-5.
44. Raymond AA, Fish DR, Sisodiya SM, Alsanjari N, Stevens JM, Shorvon SD. Abnormalities of gyration, heterotopias, tuberous sclerosis, focal cortical dysplasia, microdysgenesis, dysembryoplastic neuroepithelial tumour and dysgenesis of the archicortex in epilepsy. Clinical, EEG and neuroimaging features in 100 adult patients. *Brain* 1995;118:629-60.
45. Li LM, Fish DR, Sisodiya SM, Shorvon SD, Alsanjari N, Stevens JM. High resolution magnetic resonance imaging in adults with partial or secondary generalised epilepsy attending a tertiary referral unit. *J Neurol Neurosurg Psychiatry* 1995;59:384-7.
46. Cendes F, Cook MJ, Watson C, et al. Frequency and characteristics of dual pathology in patients with lesional epilepsy. *Neurology* 1995;45:2058-64.
47. Cascino GD, Jack CR, Jr., Parisi JE, et al. Operative strategy in patients with MRI-identified dual pathology and temporal lobe epilepsy. *Epilepsy Res* 1993;14:175-82.
48. Raymond AA, Fish DR, Stevens JM, Cook MJ, Sisodiya SM, Shorvon SD. Association of hippocampal sclerosis with cortical dysgenesis in patients with epilepsy [see comments]. *Neurology* 1994;44:1841-5.
49. Levesque MF, Nakasato N, Vinters HV, Babb TL. Surgical treatment of limbic epilepsy associated with extrahippocampal lesions: the problem of dual pathology. *J Neurosurg* 1991;75:364-70.

50. MacDonald RL, Meldrum BS. Principles of antiepileptic drug action. In: Levy RH, Mattson RH, Meldrum BS, eds. Antiepileptic drugs. fourth edition ed. New York: Raven Press, Ltd., 1995:61-77.
51. MacDonald RL, Greenfield LJ, Jr. Mechanisms of action of new antiepileptic drugs. *Curr Opin Neurol* 1997;10:121-8.
52. MacDonald RL, Kelly KM. Mechanisms of action of currently prescribed and newly developed antiepileptic drugs. *Epilepsia* 1994;35:41-50.
53. Sander JW. Some aspects of prognosis in the epilepsies: a review. *Epilepsia* 1993;34:1007-16.
54. Wirrell EC. Benign epilepsy of childhood with centrotemporal spikes. *Epilepsia* 1998;39:32-41.
55. Casanovas A, Ribera J, Hukkanen M, Riveros-Moreno V, Esquerda JE. Prevention by lamotrigine, MK-801 and N omega-nitro-L-arginine methyl ester of motoneuron cell death after neonatal axotomy. *Neuroscience* 1996;71:313-25.
56. Shuaib A, Mahmood RH, Wishart T, et al. Neuroprotective effects of lamotrigine in global ischemia in gerbils. A histological, in vivo microdialysis and behavioral study. *Brain Res* 1995;702:199-206.
57. Halonen T, Nissinen J, Jansen JA, Pitkanen A. Tiagabine prevents seizures, neuronal damage and memory impairment in experimental status epilepticus. *Eur J Pharmacol* 1996;299:69-81.
58. Pitkanen A. Treatment with antiepileptic drugs: possible neuroprotective effects. *Neurology* 1996;47:12-6.
59. Pitkanen A, Halonen T. Prevention of neuronal cell death by anticonvulsants in experimental epilepsy. *Acta Neurol Scand Suppl* 1995;162:22-3.
60. Pitkanen A, Tuunanen J, Halonen T. Vigabatrin and carbamazepine have different efficacies in the prevention of status epilepticus induced neuronal damage in the hippocampus and amygdala. *Epilepsy Res* 1996;24:29-45.
61. Loscher W, Honack D, Rundfeldt C. Antiepileptogenic effects of the novel anticonvulsant levetiracetam (ucb L059) in the kindling model of temporal lobe epilepsy. *J Pharmacol Exp Ther* 1998;284:474-9.
62. Loscher W, Honack D, Bloms-Funke P. The novel antiepileptic drug levetiracetam (ucb L059) induces alterations in GABA metabolism and turnover in discrete areas of rat brain and reduces neuronal activity in substantia nigra pars reticulata. *Brain Res* 1996;735:208-16.
63. Marson AG, Kadir ZA, Chadwick DW. New antiepileptic drugs: a systematic review of their efficacy and tolerability [see comments]. *Bmj* 1996;313:1169-74.
64. Pennell PB, Ogaily MS, MacDonald RL. Aplastic anemia in a patient receiving felbamate for complex partial seizures. *Neurology* 1995;45:456-60.
65. Arndt CF, Derambure P, Defoort-Dhellemmes S, Hache JC. Outer retinal dysfunction in patients treated with vigabatrin. *Neurology* 1999;52:1201-5.
66. Spencer DD, Spencer SS. Surgery for epilepsy. *Neurol Clin* 1985;3:313-30.
67. Awad LA, Katz A, Hahn JF, Kong AK, Ahl J, Luders H. Extent of resection in temporal lobectomy for epilepsy. I. Interobserver analysis and correlation with seizure outcome. *Epilepsia* 1989;30:756-62.

68. Awad LA, Rosenfeld J, Ahl J, Hahn JF, Luders H. Intractable epilepsy and structural lesions of the brain: mapping, resection strategies, and seizure outcome. *Epilepsia* 1991;32:179-86.
69. Gloor P. Commentary: Approaches to localization of epileptogenic lesion. In: Engel J, Jr., ed. *Surgical treatment of epilepsies*. first ed. New York: Raven Press, 1987:97-100.
70. ILAE. A global survey on epilepsy surgery, 1980-1990: a report by the Commission on Neurosurgery of Epilepsy, the International League Against Epilepsy. *Epilepsia* 1997;38:249-55.
71. Luders HO, Awad I. Conceptual considerations. In: Luders H, ed. *Epilepsy surgery*. New York: Raven Press Ltd, 1991:51-62.
72. Barkovich AJ, Kuzniecky RI. Neuroimaging of focal malformations of cortical development. *J Clin Neurophysiol* 1996;13:481-94.
73. Kuzniecky R. Magnetic resonance and functional magnetic resonance imaging: tools for the study of human epilepsy. *Curr Opin Neurol* 1997;10:88-91.
74. Laxer KD, Garcia PA. Imaging criteria to identify the epileptic focus. Magnetic resonance imaging, magnetic resonance spectroscopy, positron emission tomography scanning, and single photon emission computed tomography. *Neurosurg Clin N Am* 1993;4:199-209.
75. ILAE. Guidelines for neuroimaging evaluation of patients with uncontrolled epilepsy considered for surgery. Commission on Neuroimaging of the International League Against Epilepsy. *Epilepsia* 1998;39:1375-6.
76. ILAE. Recommendations for neuroimaging of patients with epilepsy. Commission on Neuroimaging of the International League Against Epilepsy. *Epilepsia* 1997;38:1255-6.
77. Fish DR. MRI in focal lesions. *Acta Neurol Scand Suppl* 1994;152:101-4.
78. Fish DR, Spencer SS. Clinical correlations: MRI and EEG. *Magn Reson Imaging* 1995;13:1113-7.
79. Jack CR, Jr. Magnetic resonance imaging in epilepsy. *Mayo Clin Proc* 1996;71:695-711.
80. Jack CR, Jr., Rydberg CH, Krecke KN, et al. Mesial temporal sclerosis: diagnosis with fluid-attenuated inversion-recovery versus spin-echo MR imaging. *Radiology* 1996;199:367-73.
81. Bergin PS, Fish DR, Shorvon SD, Oatridge A, deSouza NM, Bydder GM. Magnetic resonance imaging in partial epilepsy: additional abnormalities shown with the fluid attenuated inversion recovery (FLAIR) pulse sequence. *J Neurol Neurosurg Psychiatry* 1995;58:439-43.
82. Wieshmann UC, Free SL, Everitt AD, et al. Magnetic resonance imaging in epilepsy with a fast FLAIR sequence. *J Neurol Neurosurg Psychiatry* 1996;61:357-61.
83. Jack CR, Jr., Sharbrough FW, Twomey CK, et al. Temporal lobe seizures: lateralization with MR volume measurements of the hippocampal formation [see comments]. *Radiology* 1990;175:423-9.
84. Cook MJ, Fish DR, Shorvon SD, Straughan K, Stevens JM. Hippocampal volumetric and morphometric studies in frontal and temporal lobe epilepsy. *Brain* 1992;115:1001-15.

85. Cendes F, Andermann F, Gloor P, et al. MRI volumetric measurement of amygdala and hippocampus in temporal lobe epilepsy. *Neurology* 1993;43:719-25.
86. Bronen RA, Cheung G, Charles JT, et al. Imaging findings in hippocampal sclerosis: correlation with pathology. *AJNR Am J Neuroradiol* 1991;12:933-40.
87. Lencz T, McCarthy G, Bronen RA, et al. Quantitative magnetic resonance imaging in temporal lobe epilepsy: relationship to neuropathology and neuropsychological function. *Ann Neurol* 1992;31:629-37.
88. Kuzniecky RI, Burgard S, Bilir E, et al. Qualitative MRI segmentation in mesial temporal sclerosis: clinical correlations. *Epilepsia* 1996;37:433-9.
89. Jackson GD, Connelly A, Duncan JS, Grunewald RA, Gadian DG. Detection of hippocampal pathology in intractable partial epilepsy: increased sensitivity with quantitative magnetic resonance T2 relaxometry. *Neurology* 1993;43:1793-9.
90. van Paesschen W, Sisodiya S, Connelly A, et al. Quantitative hippocampal MRI and intractable temporal lobe epilepsy. *Neurology* 1995;45:2233-40.
91. Woermann FG, Barker GJ, Birnie KD, Meencke HJ, Duncan JS. Regional changes in hippocampal T2 relaxation and volume: a quantitative magnetic resonance imaging study of hippocampal sclerosis. *J Neurol Neurosurg Psychiatry* 1998;65:656-64.
92. Watson C, Cendes F, Fuerst D, et al. Specificity of volumetric magnetic resonance imaging in detecting hippocampal sclerosis. *Arch Neurol* 1997;54:67-73.
93. Watson C, Jack CR, Jr., Cendes F. Volumetric magnetic resonance imaging. Clinical applications and contributions to the understanding of temporal lobe epilepsy. *Arch Neurol* 1997;54:1521-31.
94. Kuzniecky RI. Magnetic resonance imaging in developmental disorders of the cerebral cortex. *Epilepsia* 1994;35:44-56.
95. Kuzniecky RI. MRI in cerebral developmental malformations and epilepsy. *Magn Reson Imaging* 1995;13:1137-45.
96. Palmini A, Andermann F, Olivier A, et al. Neuronal migration disorders: a contribution of modern neuroimaging to the etiologic diagnosis of epilepsy. *Can J Neurol Sci* 1991;18:580-7.
97. Bastos AC, Korah IP, Cendes F, et al. Curvilinear reconstruction of 3D magnetic resonance imaging in patients with partial epilepsy: a pilot study. *Magn Reson Imaging* 1995;13:1107-12.
98. Bastos AC, Comeau RM, Andermann F, et al. Diagnosis of subtle focal dysplastic lesions: curvilinear reformatting from three-dimensional magnetic resonance imaging. *Ann Neurol* 1999;46:88-94.
99. Bronen RA, Fulbright RK, Spencer DD, et al. Refractory epilepsy: comparison of MR imaging, CT, and histopathologic findings in 117 patients. *Radiology* 1996;201:97-105.
100. Peretti P, Raybaud C, Dravet C, Mancini J, Pinsard N. Magnetic resonance imaging in partial epilepsy of childhood. Seventy-nine cases. *J Neuroradiol* 1989;16:308-16.
101. Zentner J, Hufnagel A, Wolf HK, et al. Surgical treatment of temporal lobe epilepsy: clinical, radiological, and histopathological findings in 178 patients. *J Neurol Neurosurg Psychiatry* 1995;58:666-73.

102. Ryvlin P, Bouvard S, Le Bars D, et al. Clinical utility of flumazenil-PET versus [18F]fluorodeoxyglucose-PET and MRI in refractory partial epilepsy. A prospective study in 100 patients. *Brain* 1998;121:2067-81.
103. Menzel C, Grunwald F, Ostertun B, et al. [Incidence of lesions described by magnetic resonance imaging in the clarification of focal epilepsy of frontal and temporal origin]. *Nuklearmedizin* 1997;36:187-93.
104. Ferone E, Pierallini A, Bonamini M, et al. Assessment with magnetic resonance with Turbo-FLAIR sequences and volumetric analysis of the hippocampal region in drug-resistant temporal epilepsy. *Radiol Med (Torino)* 1998;95:456-60.
105. Wang PJ, Liu HM, Fan PC, et al. Magnetic resonance imaging in symptomatic/cryptogenic partial epilepsies of infants and children. *Chung Hua Min Kuo Hsiao Erh Ko I Hsueh Hui Tsa Chih* 1997;38:127-36.
106. Kramer U, Nevo Y, Reider-Groswasser I, et al. Neuroimaging of children with partial seizures. *Seizure* 1998;7:115-8.
107. Kilpatrick CJ, Tress BM, O'Donnell C, Rossiter SC, Hopper JL. Magnetic resonance imaging and late-onset epilepsy. *Epilepsia* 1991;32:358-64.
108. Convers P, Bierme T, Ryvlin P, et al. Contribution of magnetic resonance imaging in 100 cases of refractory partial epilepsy with normal CT scans. *Rev Neurol* 1990;146:330-7.
109. Paterson A, Winder J, Bell KE, McKinstry CS. An evaluation of how MRI is used as a pre-operative screening investigation in patients with temporal lobe epilepsy. *Clin Radiol* 1998;53:353-6.
110. Namer IJ, Waydelich R, Armspach JP, Hirsch E, Marescaux C, Grucker D. Contribution of T2 relaxation time mapping in the evaluation of cryptogenic temporal lobe epilepsy. *Neuroimage* 1998;7:304-13.
111. Lawson JA, Cook MJ, Bleasel AF, Nayanar V, Morris KF, Bye AM. Quantitative MRI in outpatient childhood epilepsy. *Epilepsia* 1997;38:1289-93.
112. Christensen T, Pedersen B, Jensen FT. MR-scanning in complex partial epilepsy. *Ugeskr Laeger* 1996;158:5624-6.
113. Cascino GD, Jack CR, Jr., Parisi JE, et al. Magnetic resonance imaging-based volume studies in temporal lobe epilepsy: pathological correlations. *Ann Neurol* 1991;30:31-6.
114. Adam C, Baulac M, Saint-Hilaire JM, Landau J, Granat O, Laplane D. Value of magnetic resonance imaging-based measurements of hippocampal formations in patients with partial epilepsy. *Arch Neurol* 1994;51:130-8.
115. Cendes F, Caramanos Z, Andermann F, Dubeau F, Arnold DL. Proton magnetic resonance spectroscopic imaging and magnetic resonance imaging volumetry in the lateralization of temporal lobe epilepsy: a series of 100 patients. *Ann Neurol* 1997;42:737-46.
116. Kuzniecky R, Hugg JW, Hetherington H, et al. Relative utility of 1H spectroscopic imaging and hippocampal volumetry in the lateralization of mesial temporal lobe epilepsy. *Neurology* 1998;51:66-71.
117. van Paesschen W, Connelly A, King MD, Jackson GD, Duncan JS. The spectrum of hippocampal sclerosis: a quantitative magnetic resonance imaging study. *Ann Neurol* 1997;41:41-51.

118. Gadian DG. NMR and its applications to living systems. Second edition ed. New York:Oxford Science Publications, 1995:1.
119. Salibi N, Brown MA. Clinical MR spectroscopy: First principles. New York:Wiley-Liss, Inc., 1998:
120. Knizley H, Jr. The enzymatic synthesis of N-acetyl-L-aspartic acid by a water- insoluble preparation of a cat brain acetone powder. *J Biol Chem* 1967;242:4619-22.
121. Goldstein FB. The enzymatic synthesis of N-acetyl-L-aspartic acid by subcellular preparations of rat brain. *J Biol Chem* 1969;244:4257-60.
122. Patel TB, Clark JB. Synthesis of N-acetyl-L-aspartate by rat brain mitochondria and its involvement in mitochondrial/cytosolic carbon transport. *Biochem J* 1979;184:539-46.
123. Truckenmiller ME, Namboodiri MA, Brownstein MJ, Neale JH. N-Acetylation of L-aspartate in the nervous system: differential distribution of a specific enzyme. *J Neurochem* 1985;45:1658-62.
124. Moffett JR, Namboodiri MA, Cangro CB, Neale JH. Immunohistochemical localization of N-acetylaspartate in rat brain. *Neuroreport* 1991;2:131-4.
125. Simmons ML, Frondoza CG, Coyle JT. Immunocytochemical localization of N-acetyl-aspartate with monoclonal antibodies. *Neuroscience* 1991;45:37-45.
126. Urenjak J, Williams SR, Gadian DG, Noble M. Specific expression of N-acetylaspartate in neurons, oligodendrocyte- type-2 astrocyte progenitors, and immature oligodendrocytes in vitro. *J Neurochem* 1992;59:55-61.
127. Clarke DD, Greenfield S, Dicker E, Tirri LJ, Ronan EJ. A relationship of N-acetylaspartate biosynthesis to neuronal protein synthesis. *J Neurochem* 1975;24:479-85.
128. D'Adamo AF, Jr., Gidez LI, Yatsu FM. Acetyl transport mechanisms. Involvement of N-acetyl aspartic acid in de novo fatty acid biosynthesis in the developing rat brain. *Exp Brain Res* 1968;5:267-73.
129. D'Adamo AF, Jr., Yatsu FM. Acetate metabolism in the nervous system. N-acetyl-L-aspartic acid and the biosynthesis of brain lipids. *J Neurochem* 1966;13:961-5.
130. Patel TB, Clark JB. Lipogenesis in the brain of suckling rats. Studies on the mechanism of mitochondrial-cytosolic carbon transfer. *Biochem J* 1980;188:163-8.
131. Burri R, Steffen C, Herschkowitz N. N-acetyl-L-aspartate is a major source of acetyl groups for lipid synthesis during rat brain development. *Dev Neurosci* 1991;13:403-11.
132. Cangro CB, Namboodiri MA, Sklar LA, Corigliano-Murphy A, Neale JH. Immunohistochemistry and biosynthesis of N-acetylaspartylglutamate in spinal sensory ganglia. *J Neurochem* 1987;49:1579-88.
133. Taylor DL, Davies SE, Obrenovitch TP, et al. Investigation into the role of N-acetylaspartate in cerebral osmoregulation. *J Neurochem* 1995;65:275-81.
134. Kato T, Nishina M, Matsushita K, Hori E, Mito T, Takashima S. Neuronal maturation and N-acetyl-L-aspartic acid development in human fetal and child brains. *Brain Dev* 1997;19:131-3.
135. Kreis R, Ernst T, Ross BD. Development of the human brain: in vivo quantification of metabolite and water content with proton magnetic resonance spectroscopy. *Magn Reson Med* 1993;30:424-37.

136. Saunders DE, Howe FA, van den Boogaart A, Griffiths JR, Brown MM. Aging of the adult human brain: in vivo quantitation of metabolite content with proton magnetic resonance spectroscopy. *J Magn Reson Imaging* 1999;9:711-6.
137. Guimaraes AR, Schwartz P, Prakash MR, et al. Quantitative in vivo ¹H nuclear magnetic resonance spectroscopic imaging of neuronal loss in rat brain. *Neuroscience* 1995;69:1095-1101.
138. Strauss I, Williamson JM, Bertram EH, Lothman EW, Fernandez EJ. Histological and ¹H magnetic resonance spectroscopic imaging analysis of quinolinic acid-induced damage to the rat striatum. *Magn Reson Med* 1997;37:24-33.
139. Najm IM, Wang Y, Hong SC, Luders HO, Ng TC, Comair YG. Temporal changes in proton MRS metabolites after kainic acid-induced seizures in rat brain. *Epilepsia* 1997;38:87-94.
140. Najm IM, Wang Y, Shedid D, Luders HO, Ng TC, Comair YG. MRS metabolic markers of seizures and seizure-induced neuronal damage. *Epilepsia* 1998;39:244-50.
141. Ebisu T, Rooney WD, Graham SH, Weiner MW, Maudsley AA. N-acetylaspartate as an in vivo marker of neuronal viability in kainate-induced status epilepticus: ¹H magnetic resonance spectroscopic imaging. *J Cereb Blood Flow Metab* 1994;14:373-82.
142. Tokumitsu T, Mancuso A, Weinstein PR, Weiner MW, Naruse S, Maudsley AA. Metabolic and pathological effects of temporal lobe epilepsy in rat brain detected by proton spectroscopy and imaging. *Brain Res* 1997;744:57-67.
143. Pioro EP, Wang Y, Moore JK, et al. Neuronal pathology in the wobbler mouse brain revealed by in vivo proton magnetic resonance spectroscopy and immunocytochemistry. *Neuroreport* 1998;9:3041-6.
144. Nakano M, Ueda H, Li JY, Matsumoto M, Yanagihara T. Measurement of regional N-acetylaspartate after transient global ischemia in gerbils with and without ischemic tolerance: an index of neuronal survival. *Ann Neurol* 1998;44:334-40.
145. Pioro EP, Antel JP, Cashman NR, Arnold DL. Detection of cortical neuron loss in motor neuron disease by proton magnetic resonance spectroscopic imaging in vivo. *Neurology* 1994;44:1933-8.
146. Moller HE, Vermathen P, Lentschig MG, et al. Metabolic characterization of AIDS dementia complex by spectroscopic imaging. *J Magn Reson Imaging* 1999;9:10-8.
147. Wardlaw JM, Marshall I, Wild J, Dennis MS, Cannon J, Lewis SC. Studies of acute ischemic stroke with proton magnetic resonance spectroscopy: relation between time from onset, neurological deficit, metabolite abnormalities in the infarct, blood flow, and clinical outcome. *Stroke* 1998;29:1618-24.
148. van der Grond J, Balm R, Kappelle LJ, Eikelboom BC, Mali WP. Cerebral metabolism of patients with stenosis or occlusion of the internal carotid artery. A ¹H-MR spectroscopic imaging study. *Stroke* 1995;26:822-8.
149. Petroff OA, Graham GD, Blamire AM, et al. Spectroscopic imaging of stroke in humans: histopathology correlates of spectral changes. *Neurology* 1992;42:1349-54.
150. Chong WK, Sweeney B, Wilkinson ID, et al. Proton spectroscopy of the brain in HIV infection: correlation with clinical, immunologic, and MR imaging findings. *Radiology* 1993;188:119-24.
151. De Stefano N, Matthews PM, Arnold DL. Reversible decreases in N-acetylaspartate after acute brain injury. *Magn Reson Med* 1995;34:721-7.

152. Kalra S, Cashman NR, Genge A, Arnold DL. Recovery of N-acetylaspartate in corticomotor neurons of patients with ALS after riluzole therapy. *Neuroreport* 1998;9:1757-61.
153. Balm R, van der Grond J, Mali WP, Eikelboom BC. Re-establishment of cerebral metabolism after carotid endarterectomy. *Eur J Vasc Endovasc Surg* 1995;10:182-6.
154. van der Grond J, Balm R, Klijn CJ, Kapelle LJ, Eikelboom BC, Mali WP. Cerebral metabolism of patients with stenosis of the internal carotid artery before and after endarterectomy. *J Cereb Blood Flow Metab* 1996;16:320-6.
155. Matthews PM, Cianfaglia L, McLaurin J, et al. Demonstration of reversible decreases in N-acetylaspartate (NAA) in a neuronal cell line: NAA decreases as a marker of sublethal neuronal dysfunction. *Proceedings of ISMRM* 1995;1:147(Abstract)
156. Bates TE, Strangward M, Keelan J, Davey GP, Munro PM, Clark JB. Inhibition of N-acetylaspartate production: implications for 1H MRS studies in vivo. *Neuroreport* 1996;7:1397-400.
157. Cross JH, Connelly A, Jackson GD, Johnson CL, Neville BG, Gadian DG. Proton magnetic resonance spectroscopy in children with temporal lobe epilepsy. *Ann Neurol* 1996;39:107-13.
158. Connelly A, Jackson GD, Duncan JS, King MD, Gadian DG. Magnetic resonance spectroscopy in temporal lobe epilepsy. *Neurology* 1994;44:1411-7.
159. Vermathen P, Ende G, Laxer KD, Knowlton RC, Matson GB, Weiner MW. Hippocampal N-acetylaspartate in neocortical epilepsy and mesial temporal lobe epilepsy. *Ann Neurol* 1997;42:194-9.
160. Petroff OA, Pleban LA, Spencer DD. Symbiosis between in vivo and in vitro NMR spectroscopy: the creatine, N-acetylaspartate, glutamate, and GABA content of the epileptic human brain. *Magn Reson Imaging* 1995;13:1197-211.
161. Cendes F, Andermann F, Dubeau F, Matthews PM, Arnold DL. Normalization of neuronal metabolic dysfunction after surgery for temporal lobe epilepsy. Evidence from proton MR spectroscopic imaging. *Neurology* 1997;49:1525-33.
162. Matthews PM, De Stefano N, Narayanan S, et al. Putting magnetic resonance spectroscopy studies in context: axonal damage and disability in multiple sclerosis. *Semin Neurol* 1998;18:327-36.
163. Cross JH, Gadian DG, Connelly A, Leonard JV. Proton magnetic resonance spectroscopy studies in lactic acidosis and mitochondrial disorders. *J Inher Metab Dis* 1993;16:800-11.
164. Matthews PM, Berkovic SF, Shoubridge EA, et al. In vivo magnetic resonance spectroscopy of brain and muscle in a type of mitochondrial encephalomyopathy (MEERF). *Ann Neurol* 1991;29:435-8.
165. Matthews PM, Allaire C, Shoubridge EA, Karpati G, Carpenter S, Arnold DL. In vivo muscle magnetic resonance spectroscopy in the clinical investigation of mitochondrial disease. *Neurology* 1991;41:114-20.
166. Matthews PM, Tampieri D, Berkovic SF, et al. Magnetic resonance imaging shows specific abnormalities in the MELAS syndrome. *Neurology* 1991;41:1043-6.
167. Preul MC, Caramanos Z, Collins DL, et al. Accurate, noninvasive diagnosis of human brain tumors by using proton magnetic resonance spectroscopy. *Nat Med* 1996;2:323-5.

168. Rothman DL, Petroff OA, Behar KL, Mattson RH. Localized ¹H NMR measurements of gamma-aminobutyric acid in human brain in vivo. *Proc Natl Acad Sci U S A* 1993;90:5662-6.
169. Rothman DL, Hanstock CC, Petroff OA, Novotny EJ, Prichard JW, Shulman RG. Localized ¹H NMR spectra of glutamate in the human brain. *Magn Reson Med* 1992;25:94-106.
170. Breiter SN, Arroyo S, Mathews VP, Lesser RP, Bryan RN, Barker PB. Proton MR spectroscopy in patients with seizure disorders. *AJNR Am J Neuroradiol* 1994;15:373-84.
171. Achten E, Boon P, Van De Kerckhove T, Caemaert J, De Reuck J, Kunnen M. Value of single-voxel proton MR spectroscopy in temporal lobe epilepsy. *AJNR Am J Neuroradiol* 1997;18:1131-9.
172. Duc CO, Trabesinger AH, Weber OM, et al. Quantitative ¹H MRS in the evaluation of mesial temporal lobe epilepsy in vivo. *Magn Reson Imaging* 1998;16:969-79.
173. Hugg JW, Laxer KD, Matson GB, Maudsley AA, Weiner MW. Neuron loss localizes human temporal lobe epilepsy by in vivo proton magnetic resonance spectroscopic imaging. *Ann Neurol* 1993;34:788-94.
174. Vainio P, Userius JP, Vapalahti M, et al. Reduced N-acetylaspartate concentration in temporal lobe epilepsy by quantitative ¹H MRS in vivo. *Neuroreport* 1994;5:1733-6.
175. Cendes F, Andermann F, Preul MC, Arnold DL. Lateralization of temporal lobe epilepsy based on regional metabolic abnormalities in proton magnetic resonance spectroscopic images. *Ann Neurol* 1994;35:211-6.
176. Ng TC, Comair YG, Xue M, et al. Temporal lobe epilepsy: presurgical localization with proton chemical shift imaging. *Radiology* 1994;193:465-72.
177. Hetherington H, Kuzniecky R, Pan J, et al. Proton nuclear magnetic resonance spectroscopic imaging of human temporal lobe epilepsy at 4.1 T. *Ann Neurol* 1995;38:396-404.
178. Ende GR, Laxer KD, Knowlton RC, et al. Temporal lobe epilepsy: bilateral hippocampal metabolite changes revealed at proton MR spectroscopic imaging. *Radiology* 1997;202:809-17.
179. Margerison JH, Corsellis JA. Epilepsy and the temporal lobes. A clinical, electroencephalographic and neuropathological study of the brain in epilepsy, with particular reference to the temporal lobes. *Brain* 1966;89:499-530.
180. Fulham MJ, Dietz MJ, Duyn JH, Shih HH, Alger JR, Di Chiro G. Transsynaptic reduction in N-acetyl-aspartate in cerebellar diaschisis: a proton MR spectroscopic imaging study. *J Comput Assist Tomogr* 1994;18:697-704.
181. Rango M, Spagnoli D, Tomei G, Bamonti F, Scarlato G, Zetta L. Central nervous system trans-synaptic effects of acute axonal injury: a ¹H magnetic resonance spectroscopy study. *Magn Reson Med* 1995;33:595-600.
182. Bertolino A, Saunders RC, Mattay VS, Bachevalier J, Frank JA, Weinberger DR. Altered development of prefrontal neurons in rhesus monkeys with neonatal mesial temporo-limbic lesions: a proton magnetic resonance spectroscopic imaging study. *Cereb Cortex* 1997;7:740-8.

183. Gotman J. Relationships between interictal spiking and seizures: human and experimental evidence. *Can J Neurol Sci* 1991;18:573-6.
184. Gotman J. Relationships between triggered seizures, spontaneous seizures, and interictal spiking in the kindling model of epilepsy. *Exp Neurol* 1984;84:259-73.
185. Gotman J, Koffler DJ. Interictal spiking increases after seizures but does not after decrease in medication. *Electroencephalogr Clin Neurophysiol* 1989;72:7-15.
186. Gotman J, Marciani MG. Electroencephalographic spiking activity, drug levels, and seizure occurrence in epileptic patients. *Ann Neurol* 1985;17:597-603.
187. Peeling J, Sutherland G. 1H magnetic resonance spectroscopy of extracts of human epileptic neocortex and hippocampus. *Neurology* 1993;43:589-94.
188. Edzes, H. T. and Samulski, E. D. The measurement of cross-relaxation effects in the proton NMR spin-lattice relaxation of water in biological systems: hydrated collagen and muscle. *J Magn Reson* 31, 207-229. 1978.
189. Fung B. Nuclear magnetic resonance study of water interactions with proteins, biomolecules, membranes, and tissues. In: Parker L, ed. *Methods in Enzymology*. San Diego: Academic Press, 1986:
190. Pike GB. Pulsed magnetization transfer contrast in gradient echo imaging: a two-pool analytic description of signal response. *Magn Reson Med* 1996;36:95-103.
191. Pike GB, Glover GH, Hu BS, Enzmann DR. Pulsed magnetization transfer spin-echo MR imaging. *J Magn Reson Imaging* 1993;3:531-9.
192. Wolff SD, Balaban RS. Magnetization transfer contrast (MTC) and tissue water proton relaxation in vivo. *Magn Reson Med* 1989;10:135-44.
193. Hu BS, Conolly SM, Wright GA, Nishimura DG, Macovski A. Pulsed saturation transfer contrast. *Magn Reson Med* 1992;26:231-40.
194. Yeung HN, Aisen AM. Magnetization transfer contrast with periodic pulsed saturation. *Radiology* 1992;183:209-14.
195. Pike GB, De Stefano N, Narayanan S, Francis GS, Antel JP, Arnold DL. Combined magnetization transfer and proton spectroscopic imaging in the assessment of pathologic brain lesions in multiple sclerosis. *AJNR Am J Neuroradiol* 1999;20:829-37.
196. Eriksson S, Malmgren K, Rydenhag B, Jonsson L, Uvebrant P, Nordborg C. Surgical treatment of epilepsy--clinical, radiological and histopathological findings in 139 children and adults. *Acta Neurol Scand* 1999;99:8-15.
197. Palmi A, Andermann F, Olivier A, et al. Focal neuronal migration disorders and intractable partial epilepsy: a study of 30 patients. *Ann Neurol* 1991;30:741-9.
198. Palmi A, Gambardella A, Andermann F, et al. Intrinsic epileptogenicity of human dysplastic cortex as suggested by corticography and surgical results. *Ann Neurol* 1995;37:476-87.
199. Palmi A, Gambardella A, Andermann F, et al. Operative strategies for patients with cortical dysplastic lesions and intractable epilepsy. *Epilepsia* 1994;35:57-71.
200. Engel J, Jr. Update on surgical treatment of the epilepsies. Summary of the Second International Palm Desert Conference on the Surgical Treatment of the Epilepsies (1992). *Neurology* 1993;43:1612-7.

201. Arruda F, Cendes F, Andermann F, et al. Mesial atrophy and outcome after amygdalohippocampectomy or temporal lobe removal. *Ann Neurol* 1996;40:446-50.
202. Jack CR, Jr., Sharbrough FW, Cascino GD, Hirschorn KA, O'Brien PC, Marsh WR. Magnetic resonance image-based hippocampal volumetry: correlation with outcome after temporal lobectomy. *Ann Neurol* 1992;31:138-46.
203. Jack CR, Jr., Trenerry MR, Cascino GD, Sharbrough FW, So EL, O'Brien PC. Bilaterally symmetric hippocampi and surgical outcome [see comments]. *Neurology* 1995;45:1353-8.
204. Berkovic SF, McIntosh AM, Kalnins RM, et al. Preoperative MRI predicts outcome of temporal lobectomy: an actuarial analysis [see comments]. *Neurology* 1995;45:1358-63.
205. Radhakrishnan K, So EL, Silbert PL, et al. Predictors of outcome of anterior temporal lobectomy for intractable epilepsy: a multivariate study. *Neurology* 1998;51:465-71.
206. Holshouser BA, Ashwal S, Luh GY, et al. Proton MR spectroscopy after acute central nervous system injury: outcome prediction in neonates, infants, and children. *Radiology* 1997;202:487-96.
207. Shu SK, Ashwal S, Holshouser BA, Nystrom G, Hinshaw DB, Jr. Prognostic value of ¹H-MRS in perinatal CNS insults. *Pediatr Neurol* 1997;17:309-18.
208. Friedman SD, Brooks WM, Jung RE, et al. Quantitative proton MRS predicts outcome after traumatic brain injury. *Neurology* 1999;52:1384-91.
209. Cavazos JE, Das I, Sutula TP. Neuronal loss induced in limbic pathways by kindling: evidence for induction of hippocampal sclerosis by repeated brief seizures. *J Neurosci* 1994;14:3106-21.
210. Bertram EHD, Lothman EW. Morphometric effects of intermittent kindled seizures and limbic status epilepticus in the dentate gyrus of the rat. *Brain Res* 1993;603:25-31.
211. Liu Z, Nagao T, Desjardins GC, Gloor P, Avoli M. Quantitative evaluation of neuronal loss in the dorsal hippocampus in rats with long-term pilocarpine seizures. *Epilepsy Res* 1994;17:237-47.
212. Dam AM. Epilepsy and neuron loss in the hippocampus. *Epilepsia* 1980;21:617-29.
213. Meencke HJ, Veith G. Hippocampal sclerosis in epilepsy. In: Luders HO, ed. *Epilepsy surgery*. New York: Raven Press, 1991:705-715.
214. Mathern GW, Babb TL, Leite JP, Pretorius K, Yeoman KM, Kuhlman PA. The pathogenic and progressive features of chronic human hippocampal epilepsy. *Epilepsy Res* 1996;26:151-61.
215. Mathern GW, Babb TL, Mischel PS, et al. Childhood generalized and mesial temporal epilepsies demonstrate different amounts and patterns of hippocampal neuron loss and mossy fibre synaptic reorganization. *Brain* 1996;119:965-87.
216. Mathern GW, Babb TL, Vickrey BG, Melendez M, Pretorius JK. The clinical-pathogenic mechanisms of hippocampal neuron loss and surgical outcomes in temporal lobe epilepsy. *Brain* 1995;118:105-18.
217. Mathern GW, Leite JP, Pretorius JK, Quinn B, Peacock WJ, Babb TL. Children with severe epilepsy: evidence of hippocampal neuron losses and aberrant mossy fiber

sprouting during postnatal granule cell migration and differentiation. *Brain Res Dev Brain Res* 1994;78:70-80.

218. Mathern GW, Leite JP, Pretorius JK, Quinn B, Peacock WJ, Babb TL. Severe seizures in young children are associated with hippocampal neuron losses and aberrant mossy fiber sprouting during fascia dentata postnatal development. *Epilepsy Res Suppl* 1996;12:33-43.
219. Mathern GW, Pretorius JK, Babb TL. Influence of the type of initial precipitating injury and at what age it occurs on course and outcome in patients with temporal lobe seizures. *J Neurosurg* 1995;82:220-7.
220. Cendes F, Andermann F, Gloor P, et al. Atrophy of mesial structures in patients with temporal lobe epilepsy: cause or consequence of repeated seizures? *Ann Neurol* 1993;34:795-801.
221. Kalviainen R, Salmenpera T, Partanen K, Vainio P, Riekkinen P, Pitkanen A. Recurrent seizures may cause hippocampal damage in temporal lobe epilepsy. *Neurology* 1998;50:1377-82.
222. Theodore WH, Bhatia S, Hatta J, et al. Hippocampal atrophy, epilepsy duration, and febrile seizures in patients with partial seizures. *Neurology* 1999;52:132-6.
223. van Paesschen W, Duncan JS, Stevens JM, Connelly A. Etiology and early prognosis of newly diagnosed partial seizures in adults: a quantitative hippocampal MRI study. *Neurology* 1997;49:753-7.
224. Lynch MW, Rutecki PA, Sutula TP. The effects of seizures on the brain. *Curr Opin Neurol* 1996;9:97-102.
225. Regis J, Semah F, Bryan RN, et al. Early and delayed MR and PET changes after selective temporomesial radiosurgery in mesial temporal lobe epilepsy. *AJNR Am J Neuroradiol* 1999;20:213-6.
226. Akimura T, Yeh HS, Mantil JC, Privitera MD, Gartner M, Tomsick TA. Cerebral metabolism of the remote area after epilepsy surgery. *Neurol Med Chir (Tokyo)* 1999;39:16-25.
227. Chugani HT, Jacobs B. Metabolic recovery in caudate nucleus of children following cerebral hemispherectomy. *Ann Neurol* 1994;36:794-7.
228. Hajek M, Wieser HG, Khan N, et al. Preoperative and postoperative glucose consumption in mesiobasal and lateral temporal lobe epilepsy. *Neurology* 1994;44:2125-32.
229. Savic I, Blomqvist G, Halldin C, Litton JE, Gulyas B. Regional increases in [11C]flumazenil binding after epilepsy surgery. *Acta Neurol Scand* 1998;97:279-86.
230. Dasheiff RM, Rosenbek J, Matthews C, et al. Epilepsy surgery improves regional glucose metabolism on PET scan. A case report. *J Neurol* 1987;234:283-8.
231. Vermathen P, Ende G, Laxer KD, et al. 1H-MRSI follow-up studies of epilepsy show strongly altered metabolite concentrations after surgery. *Proceedings of ISMRM* 1996;2:957(Abstract)
232. Hugg JW, Kuzniecky RI, Gilliam FG, Morawetz RB, Fraught RE, Hetherington HP. Normalization of contralateral metabolic function following temporal lobectomy demonstrated by 1H magnetic resonance spectroscopic imaging. *Ann Neurol* 1996;40:236-9.

233. Watson C, Moore GJ. Comparison of preoperative vs. postoperative 1H MR spectroscopic imaging findings in the contralateral temporal lobe following ipsilateral resection in adult temporal lobe epilepsy patients. *Neurology* 1998;50:A286(Abstract)
234. Jokeit H, Ebner A. Long term effects of refractory temporal lobe epilepsy on cognitive abilities: a cross sectional study. *J Neurol Neurosurg Psychiatry* 1999;67:44-50.
235. Selwa LM, Berent S, Giordani B, Henry TR, Buchtel HA, Ross DA. Serial cognitive testing in temporal lobe epilepsy: longitudinal changes with medical and surgical therapies. *Epilepsia* 1994;35:743-9.
236. Novelty RA, Augustine EA, Mattson RH, et al. Selective memory improvement and impairment in temporal lobectomy for epilepsy. *Ann Neurol* 1984;15:64-7.
237. Ivnik RJ, Sharbrough FW, Laws ER, Jr. Effects of anterior temporal lobectomy on cognitive function. *J Clin Psychol* 1987;43:128-37.
238. Ivnik RJ, Sharbrough FW, Laws ER, Jr. Anterior temporal lobectomy for the control of partial complex seizures: information for counseling patients. *Mayo Clin Proc* 1988;63:783-93.
239. Martin RC, Sawrie SM, Roth DL, et al. Individual memory change after anterior temporal lobectomy: a base rate analysis using regression-based outcome methodology. *Epilepsia* 1998;39:1075-82.
240. Gaillard WD, Weinstein S, Pearl PL, et al. Natural history of metabolic abnormalities in children with partial epilepsy determined by FDG-PET. *Epilepsia* 1998;39:101(Abstract)
241. Leiderman DB, Albert P, Balish M, Bromfield E, Theodore WH. The dynamics of metabolic change following seizures as measured by positron emission tomography with fludeoxyglucose F 18. *Arch Neurol* 1994;51:932-6.
242. Mendes-Ribeiro JA, Soares R, Simoes-Ribeiro F, Guimaraes ML. Reduction in temporal N-acetylaspartate and creatine (or choline) ratio in temporal lobe epilepsy: does this 1H-magnetic resonance spectroscopy finding mean poor seizure control? *J Neurol Neurosurg Psychiatry* 1998;65:518-22.
243. Holopainen IE, Valtonen ME, Komu ME, et al. Proton spectroscopy in children with epilepsy and febrile convulsions. *Pediatr Neurol* 1998;19:93-9.
244. Tasch E, Li LM, Cendes F, Dubeau F, Andermann F, Arnold DL. Seizure-related neuronal damage: a magnetic resonance spectroscopic study of temporal lobe epilepsy. *Epilepsia* 1998;39:104(Abstract)
245. Sisodiya SM, Free SL, Stevens JM, Fish DR, Shorvon SD. Widespread cerebral structural changes in patients with cortical dysgenesis and epilepsy. *Brain* 1995;118:1039-50.
246. Sisodiya SM, Moran N, Free SL, et al. Correlation of widespread preoperative magnetic resonance imaging changes with unsuccessful surgery for hippocampal sclerosis. *Ann Neurol* 1997;41:490-6.
247. Gadian DG. N-acetylaspartate and epilepsy. *Magn Reson Imaging* 1995;13:1193-5.
248. de Beer R, van den Boogaart A, van Ormondt D, et al. Application of time-domain fitting in the quantification of in vivo 1H spectroscopic imaging data sets. *NMR Biomed* 1992;5:171-178.

249. Cendes F, Stanley JA, Dubeau F, Andermann F, Arnold DL. Proton magnetic resonance spectroscopic imaging for discrimination of absence and complex partial seizures. *Ann Neurol* 1997;41:74-81.
250. Meencke HJ. The density of dystopic neurons in the white matter of the gyrus frontalis inferior in epilepsies. *J Neurol* 1983;230:171-81.
251. Meencke HJ, Janz D. Neuropathological findings in primary generalized epilepsy: a study of eight cases. *Epilepsia* 1984;25:8-21.
252. Li LM, Dubeau F, Andermann F, et al. Periventricular nodular heterotopia and intractable temporal lobe epilepsy: poor outcome after temporal lobe resection. *Ann Neurol* 1997;41:662-8.
253. Morrell F. Secondary epileptogenic lesions. *Epilepsia* 1959;1:538-560.
254. Wilder BJ, King RL, Schmidt RP. Comparative study of secondary epileptogenesis. *Epilepsia* 1968;9:275-89.
255. Racine R. Kindling: the first decade. *Neurosurgery* 1978;3:234-52.
256. Sarnat HB. Cerebral dysgenesis: embryology and clinical expression. New York:Oxford University Press, 1992:
257. Battaglia G, Arcelli P, Granata T, et al. Neuronal migration disorders and epilepsy: a morphological analysis of three surgically treated patients. *Epilepsy Res* 1996;26:49-58.
258. Lee N, Radtke RA, Gray L, et al. Neuronal migration disorders: positron emission tomography correlations. *Ann Neurol* 1994;35:290-7.
259. Marsh L, Lim KO, Sullivan EV, Lane B, Spielman D. Proton magnetic resonance spectroscopy of a gray matter heterotopia. *Neurology* 1996;47:1571-4.
260. Preul MC, Leblanc R, Cendes F, et al. Function and organization in dysgenic cortex. Case report. *J Neurosurg* 1997;87:113-21.
261. Kuzniecky R, Hetherington H, Pan J, Hugg J, Gilliam F, Faught E. Identification of metabolic abnormalities by proton MRSI in patients with malformations of cortical development. *Epilepsia* 1996;37:194(Abstract)
262. Peters T, Davey B, Munger P, Comeau R, Evans A, Olivier A. Three-dimensional multimodal image-guidance for neurosurgery. *IEEE Trans Med Imaging* 1996;15:121-128.
263. Preul MC, Leblanc R, Caramanos Z, Kasrai R, Narayanan S, Arnold DL. Magnetic resonance spectroscopy guided brain tumor resection: differentiation between recurrent glioma and radiation change in two diagnostically difficult cases. *Can J Neurol Sci* 1998;25:13-22.
264. Kauppinen RA, Williams SR. Nuclear magnetic resonance spectroscopy studies of the brain. *Prog Neurobiol* 1994;44:87-118.
265. Peeling J, Sutherland G. High-resolution ¹H NMR spectroscopy studies of extracts of human cerebral neoplasms. *Magn Reson Med* 1992;24:123-36.
266. Gadian DG, Connelly A, Duncan JS, et al. ¹H magnetic resonance spectroscopy in the investigation of intractable epilepsy. *Acta Neurol Scand Suppl* 1994;152:116-21.

267. Engel J, Jr., Van Ness P, Rasmussen T, Ojemann LM. Outcome with respect to epileptic seizures. In: Engel J, Jr., ed. *Surgical treatment of the epilepsies*. 2nd edition ed. New York: Raven Press, 1993:609-621.
268. Stanley JA, Cendes F, Dubeau F, Andermann F, Arnold DL. Proton magnetic resonance spectroscopic imaging in patients with extratemporal epilepsy. *Epilepsia* 1998;39:267-73.
269. Roth K, Kimber BJ, Feeney J. Data shift accumulation and alternate delay accumulation techniques for overcoming dynamic range problems. *J Magn Reson* 1980;41:302-309.
270. Watson C, Andermann F, Gloor P, et al. Anatomic basis of amygdaloid and hippocampal volume measurement by magnetic resonance imaging. *Neurology* 1992;42:1743-50.
271. ILAE. Proposal for revised classification of epilepsies and epileptic syndromes. Commission on Classification and Terminology of the International League Against Epilepsy. *Epilepsia* 1989;30:389-99.
272. Vermathen P, Laxer KD, Schuff N, Maudsley AA, Matson GB, Weiner MW. Simultaneous detection of reduced NAA in hippocampal and other regions in mesial temporal lobe epilepsy using multislice proton MRSI. *Proceedings of ISMRM* 1998;3:1729(Abstract)
273. Vermathen P, Laxer KD, El Din M, Matson GB, Weiner MW. Hippocampal NAA loss in mesial temporal lobe epilepsy is not accompanied by changes in other brain regions. A combined multislice and PRESS MRSI study. *Proceedings of ISMRM* 1997;2:1185(Abstract)
274. Li LM, Cendes F, Watson C, et al. Surgical treatment of patients with single and dual pathology: relevance of lesion and of hippocampal atrophy to seizure outcome. *Neurology* 1997;48:437-44.
275. Li LM, Cendes F, Andermann F, et al. Surgical outcome in patients with epilepsy and dual pathology. *Brain* 1999;122:799-805.
276. Li LM, Cendes F, Antel S, et al. Prognostic features in surgical outcome of patients with bilateral hippocampal atrophy and intractable temporal lobe epilepsy. *Neurology* 1999;52:161-162.(Abstract)
277. Matthews PM, Francis G, Antel J, Arnold DL. Proton magnetic resonance spectroscopy for metabolic characterization of plaques in multiple sclerosis [published erratum appears in *Neurology* 1991 Nov;41(11):1828]. *Neurology* 1991;41:1251-6.
278. Frahm J, Bruhn H, Gyngell ML, Merboldt KD, Hanicke W, Sauter R. Localized proton NMR spectroscopy in different regions of the human brain in vivo. Relaxation times and concentrations of cerebral metabolites. *Magn Reson Med* 1989;11:47-63.
279. Hetherington HP, Mason GF, Pan JW, et al. Evaluation of cerebral gray and white matter metabolite differences by spectroscopic imaging at 4.1T. *Magn Reson Med* 1994;32:565-71.
280. Prince DA, Connors BW. Mechanisms of interictal epileptogenesis. *Adv Neurol* 1986;44:275-99.
281. Speckmann EJ, Elger CE. Introduction to the neurophysiological basis of the EEG and DC potentials. In: Niedermeyer E, Lopes da Silva F, eds. *Electroencephalography*. 2nd edition ed. Baltimore: Williams & Wilkins, 1993:15-26.

282. Gloor P. Contributions of electroencephalography and electrocorticography to the neurosurgical treatment of the epilepsies. *Adv Neurol* 1975;8:59-105.
283. Cooper R, Winter AL, Crow HJ, Walter WG. Comparison of subcortical, cortical and scalp activity using chronically indwelling electrodes in man. *Electroencephalogr Clin Neurophysiol* 1965;18:217-228.
284. Chung MY, Walczak TS, Lewis DV, Dawson DV, Radtke R. Temporal lobectomy and independent bitemporal interictal activity: what degree of lateralization is sufficient? *Epilepsia* 1991;32:195-201.
285. Sperling MR, O'Connor MJ, Saykin AJ, et al. A noninvasive protocol for anterior temporal lobectomy. *Neurology* 1992;42:416-22.
286. De Stefano N, Matthews PM, Fu L, et al. Axonal damage correlates with disability in patients with relapsing- remitting multiple sclerosis. Results of a longitudinal magnetic resonance spectroscopy study. *Brain* 1998;121:1469-77.
287. Pendlebury ST, Blamire AM, Lee MA, Styles P, Matthews PM. Axonal injury in the internal capsule correlates with motor impairment after stroke. *Stroke* 1999;30:956-62.
288. Garcia PA, Laxer KD, van der Grond J, Hugg JW, Matson GB, Weiner MW. Correlation of seizure frequency with N-acetyl-aspartate levels determined by 1H magnetic resonance spectroscopic imaging. *Magn Reson Imaging* 1997;15:475-8.
289. Tasch E, Cendes F, Li LM, Dubeau F, Andermann F, Arnold DL. Neuroimaging evidence of progressive neuronal loss and dysfunction in temporal lobe epilepsy. *Ann Neurol* 1999;45:568-576.
290. Karlik SJ, Stavray RT, Taylor AW, Fox AJ, McLachlan RS. Magnetic resonance imaging and 31P spectroscopy of an interictal cortical spike focus in the rat. *Epilepsia* 1991;32:446-53.
291. Li LM, Cendes F, Bastos AC, Andermann F, Dubeau F, Arnold DL. Neuronal metabolic dysfunction in patients with cortical developmental malformations: a proton magnetic resonance spectroscopic imaging study. *Neurology* 1998;50:755-9.
292. Connelly A, van Paesschen W, Porter DA, Johnson CL, Duncan JS, Gadian DG. Proton magnetic resonance spectroscopy in MRI-negative temporal lobe epilepsy. *Neurology* 1998;51:61-6.
293. Sammaritano M, Gigli GL, Gotman J. Interictal spiking during wakefulness and sleep and the localization of foci in temporal lobe epilepsy. *Neurology* 1991;41:290-7.
294. Collins DL, Neelin P, Peters TM, Evans AC. Automatic 3D intersubject registration of MR volumetric data in standardized Talairach space. *J Comput Assist Tomogr* 1994;18:192-205.
295. Bronen RA, Fulbright RK, Kim JH, Spencer SS, Spencer DD, al-Rodhan NR. Regional distribution of MR findings in hippocampal sclerosis. *AJNR Am J Neuroradiol* 1995;16:1193-200.
296. Bilir E, Craven W, Hugg J, et al. Volumetric MRI of the limbic system: anatomic determinants. *Neuroradiology* 1998;40:138-44.
297. Lee N, Tien RD, Lewis DV, et al. Fast spin-echo, magnetic resonance imaging-measured hippocampal volume: correlation with neuronal density in anterior temporal lobectomy patients. *Epilepsia* 1995;36:899-904.

298. van Paesschen W, Revesz T, Duncan JS, King MD, Connelly A. Quantitative neuropathology and quantitative magnetic resonance imaging of the hippocampus in temporal lobe epilepsy. *Ann Neurol* 1997;42:756-66.
299. Engel J, Jr. Update on surgical treatment of the epilepsies. *Clin Exp Neurol* 1992;29:32-48.
300. So N, Olivier A, Andermann F, Gloor P, Quesney LF. Results of surgical treatment in patients with bitemporal epileptiform abnormalities. *Ann Neurol* 1989;25:432-9.
301. Sato M, Racine RJ, McIntyre DC. Kindling: basic mechanisms and clinical validity. *Electroencephalogr Clin Neurophysiol* 1990;76:459-72.
302. Cavazos JE, Sutula TP. Progressive neuronal loss induced by kindling: a possible mechanism for mossy fiber synaptic reorganization and hippocampal sclerosis [published erratum appears in *Brain Res* 1991 Feb 8;541(1):179]. *Brain Res* 1990;527:1-6.
303. Sisodiya SM, Stevens JM, Fish DR, Free SL, Shorvon SD. The demonstration of gyral abnormalities in patients with cryptogenic partial epilepsy using three-dimensional MRI. *Arch Neurol* 1997;53:28-34.
304. Scott CA, Fish DR, Smith SJ, et al. Presurgical evaluation of patients with epilepsy and normal MRI: role of scalp video-EEG telemetry. *J Neurol Neurosurg Psychiatry* 1999;66:69-71.
305. Cascino GD, Trenerry MR, Sharbrough FW, So EL, Marsh WR, Strelow DC. Depth electrode studies in temporal lobe epilepsy: relation to quantitative magnetic resonance imaging and operative outcome. *Epilepsia* 1995;36:230-5.
306. Cascino GD, Trenerry MR, Jack CR, Jr., et al. Electroconvulsive therapy and temporal lobe epilepsy: relationship to quantitative MRI and operative outcome. *Epilepsia* 1995;36:692-6.
307. Garcia PA, Laxer KD, Barbaro NM, Dillon WP. Prognostic value of qualitative magnetic resonance imaging hippocampal abnormalities in patients undergoing temporal lobectomy for medically refractory seizures. *Epilepsia* 1994;35:520-4.
308. Mathieson G. Pathology of temporal lobe foci. *Adv Neurol* 1975;11:163-85.
309. de Lanerolle NC, Kim JH, Robbins RJ, Spencer DD. Hippocampal interneuron loss and plasticity in human temporal lobe epilepsy. *Brain Res* 1989;495:387-95.
310. Gloor P. Mesial temporal sclerosis: historical background and an overview from a modern perspective. In: Luders HO, ed. *Epilepsy surgery*. New York: Raven Press, 1991:689-703.
311. Kuzniecky R, de la Sayette V, Ethier R, et al. Magnetic resonance imaging in temporal lobe epilepsy: pathological correlations. *Ann Neurol* 1987;22:341-7.
312. Meyer A, Falconer MA, Beck E. Pathological findings in temporal lobe epilepsy. *J Neurol Neurosurg Psychiatry* 1954;17:276-285.
313. Zimmerman HM. The histopathology of convulsive disorders in children. *J Pediatr* 1940;13:359-390.
314. Ounsted C, Lindsay J, Norman R. Biological factors in temporal lobe epilepsy. London:William Heinemann Medical Books, 1966.
315. Falconer MA, Serafetinides EA, Corsellis JA. Etiology and pathogenesis of temporal lobe epilepsy. *Arch Neurol* 1964;10:233-248.

316. Harvey AS, Grattan-Smith JD, Desmond PM, Chow CW, Berkovic SF. Febrile seizures and hippocampal sclerosis: frequent and related findings in intractable temporal lobe epilepsy of childhood. *Pediatr Neurol* 1995;12:201-6.
317. Hauser WA. Status epilepticus: frequency, etiology, and neurological sequelae. *Adv Neurol* 1983;34:3-14.
318. Meldrum BS, Brierley JB. Prolonged epileptic seizures in primates. Ischemic cell change and its relation to ictal physiological events. *Arch Neurol* 1973;28:10-7.
319. Shorvon S. Neurophysiology, neuropathology and neurochemistry of status epilepticus. In: Anonymous Status epilepticus. Cambridge: Cambridge University Press, 1994:139-174.
320. Mouritze Dam A. Hippocampal neuron loss in epilepsy and after experimental seizures. *Acta Neurol Scand* 1982;66:601-42.
321. Cendes F, Andermann F, Dubeau F, Arnold DL. Proton magnetic resonance spectroscopic images and MRI volumetric studies for lateralization of temporal lobe epilepsy. *Magn Reson Imaging* 1995;13:1187-91.
322. Luby M, Spencer DD, Kim JH, deLanerolle N, McCarthy G. Hippocampal MRI volumetrics and temporal lobe substrates in medial temporal lobe epilepsy. *Magn Reson Imaging* 1995;13:1065-71.
323. Jackson GD, Kuzniecky RI, Cascino GD. Hippocampal sclerosis without detectable hippocampal atrophy. *Neurology* 1994;44:42-6.
324. Nohria V, Lee N, Tien RD, et al. Magnetic resonance imaging evidence of hippocampal sclerosis in progression: a case report. *Epilepsia* 1994;35:1332-6.
325. Saukkonen A, Kalviainen R, Partanen K, Vainio P, Riekkinen P, Pitkanen A. Do seizures cause neuronal damage? A MRI study in newly diagnosed and chronic epilepsy. *Neuroreport* 1994;6:219-23.
326. Trenerry MR, Jack CR, Jr., Sharbrough FW, et al. Quantitative MRI hippocampal volumes: association with onset and duration of epilepsy, and febrile convulsions in temporal lobectomy patients. *Epilepsy Res* 1993;15:247-52.
327. Salmenpera T, Kalviainen R, Partanen K, Pitkanen A. Hippocampal damage caused by seizures in temporal lobe epilepsy [letter] [see comments]. *Lancet* 1998;351:35
328. Matthews PM, Andermann F, Arnold DL. A proton magnetic resonance spectroscopy study of focal epilepsy in humans. *Neurology* 1990;40:985-9.
329. Petroff OA, Spencer DD, Alger JR, Prichard JW. High-field proton magnetic resonance spectroscopy of human cerebrum obtained during surgery for epilepsy. *Neurology* 1989;39:1197-202.
330. Davies KG, Hermann BP, Dohan FC, Jr., Foley KT, Bush AJ, Wyler AR. Relationship of hippocampal sclerosis to duration and age of onset of epilepsy, and childhood febrile seizures in temporal lobectomy patients. *Epilepsy Res* 1996;24:119-26.
331. Harvey AS, Berkovic SF, Wrennall JA, Hopkins IJ. Temporal lobe epilepsy in childhood: clinical, EEG, and neuroimaging findings and syndrome classification in a cohort with new-onset seizures. *Neurology* 1997;49:960-8.
332. Golomb J, de Leon MJ, Kluger A, George AE, Tarshish C, Ferris SH. Hippocampal atrophy in normal aging. An association with recent memory impairment. *Arch Neurol* 1993;50:967-73.

333. Mani RB, Lohr JB, Jeste DV. Hippocampal pyramidal cells and aging in the human: a quantitative study of neuronal loss in sectors CA1 to CA4. *Exp Neurol* 1986;94:29-40.
334. Dam AM, Hertz M, Bolwig TG. The number of hippocampal neurons in rats after electrically-induced generalized seizures. *Brain Res* 1980;193:268-72.
335. Bevington PR. Data reduction and error analysis for the physical sciences. New York:McGraw-Hill, 1969:
336. Bertolino A, Callicott JH, Nawroz S, et al. Reproducibility of proton magnetic resonance spectroscopic imaging in patients with schizophrenia. *Neuropsychopharmacology* 1998;18:1-9.
337. Kaplan MS, Hinds JW. Neurogenesis in the adult rat: electron microscopic analysis of light radioautographs. *Science* 1977;197:1092-4.
338. Mootha SL, Barkovich AJ, Grumbach MM, et al. Idiopathic hypothalamic diabetes insipidus, pituitary stalk thickening, and the occult intracranial germinoma in children and adolescents. *J Clin Endocrinol Metab* 1997;82:1362-7.
339. Gould E, Tanapat P, McEwen BS, Flugge G, Fuchs E. Proliferation of granule cell precursors in the dentate gyrus of adult monkeys is diminished by stress. *Proc Natl Acad Sci U S A* 1998;95:3168-71.
340. Eriksson PS, Perfilieva E, Bjork-Eriksson T, et al. Neurogenesis in the adult human hippocampus [see comments]. *Nat Med* 1998;4:1313-7.
341. De Stefano N, Narayanan S, Matthews PM, Francis GS, Antel JP, Arnold DL. Transient axonal dysfunction contralateral to large brain hemispheric demyelinating lesions of the type seen in multiple sclerosis. *Ann Neurol* 1998;44:465(Abstract)
342. Serles W, Li LM, Cendes F, et al. Time course of postoperative NAA recovery in patients with intractable temporal lobe epilepsy. *Neurology* 1999;52:A18-A19(Abstract)
343. Marson AG, Chadwick D. Comparing antiepileptic drugs. *Curr Opin Neurol* 1996;9:103-6.
344. Walker MC, Li LM, Sander JW. Long-term use of lamotrigine and vigabatrin in severe refractory epilepsy: audit of outcome [see comments]. *Bmj* 1996;313:1184-5.
345. Bland JM, Altman DG. Statistical methods for assessing agreement between two methods of clinical measurement. *Lancet* 1986;1:307-10.
346. King MA, Newton MR, Jackson GD, et al. Epileptology of the first-seizure presentation: a clinical, electroencephalographic, and magnetic resonance imaging study of 300 consecutive patients [see comments]. *Lancet* 1998;352:1007-11.
347. Germano IM, Sperber EF, Ahuja S, Moshe SL. Evidence of enhanced kindling and hippocampal neuronal injury in immature rats with neuronal migration disorders. *Epilepsia* 1998;39:1253-60.
348. Nguyen DK, Botez MI. Diaschisis and neurobehavior. *Can J Neurol Sci* 1998;25:5-12.
349. Dalby NO, Nielsen EB. Tiagabine exerts an anti-epileptogenic effect in amygdala kindling epileptogenesis in the rat. *Neurosci Lett* 1997;229:135-7.
350. Preul MC, Caramanos Z, Leblanc R, Villemure JG, Arnold DL. Using pattern analysis of in vivo proton MRSI data to improve the diagnosis and surgical management of patients with brain tumors. *NMR Biomed* 1998;11:192-200.

351. Tedeschi G, Lundbom N, Raman R, et al. Increased choline signal coinciding with malignant degeneration of cerebral gliomas: a serial proton magnetic resonance spectroscopy imaging study. *J Neurosurg* 1997;87:516-24.
352. Simone IL, Federico F, Tortorella C, et al. Metabolic changes in neuronal migration disorders: evaluation by combined MRI and proton MR spectroscopy. *Epilepsia* 1999;40:872-9.
353. Knowlton RC, Laxer KD, Ende G, et al. Presurgical multimodality neuroimaging in electroencephalographic lateralized temporal lobe epilepsy. *Ann Neurol* 1997;42:829-37.
354. Kuzniecky R, Hugg J, Hetherington H, et al. Predictive value of 1H MRSI for outcome in temporal lobectomy. *Neurology* 1999;53:694-8.
355. Semah F, Picot MC, Adam C, et al. Is the underlying cause of epilepsy a major prognostic factor for recurrence? [see comments]. *Neurology* 1998;51:1256-62.
356. Walker MC, Sander JW. The impact of new antiepileptic drugs on the prognosis of epilepsy: seizure freedom should be the ultimate goal. *Neurology* 1996;46:912-4.
357. Chadwick D, Taylor J, Johnson T. Outcomes after seizure recurrence in people with well-controlled epilepsy and the factors that influence it. The MRC Antiepileptic Drug Withdrawal Group [see comments]. *Epilepsia* 1996;37:1043-50.
358. Chadwick D. Does withdrawal of different antiepileptic drugs have different effects on seizure recurrence? Further results from the MRC Antiepileptic Drug Withdrawal Study. *Brain* 1999;122:441-8.